UNLIMITED DISTRIBUTION

National Defence
Research and
Development Branch

Défense Nationale
Bureau de Recherche
et Développment

DREA CR/90/424

ANALYSIS OF THE WEST COAST WAVE CLIMATE

by
Barbara-Ann Juszko

JUSZKO SCIENTIFIC SERVICES
483 Sue Mar Place
Victoria, British Columbia, Canada
V9C 3E1

Scientific Authority
Ross Graham

Contract Number
W7077-9-0286/01-OSC

31 March 1990

CONTRACTOR REPORT

Prepared for

Defence
Research
Establishment
Atlantic

Centre de
Recherches pour la
Défense
Atlantique

ABSTRACT

Surface displacement spectra, collected at five locations off Canada's West Coast over a period extending from 1984 to 1989, were used to describe the overall wave climate, spectral types and storm characteristics of this region. Offshore waters experienced the most severe wave climate, as indicated by the joint occurrence of significant wave height (HSIG) and peak period (TP). Conditions of HSIG > 8m and TP > 17s were observed at all locations while the most severe record was represented by an HSIG > 13m and TP of 20s. Examination of the spectral types indicated a large percentage of swell dominant and multiple peak spectra which has implications towards both their numerical and parametric modelling. Fifteen storms, driven by both small and large scale pressure systems, were examined in detail and showed the presence of rapid sea growth (maximum rates on the order of 1 m/hr and 1s/hr for HSIG and TP) and, with the exception of Queen Charlotte Sound, an average 30% decrease in energy between offshore and inshore stations, intensification of sea conditions in Queen Charlotte Sound was observed on occasion (maximum intensification of 60%). The Ochi and Hubble six-parameter model was fit to all spectra. The statistical distribution of the fit parameters was calculated and an attempt was made to predict these parameters with varying success. The probability distribution of the fit parameters was also examined to define design spectra with known confidence limits.

RÉSUMÉ

Des spectres de déplacement de surface, recueillis en cinq endroits au large de la cote ouest du Canada entre 1984 et 1989, ont été utilisés pour décrire le régime global des vagues, les types spectraux et les caractéristiques des tempêtes de cette région. Les eaux du large ont été le siège du régime de vagues le plus violent, caractérisé à la fois par des hauteurs de vagues (HSIG) élevées et par des longues périodes principales (TP). Des vagues de HSIG > 8m et de TP > 17s ont été observées à tous les endroits, tandis que les vagues les plus grosses avaient des HSIG > 13m et des TP = 20s. L'examen des types spectraux a révélé un fort pourcentage de spectres dominés par la houle et de spectres a plusieurs pics, ce qui influe sur leur modélisation tant numérique que paramétrique. Quinze tempêtes, soulevées par des systèmes de pression a petite comme à grande échelle, ont été examinées en détail et ont révélé une croissance rapide de la mer (taux maximums de l'ordre de 1 m/h et de 1 s/h pour HSIG et TP) et, sauf dans le détroit de la Reine-Charlotte, une diminution moyenne d'énergie entre le large et la cote de 30%. L'intensification de l'état de la mer dans le détroit de la Reine-Charlotte a été observe par moments (intensification maximale de 60%). Le modèle a six paramètres d'Ochi et Hubble a été ajusté tous

les spectres. La distribution statistique des paramètres d'ajustement a été calculée, et on a tenté de prévoir ces paramètres avec, plus ou moins de succès. La distribution des probabilités des paramètres d'ajustement a aussi été examinée dans le but de définir des spectres théorique de conception avec des limites de confiance connues.

TABLE OF CONTENTS

LIST OF FIGURES

LIST OF TABLES

1INTRODUCTION

Since 1982, an on-going wave measurement program has been conducted on the West Coast by the Canadian government in order to characterize the wave climate in Queen Charlotte Sound, Hecate Strait, and Dixon Entrance. This program is supplemented by the long time series of waverider measurements off Tofino (West coast of Vancouver Island) and by an offshore array of 10m discus buoys, operated by the United States National Data Buoy Office, throughout the Northeast Pacific.

In this study, wave spectral information, collected from 1984 to January 1989 at three inshore and two offshore sites, were analyzed to develop an understanding of the wave climate in the region. Summary spectral statistics were used to develop a seasonal and geographic picture of the mean and extreme wave conditions. Though useful, these statistics do not provide sufficient detail on the characteristics of individual spectra for many model and engineering applications. More detailed information was obtained by first classifying the spectra according to total energy, number and position of spectral peaks and then by fitting a parametric model to the individual spectrum and assessing the model's behavior. A detailed analysis of individual spectra, concentrating on storm occurrences, provided further information on the regional, time and energy dependent growth and decay of wave spectra. Finally, the ability to predict the model parameters from external information was examined and their probability density distribution used to establish model spectra of known statistical confidence.

2STUDY BACKGROUND

2.1 Study Objectives

There were two primary objectives of this study. The first was to perform a wave climate analysis on a minimum cumulative 15 years of data from five locations off Canada's West coast. The analysis consisted of examining the behavior of standard spectral statistics, of classifying the spectra based on characteristics of scanned spectral peaks, and in selecting and analysing storm occurrences. The second objective was to perform the fit of a selected parametric model to the data spectra. The ability of the model to represent the data spectra was assessed and the statistical and predictive behavior of the parameters was determined.

2.2 Data Sources

Surface displacement energy density spectra, for five locations on Canada's West Coast, spanning a time period from January 1984 through January 1989, were supplied by the Marine Environmental Data Service (MEDS). As part of the storm analysis, surface atmospheric pressure charts, for selected time periods, were obtained from the Atmospheric

Environmental Service (AES). The buoy mooring sites, illustrated in Fig. 1 , were chosen to provide good spatial coverage of both inshore and offshore waters and the time period was selected to allow sufficient data for statistically significant analyses.

2.3 Data Processing

The periods of good data return from each station are denoted by the solid lines in Fig. 2 . Data gaps were generally associated with instrument failure and time delays in instrument servicing. Table 1 lists information on the mooring site, sampling scheme and data spectral analysis. The three inshore stations were operated by MEDS while the two offshore stations formed part of the on-going NOAA (National Oceanographic and Atmospheric Administration) databuoy project. Due to the different buoy types and sampling schemes, each station was treated independently and some pre-processing was required. Band-averaging was performed, when necessary, to increase the number of degrees of freedom of the spectra. In order to simplify later analyses, the spectra were truncated below 0.1885 and above 2.0 rps (radians/sec) (.03 and 32 Hz) to remove spurious instrument response effects influencing energy at very low frequencies, and to provide a constant upper frequency limit as well as eliminating high frequencies containing little energy. The amount of band-averaging was dictated by the initial frequency resolution and the necessity of having a sufficient number of frequencies for model fitting. Further smoothing, using a three-band running average, was also required for all but the two NDBO stations prior to classification of the spectra, peak scanning, and model fitting, indicated in Table 1 are the initial spectral information, including the number of frequencies and frequency resolution before and after this pre-processing. A data quality code was supplied by MEDS for most of their processed spectra. Spectra noted with a poor or questionable data quality code as well as those with unacceptable significant wave heights or peak periods (e.g. spikes) were rejected.

A WRIPS buoy (Datawell waverider modified for satellite transmission) was moored at station 503W, Queen Charlotte Sound, and sampled every three hours. There were numerous data gaps of short duration possibly related to satellite transmission "misses". A second problem seen in the data was the presence of spurious low frequency energy suspected to be a result of mooring motion. The most extreme cases were rejected while truncation of the record at 0.1885 rps eliminated much of this energy for less severe occurrences. As there were only 27 frequencies describing the spectra, band-averaging to increase confidence in the spectra was not possible as the reduction in the number of frequencies would have been too great for subsequent

model fitting. Smoothing with a three-band running average was applied to the first 20 frequencies prior to model fitting.

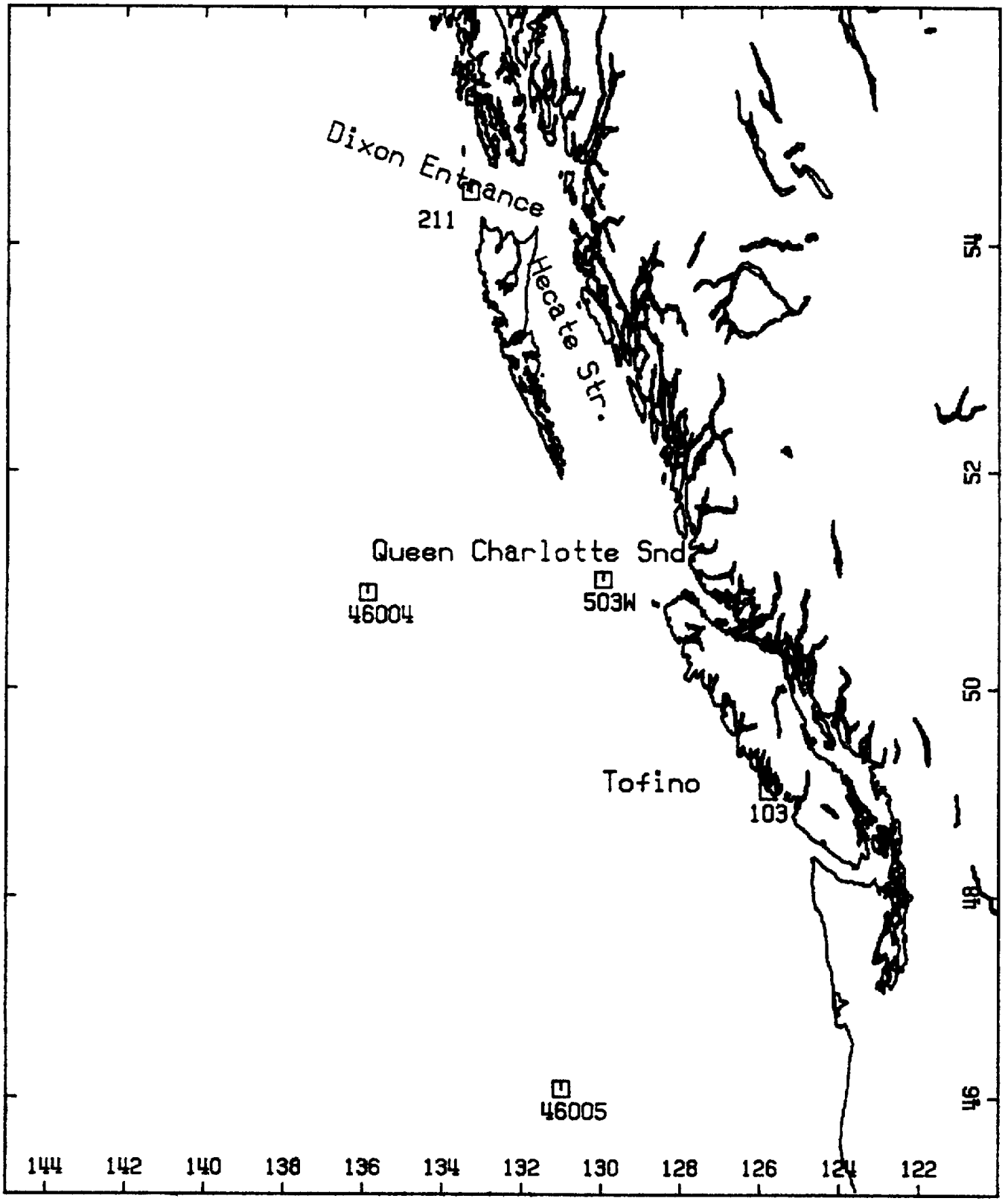

Fig. 1 Study location.

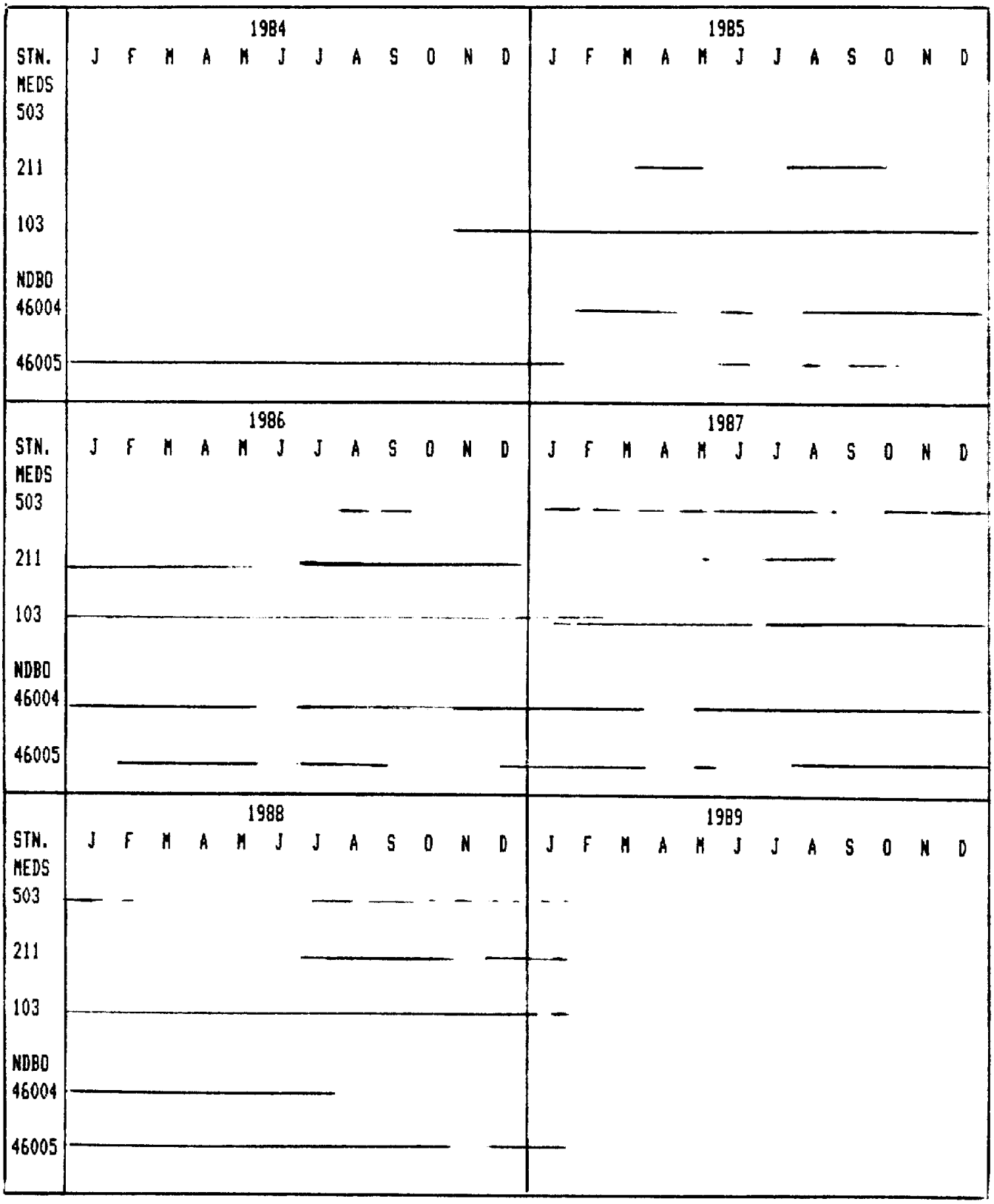

Fig. 2 Data return chart.

Table 1. Buoy locations and data processing summary.

STN.	LAT	LONG	WATER DEPTH (m)	BUOY TYPE	SAMPLING SCHEDULE (hr)	SAMPLE DURATION (min)	SAMPLING FREQ. (Hz)	NO. OF FREQ		FREQUENCY RESOLUTION (Hz)		DEGREES OF FREEDOM		TOTAL NO. OF SAMPLES
								Before	After	Before	After	Before	After	
MEDS														
503W	51.3N	129.97W	240	WRIPS	3.0	34.0	1.0	34	27	.0039	(1)	(2)	(2)	3868
211	54.45N	133.32W	293	WAVEC	3.0(3)	40.0	0.78	64	33	.005	.01	20	120	5385
103	49.04N	125.8W	37	WAVERIDER	3.0(4)	18.5	7.5	64	40	.00732		16	48	12117
			21	(6)		26.7	1.28	100	30	.005	.01	16	96	
NDBO														
46004	50.9N	135.9W	3657	NOAA DATA BUOY	3.0	20.0	1.5	48	31		.01	24	24(5)	8808
46005	46.1N	131.0W	2853	NOAA DATA BUOY	3.0	20.0	1.5	48	31		.01	24	24(5)	10608

Note: 1) Variable frequency array; no. of bands averaged: 1 for first 20 freq.
then 4,4,6,9,13,21,43. No. of degrees of freedom= No. of bands averaged * 8 * 2
2) 3 band running average performed on first 20 frequencies for smoothing prior to fit
3) Optional continuous recording during storms
4) Hourly recording for selected periods; continuous recording during storms
prior to February 1987.
5) No smoothing required
6) Processing method changed in Feb. 1987

A Datawell WAVEC buoy (directional slope-following buoy) was moored at station 211 in Dixon Entrance. It sampled every three hours except during storms when a record every 35 minutes was available. The three-hourly record was extracted for further analyses. Data quality was good when the buoy was operating.

A Datawell waverider was moored at Tofino (Station 103), normally sampling every three hours, though periods of hourly sampling occurred. Prior to February 1987, records were available every 20 minutes during storms and two 20-minute records were averaged together in order to increase confidence in the storm spectra. In order to maintain a sufficient frequency resolution, band-averaging could not be performed on this data. In February 1987, the sampling regime and data processing procedure was altered. This allowed for two-band averaging and reduction of noise in the spectra after February 87. As with Station 503W, spurious low frequency energy was sometimes observed possibly due to mooring motion. These data were the most complete for the period Nov 84 through Jan 89.

NOAA data buoys (10m discus buoys), recording both wave and wind information, were positioned at Stns. 46004 and 46005. The data quality of these spectra was high and they were relatively "noise" free. No smoothing was required.

In all, over forty thousand spectra were analyzed.

3. STATISTICAL DESCRIPTION OF THE WAVE CLIMATE

A discussion on the West Coast wave climate should include an analysis of the average and extreme behavior of selected spectral statistics, specific characteristics of sea and swell, and the observed response to the passage of storms. In this section, the behavior of spectral statistics will be discussed. Whenever possible, distinction between sea and swell will be made; however, the primary discussion on observed swell, as well as the storm behavior, will be included in Section 5 .

3.1 Methodology

The spectral statistics that were examined included the significant wave height (HSIG) (which describes the amount of wave energy present based on assumed distributions of the measured amplitude and total variance), four period statistics, peak period (TP), average period (APER), average apparent period (AAP) and apparent crest period (ACP), and two shape statistics - peakedness (QP) and spectral width (SPW). With the exception of TP, the other statistics are calculated from various moments of the spectra, as described below. Their usefulness lies in their ability to efficiently summarize given features of the spectra from which possible predictive relationships can be established or simple models could be built.

The spectral statistics were

Moments of the spectra: $Mk = \sum_{I=1}^{N} f_I^k E(f_I) df$

Significant wave height (HSIG) : 4.0 * SQRT (MO)

Peak period (TP): Period associated with the maximum spectral density value (Emax(f)).

Peakedness parameter (QP): $2 * \sum_{I=1}^{N} f_I E^2(f_I) df / (MO * MO)$

Spectral width parameter (SPW): $SQRT \left[\frac{MO*M4 - M2*M2}{MO*M4} \right]$

Average period (APER): MO/M1

Average apparent period (AAP): SQRT (MO/M2)

Apparent crest period (ACP): SQRT (M2/M4)

With the exception of TP, it should be noted that these statistics, particularly when using higher moments, are not stable (i.e. calculation over different frequency ranges would result in different values) which can cause problems for certain applications.

The overall behavior of the spectral statistics were summarized by station, season and spectral type (as discussed later), both graphically and with the following distribution statistics:

Range values: Minimum and Maximum

Mean: $\bar{X} = (1/N) * \sum_{I=1}^{N} x_I$

Average deviation (ADEV): $(1/N) * \sum_{I=1}^{N} |x_I - \bar{X}|$

Standard deviation (SDEV): $\sigma = SQRT \left[1/(N-1) * \sum_{I=1}^{N} (x_I - \bar{X})^2 \right]$

Skewness (SKEW): $(1/N) * \sum_{I=1}^{N} \left[\frac{x_I - \bar{X}}{\sigma} \right]^3$

Kurtosis (KURT): $\left\{ (1/N) * \sum_{I=1}^{N} \left[\frac{x_I - \bar{X}}{\sigma} \right]^4 \right\} - 3$

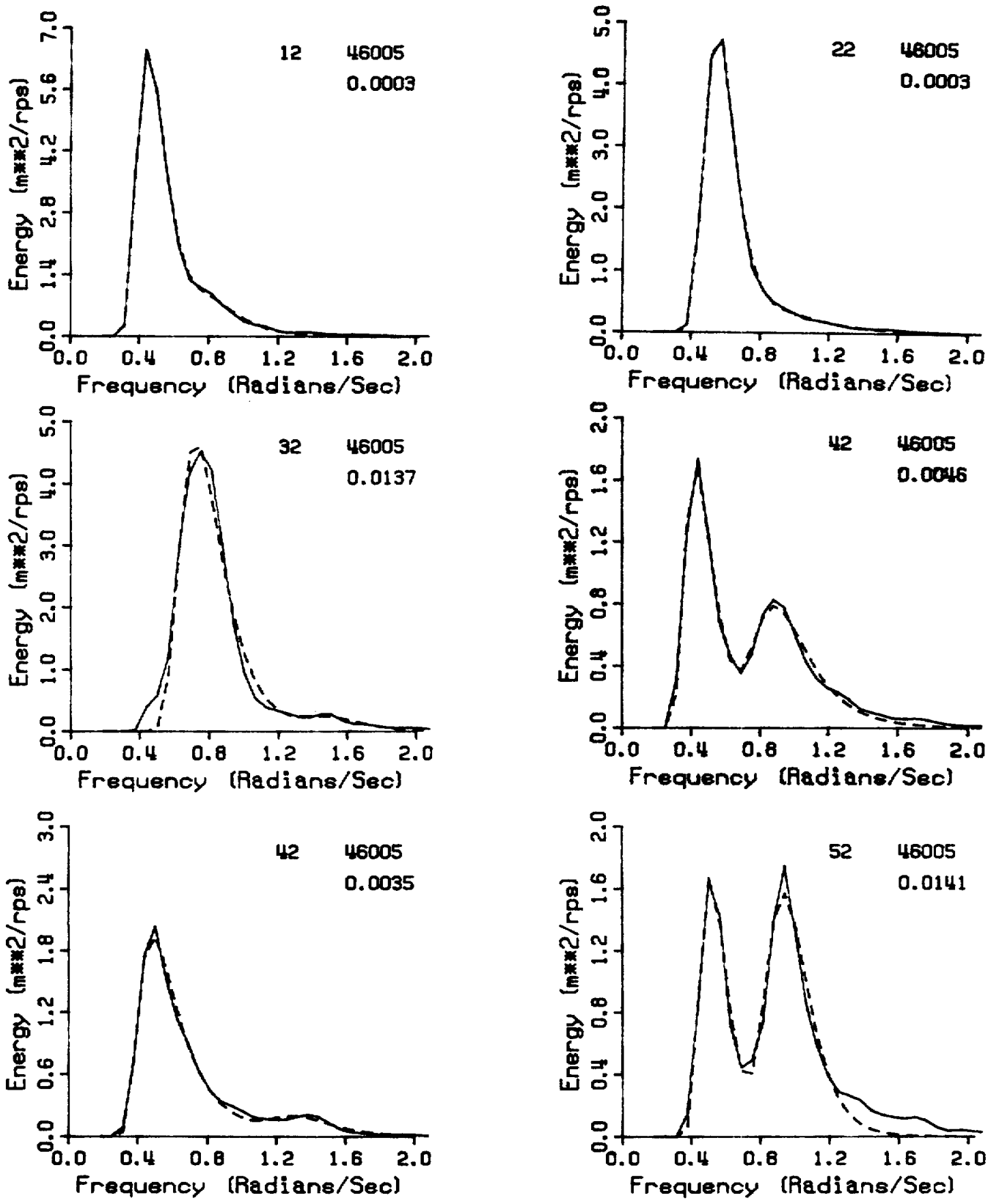

Fig. 3 Sample spectra for Stn. 46005.

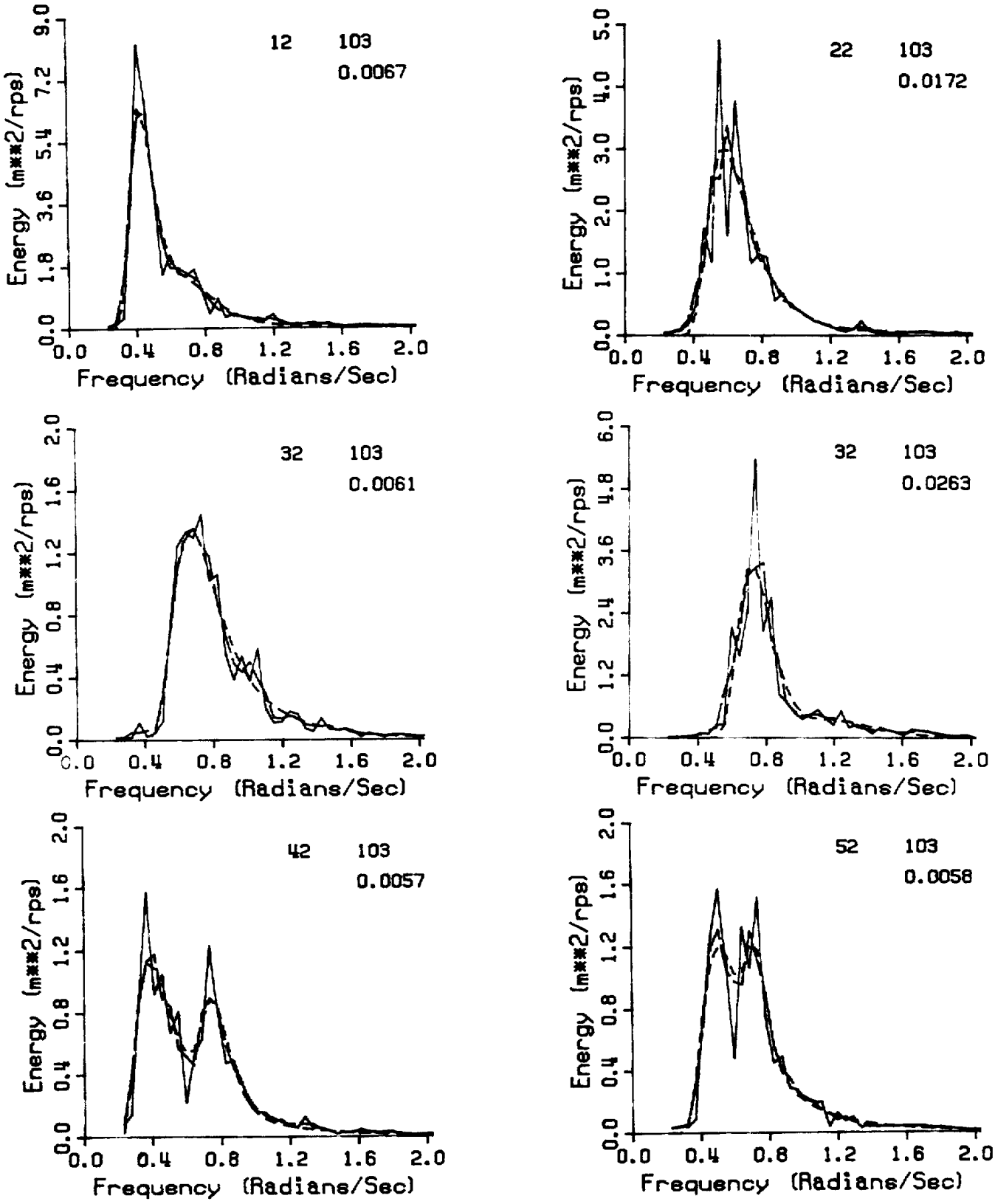

Fig. 4 Sample spectra for Stn. 103.

The wave spectra were further classified into spectral types in order to provide basic percent occurrence information and to allow for more detailed analysis of spectral statistics and model fit behavior. The classification was based on selected spectral statistics, namely HSIG and TP, and on the number and location of spectral peaks determined through a scanning procedure. The peak scanning, performed on the smoothed spectra, consisted of detecting peaks and troughs (i.e. maximum and minimum spectral densities), determining the modal peak period (TPm) associated with the local maximum, and calculating the amount of variance explained by the peak through summation over the frequency range bounded by the trough locations. As multiple peaks are often present in any given spectrum, a peak was considered significant if it explained more than 10% of the total variance. The peak scanning worked well on the Stns. 46005, 46004 and 211 records but had more difficulty with Stns. 103 and 503W as these often consisted of multiple peak conditions. One must achieve a balance between smoothing out actual data peaks and removing "peaks" that are a result of variability, while also maintaining sufficient frequency resolution. Low energy spectra were often classed as multiple peaks as the secondary peaks could readily account for 10% of the variance.

Using the above information, the data spectra were assigned a class code where the first digit represented the modal peak period information (TPm) and number of peaks, and the second digit indicated the range of significant wave height. TPm represents the period, associated with the local maximum spectral density, of the peak containing the majority of the variance in the spectrum. This coding will be referred to as Type 1 to distinguish it from a later classification based on model fit behavior (Type 2). There were fifteen classes denoted by:

Scanned single peak:	TPm $\geq$ 14s	1
	10 $\leq$ TPm < 14s	2
	TPm < 10s	3
Scanned 2 or more peaks:	TPm $\geq$ 12s	4 (low frequency dominant)
	TPm < 12s	5 (high frequency dominant)
Significant wave height	- Second Digit:	
	0 < HSIG $\leq$ 3m	1
	3 < HSIG < 6m	2
	HSIG $\geq$ 6m	3

For example, a Type 1 code of 23 would represent a single peak spectrum with HSIG greater than or equal to 6m and a peak period between 10 and 14 seconds while a code of 43 would be assigned to a multiple peak spectrum with similar HSIG whose major peak has an associated period greater than or equal to 12 seconds. Note that for

single peak spectra, TPm would be equal to TP while for multiple peak spectra this is not necessarily true (e.g. sharp swell and broad sea, where TP is associated with the swell while the sea may be explaining a greater percentage of the total variance denoted by TPm). Figs. 3 and 4 contain examples of classes 12, 22, 32, 42 and 52 for stations 46005 and 103, respectively. Indicated on the figures are the station number, class code and model fit residual value (RESH) discussed in Section 4.1 . The solid line represents the data spectra without any smoothing. The short dashed line is the parametric model fit to the data while the long dashed line, in Fig. 4 , is the smoothed spectra upon which both peak scanning and model fitting is performed. By comparing the two figures, it can be seen that the NDBO spectra show less variability than the original 103 spectra and no additional smoothing is required. Smoothing of the 103 spectra is necessary for a peak/trough scanning procedure to be effective. Two examples of class 42 spectra are shown in Fig. 3 . The relatively small high frequency peak in the lower example was an early sea which developed, in three hours, to the spectra representing class 52. In Fig. 4 , two examples of class 32 are included to illustrate differences in peak width that may be encountered. Numerous examples of a wide variety of spectral shapes are included in Appendix 3 as part of the storm analysis.

The spectral type classes can be assigned some physical meaning. Classes 11, 21 and 12 are predominantly pure swell situations. Classes 13, 23, 32 and 33(very few and possibly questionable occurrences) are primarily pure wind-driven sea spectra. Classes 22 and 31 may be sea or swell depending on the wave history. The remaining classes represent multiple peak situations which are particularly prevalent in low energy conditions. Classes 41, 42 and 52 are primarily mixed sea and swell situations, though multiple swells are possible. They often occur during early sea development, Class 51 may also be representing a mixed sea/swell situation or noisy low energy sea. The classes associated with larger energy (43,53) may represent a sea peak with smaller swell or "noisy" sea spectra under decaying, varying or veering winds when equilibrium has to be re-established. These characterizations are general and it was often more difficult to perform peak selection when multiple peaks exist or if one broad peak is present (i.e. which actually consists of more than one peak close in frequency). This was especially true for Stn. 103 and 503W data which tended to have multiple peaks even after smoothing.

3.2 Results

A qualitative understanding of the wave climate during the study period can be obtained through examination of the time series of HSIG, TP and energy density contoured by frequency, shown in Appendix 2. The contour intervals were set to 0.05, 0.1, 0.25, 0.5, 1.0, 2.5, 5., 10.,

15. and 20. m**2/rps. The relative amount of noise in the spectra can be seen by comparing the contoured spectral densities. For example, Stn. 46005 is relatively noise free while Stn. 103 spectra contain a significant noise component. The occurrence and character of storms are indicated by the relative amount of energy present, the rate of build-up and decay and its duration. The presence of mixed sea/swell or swell dominant conditions can be seen in the contour spectra as two or more energy centers. These are not always obvious in the time series of TP and HSIG alone. A clear distinction between sea and swell is most easily observed during the summer. Seasonal designations were chosen as

Winter - December, January, February
Spring - March, April, May
Summer - June, July, August
Autumn - September, October, November

There was seasonal representation from all five locations, however the presence of data gaps (see Fig. 2) reduced the number of years incorporated into the seasonal averaging. These gaps may effect the examination of inter-annual variability of the wave climate, and could introduce bias into the overall statistics. The estimated number of months of data contributing to each seasonal average and the actual percentage of records used in the calculation of both the spectral and fit (discussed in Section 4.3) summary statistics, are presented in Table 2 , Stns. 503W and 211 had the fewest number of contributing months of data in the calculation of the seasonal statistics. For Stn. 211, there were no data recorded during May with only a limited number of records available from June possibly biasing the spring statistics to more energetic and the summer values to less energetic conditions. There was more uniform data coverage at the other stations. The relative contribution of winter vs summer data would indicate the expected bias in the overall statistics. Stn. 211 was the only location for which there was greater than 6% difference between these two seasons with summer, low energy conditions associated with over 35% of all records. At the other stations, there was a slightly greater occurrence of winter recordings.

The seasonal and overall percent occurrence of HSIG, TP, QP and APER are illustrated in Figs 5 to 8 a,b and the percent exceedance of HSIG is shown in Fig.9 . Similar percent occurrence plots for the remaining spectral statistics are included in Appendix 1. The distribution statistics, as a function of location, season and spectral type are also listed in the tables of Appendix 1. As might be expected, the most energetic conditions at all locations were seen in the winter months, the calmest in the summer, with intermediate and similar conditions in the spring and autumn. The most extreme

conditions, in terms of both HSIG and TP, were observed at the two offshore NDBO stations. Here, essentially no sheltering, fetch or water depth effects would influence the spectral development. The inshore stations are sheltered by nearby land masses and the buoy at Stn. 103, which showed the least severe wave climate, was moored in shallow water (under 40m) and waves of period greater than approximately seven seconds would "feel" the bottom. Under certain conditions, however, inshore stations in Queen Charlotte Snd. and Hecate Strait, may show a more severe wave climate than offshore. This occurs when the pressure center, generating the storm conditions, intensifies while approaching the coast at a speed close to the group velocity of the low frequency waves allowing for continuous wind reinforcement of the wave field. Strong wind and tidally generated currents could also result in wave steepening particularly in Hecate Strait. Larger values of the peakedness parameter were observed for spectra associated with the inshore stations than for the offshore stations. The increased low frequency resolution of the WRIPS records may account for the larger QP values at Stn. 503W. The large values may also be a result of "filtering" of the incoming waves due to both land and bathymetry limiting directional spread of the wave energy resulting in sharper energy peaks. The distribution of APER, an energy weighted mean period with values slightly smaller then TP, were similar between the mooring sites. The largest values were seen at Stn. 103 indicating a more consistent presence of swell at this location.

The joint distribution of HSIG and TP provides further information on the severity of the wave climate. It is these combined characteristics of HSIG and TP which determine the separation between sea and swell. For example, a single-peaked record with HSIG of 3m and TP of 16s would be classified as swell but if HSIG was 9m, this record would be representing a wind forced sea. Operational criteria are often defined in terms of the most frequent joint occurrence of HSIG and TP. The seasonal and total percent joint occurrence of HSIG and TP are included in Appendix 2. Table 3 lists, by season and station, the percent occurrence and the range of HSIG and TP values associated with the maximum joint occurrence group. Also included in the table, is the % occurrence of records having HSIG>5m and TP>14s as an indication of wave climate severity. The results in the table support the previous discussion on location and seasonal effects. The most extreme single joint occurrence was observed at Stn. 46005 at the peak of a storm in December 1987. At this time, the significant wave height was estimated at over 13m and the spectral peak indicated a 20 second period. Conditions of HSIG greater than 10m with concurrent wave periods greater than 17 seconds were also observed at Stn. 46004. At the inshore stations, HSIG>8m and TP>17s were observed at all stations on at least one occasion.

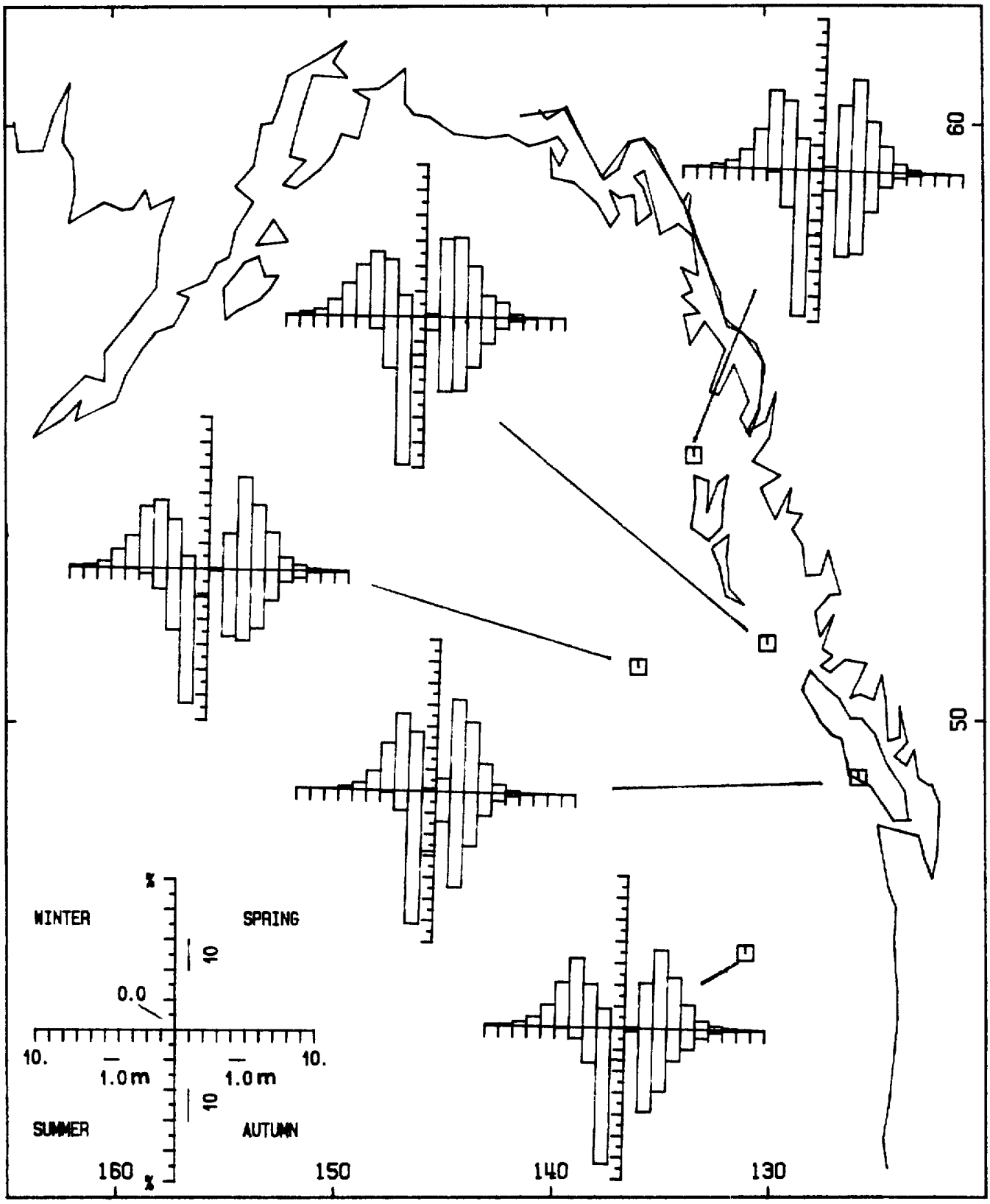

Fig. 5a Seasonal percent occurrence of significant wave hgt.

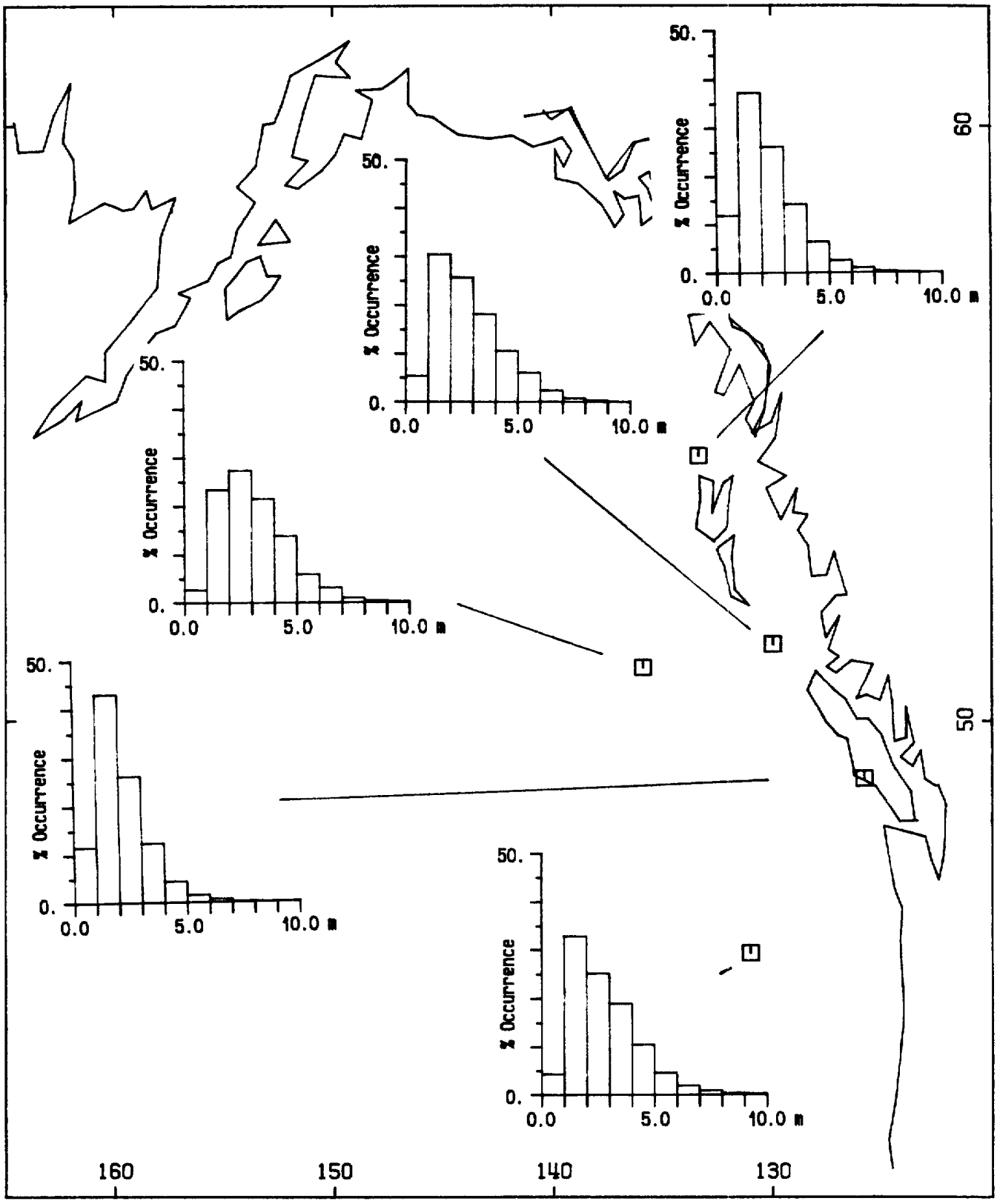

Fig. 5b Total percent occurrence of significant wave hgt.

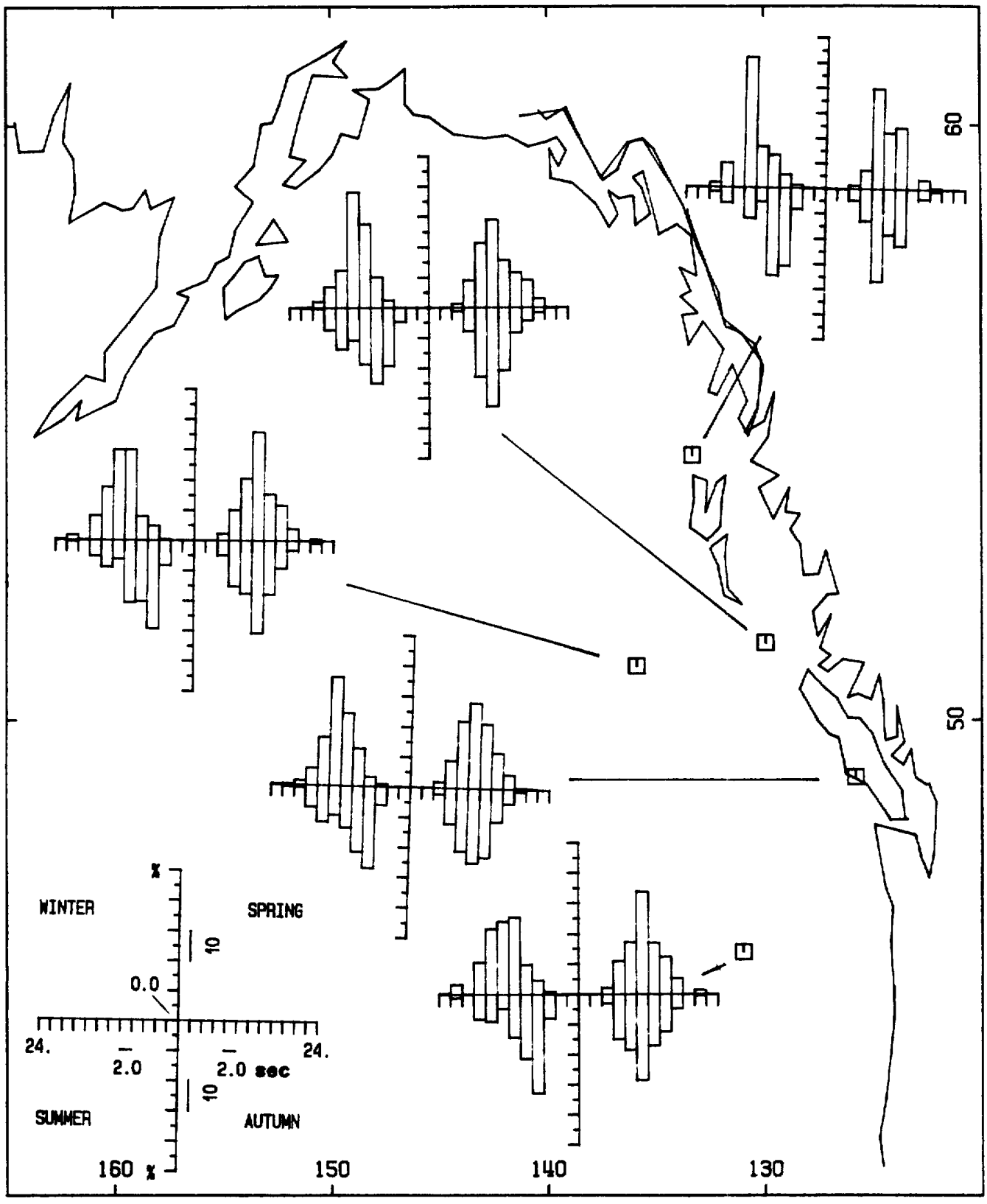

Fig. 6a Seasonal percent occurrence of peak period.

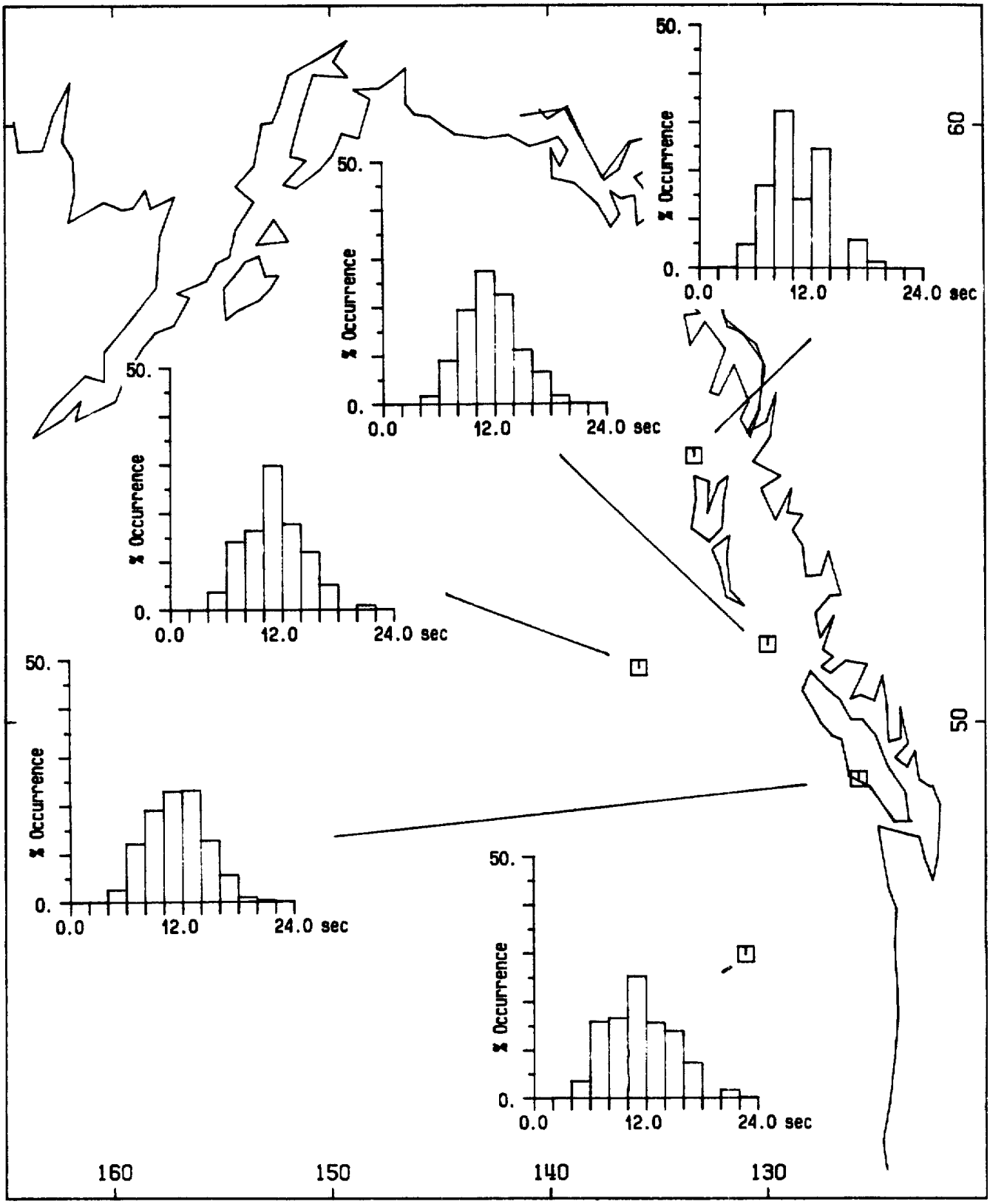

Fig. 6b Total percent occurrence of peak period.

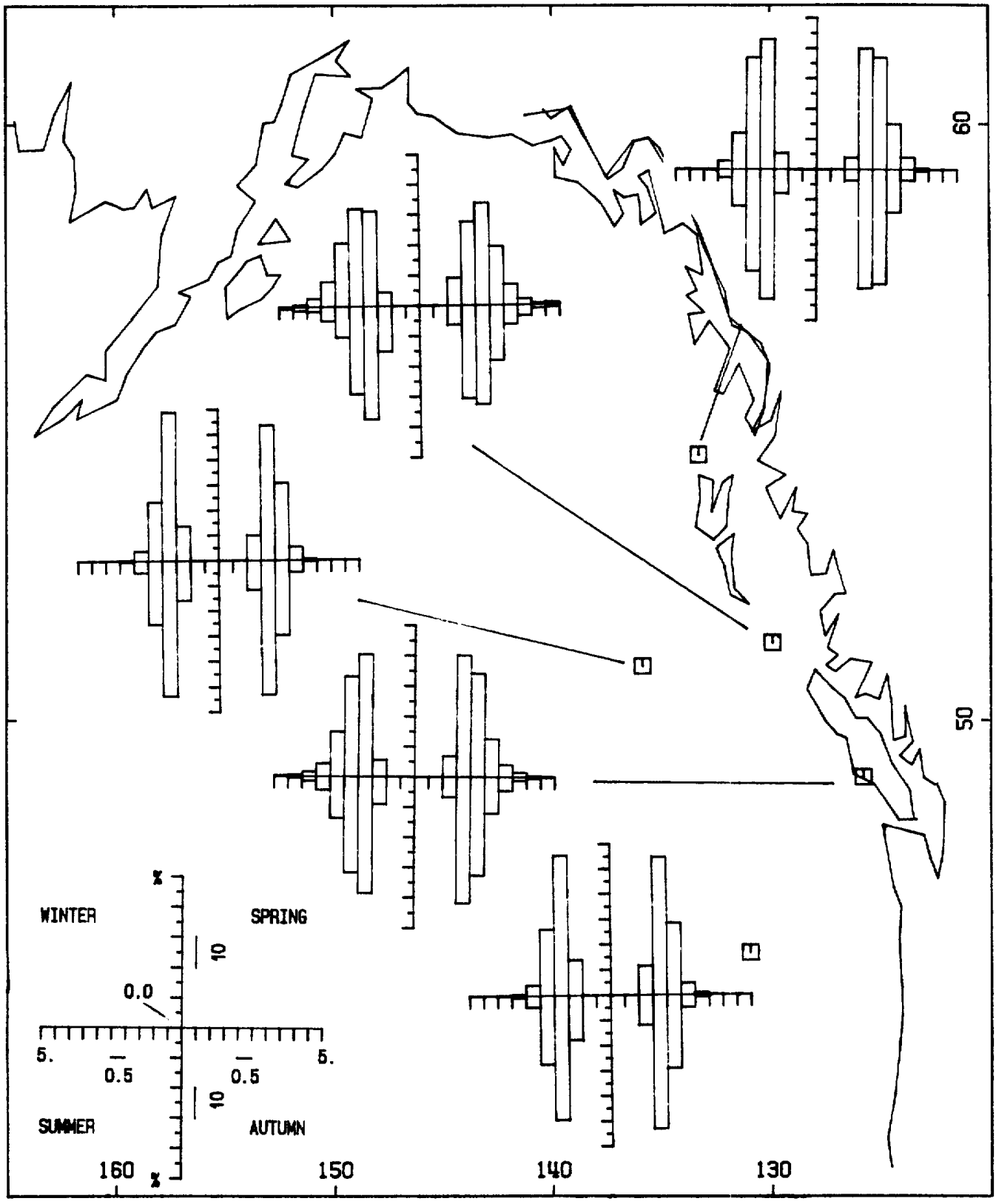

Fig. 7a Seasonal percent occurrence of peakedness parameter.

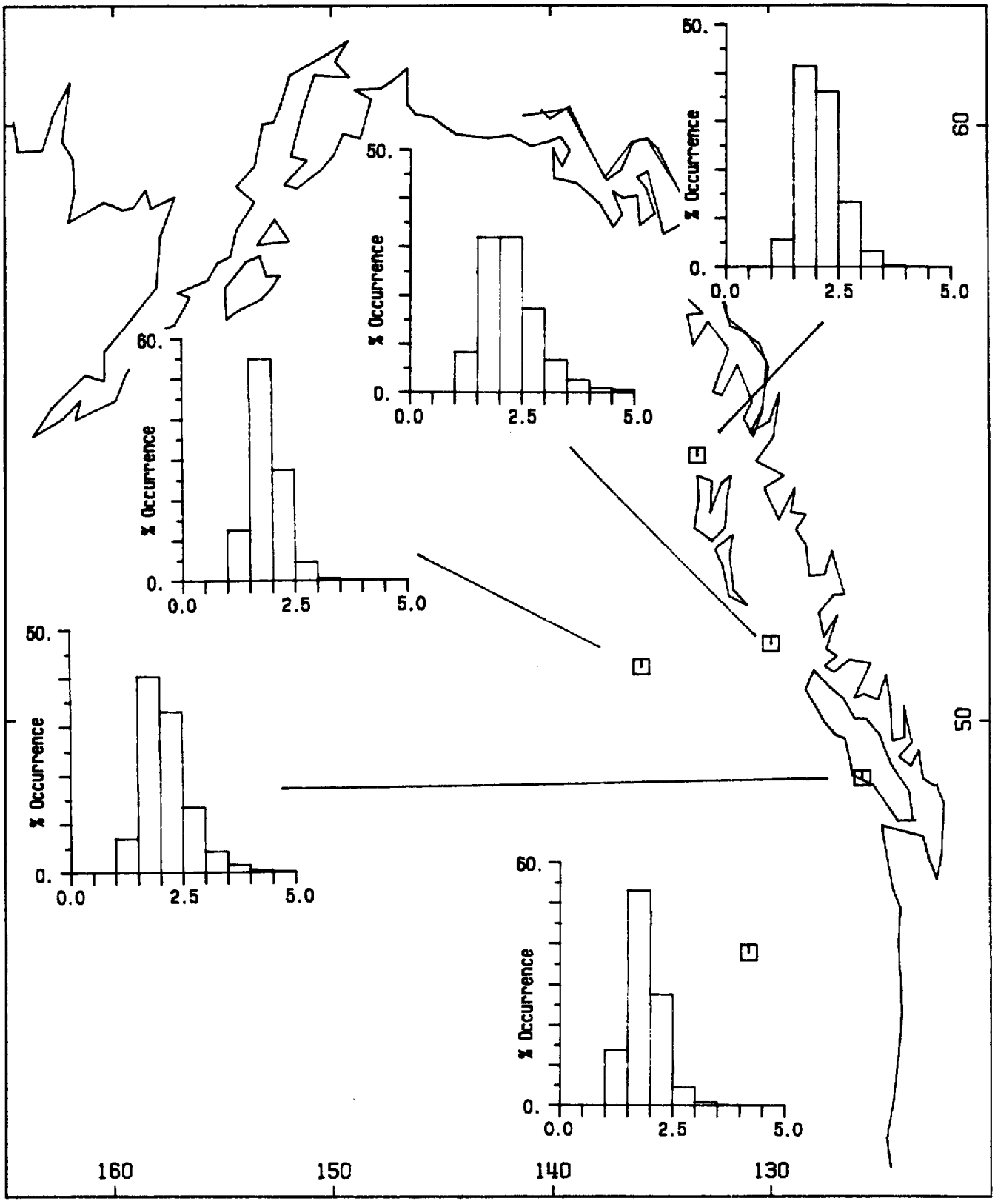

Fig. 7b Total percent occurrence of peakedness parameter.

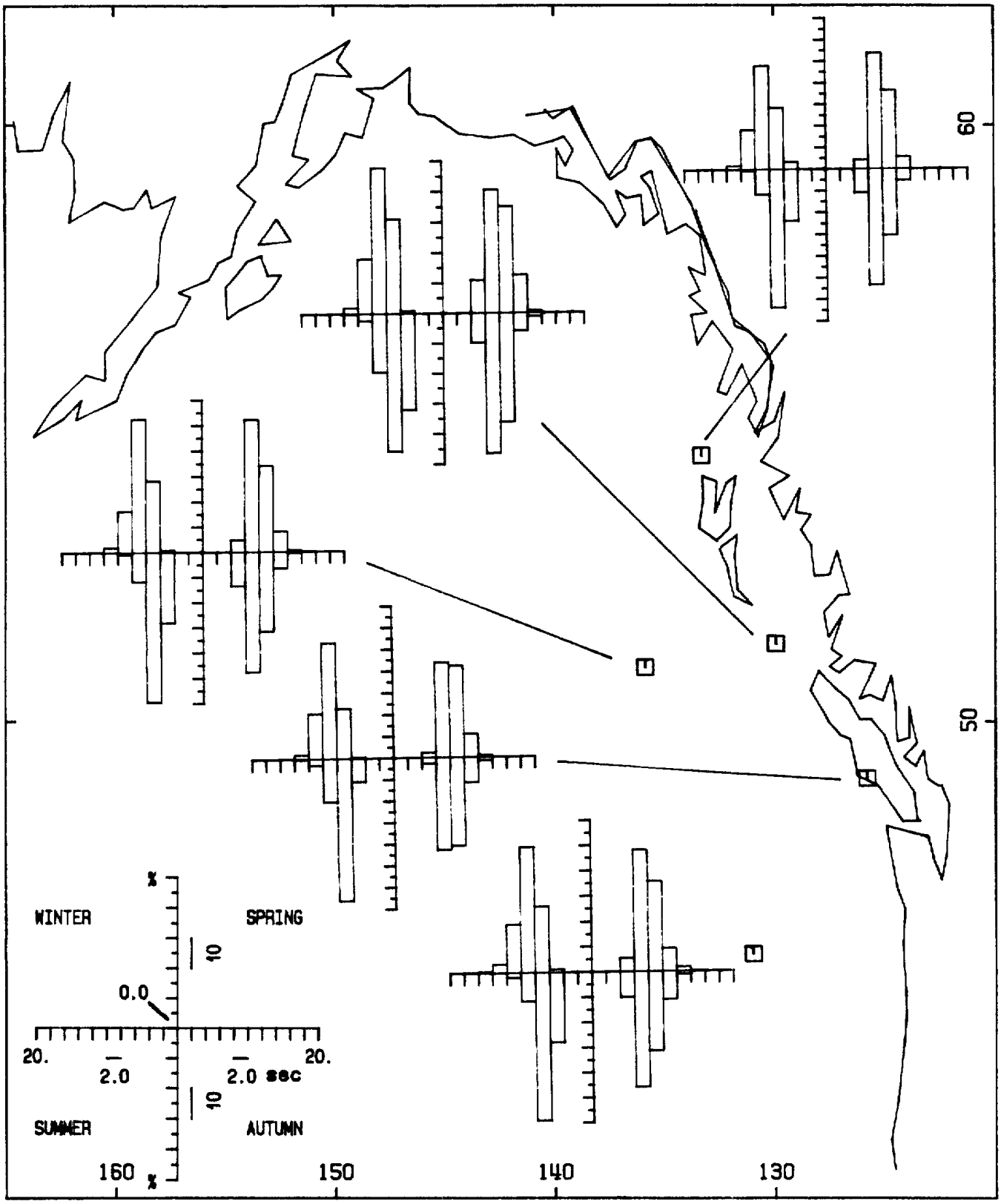

Fig. 8a Seasonal percent occurrence of average period.

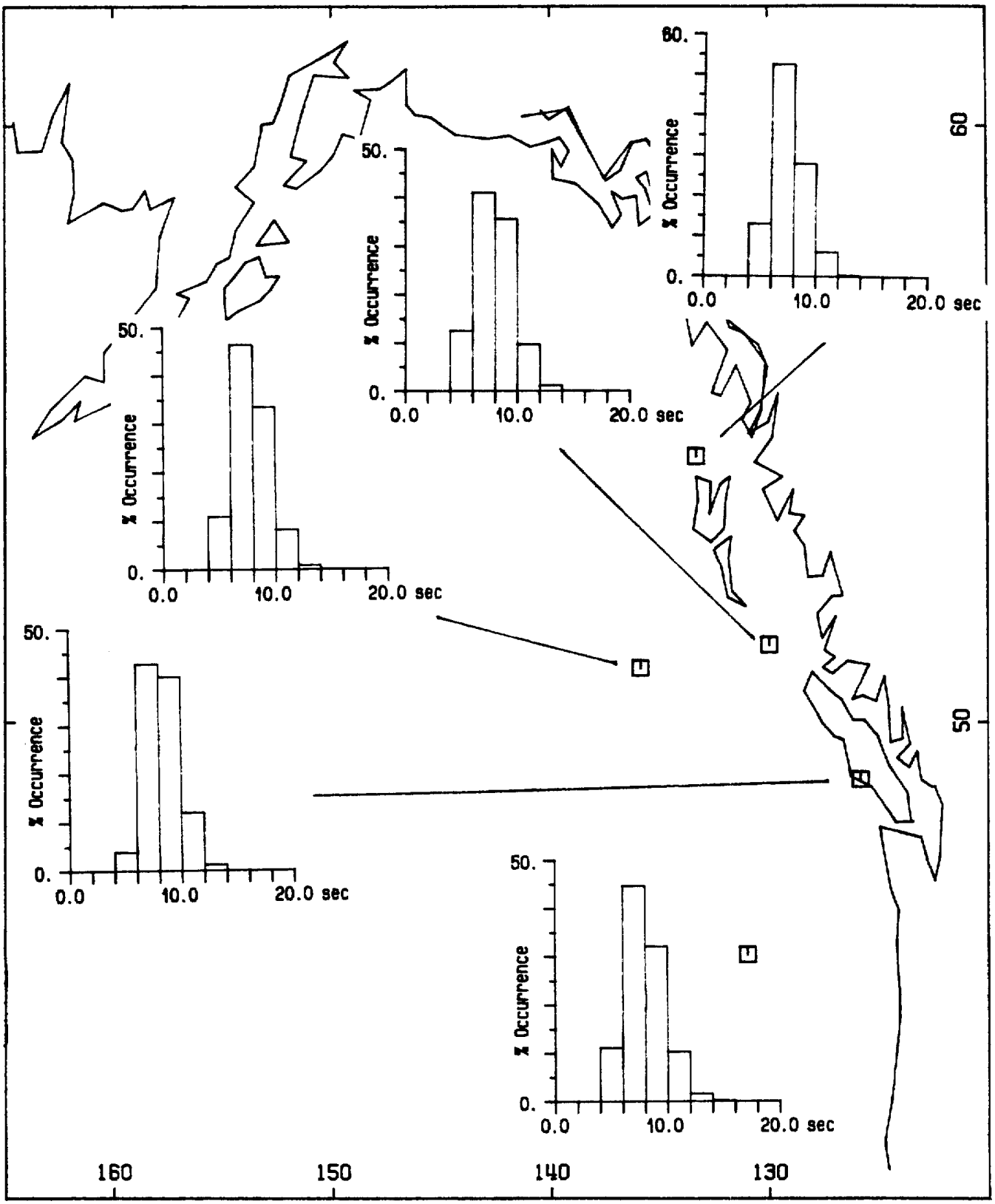

Fig. 8b Total percent occurrence of average period.

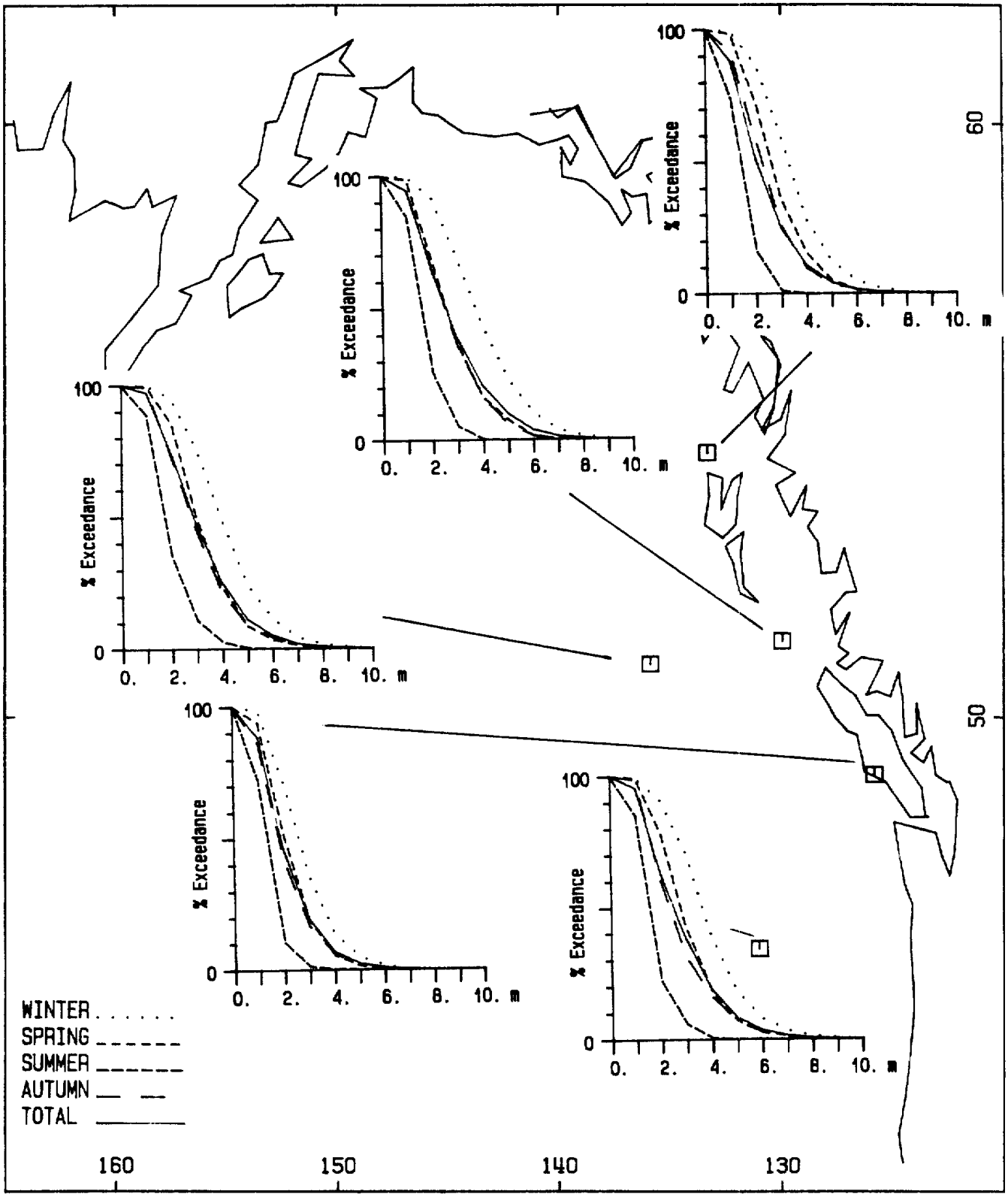

Fig. 9 Seasonal and total percent exceedance of significant wave height.

Table 2. Seasonal data coverage.

Stn.	Winter			Spring			Summer			Autumn		
	No. of Months	% of Tot. Rec.	% of Fit. Rec.	No. of Months	% of Tot. Rec.	% of Fit. Rec.	No. of Months	% of Tot. Rec.	% of Fit. Rec.	No. of Months	% of Tot. Rec.	% of Fit. Rec.
503W	5	28.4	32.5	3	16.6	15.2	4	22.6	20.8	6	32.4	31.5
211	5	18.1	19.1	3.5	16.4	17.6	7.5	35.5	32.5	6.5	30.1	30.7
103	14	28.0	30.5	12	24.4	24.9	12	22.5	19.2	13	25.1	25.4
46004	10	26.3	27.5	10.5	27.8	29.0	8.5	22.1	20.2	9	23.8	23.2
46005	12.5	26.3	28.1	10.5	25.1	25.6	11	26.2	23.5	9	22.5	22.8

Table 3. Joint occurrence of HSIG and TP.

Station	Winter				Spring				Summer				Autumn			
	% Occ.	Range HSIG	Range TP	% >5m >14s	% Occ.	Range HSIG	Range TP	% >5m >14s	% Occ.	Range HSIG	Range TP	% >5m >14s	% Occ.	Range HSIG	Range TP	% >5m >14s
503W	10.2	3-4	12-14	8.2	11.8	2-3	10-12	2.6	15.4	1-2	8-10	-	11.7	2-3	10-12	1.2
211	18.6	3-4	12-14	3.3	17.1	2-3	8-10	1.2	23.6	1-2	8-10	-	15.6	1-2	8-10	.96
103	14.2	2-3	12-14	1.1	13.7	1-2	8-10	0.9	19.9	1-2	6-8	0.15	11.1	1-2	10-12	.86
46004	8.6	3-4	12-14	10.2	13.4	2-3	10-12	3.9	17.2	1-2	6-8	0.1	9.8	2-3	10-12	3.2
46005	9.3	3-4	10-12	9.9	14.7	2-3	10-12	4.3	23.3	1-2	6-8	0.04	10.6	1-2	10-12	3.3

Table 4. Observed and/or predicted maximum HSI6.

Location	Type	Time Period	Observed max HSI6	Predicted Return Period(yrs) 10	50	100	Source
Queen Charlotte							
Snd. MEDS Stn.216	Buoy	Oct82-Nov84	11.4(18.5)				Juszko et al.(1985)
Stn.503	Buoy	Aug86-Jan89	11.3				This study
	Hindcast				17.7	19.8	Quayle and Fulbright(1975)
	Combined			14.2	16.1	16.9	Hodgins et al.(1985)
Hecate Str.							
MEDS Stn.215	Buoy	Oct82-Nov84	10.7(19.8)				Juszko et al.(1985)
	Visual		>20.				James(1969)
Dixon Entrance							
MEDS Stn.211	Buoy	Nov82-May84	9.0(14.9)				Juszko et al.(1985)
		Mar85-Jan89	9.2				This study
	Combined			13.4	14.5	16.1	Hodgins et al.(1985)
Tofino							
MEDS Stn.103	Buoy	Nov84-Jan89	8.7				This study
46003(51.9N,155.9W)	Combined			15.0	17.1	18.0	Hodgins et al.(1985)
46004	Buoy	Feb85-Jan89	14.1				This study
	Combined			11.8	13.3	13.9	Hodgins et al.(1985)
46005	Buoy	Jan84-Jan89	13.6				This study
Hibernia	METOC	1970-80	9.0(normal yr) 12.3 max		15-16		Neu (1982) (2)
	Buoy	1980-83	11-12				Baird (1984) (1)
	WIS Hindcast	1956-75	>15		16-18		(1)
	SOWM Hind.	1956-75			17-20		(1)
Sable Isl.	METOC	1970-80	8.7(normal yr) 11.7 max		15		(2)
	Buoy	1981-83	8-9				(1)
	WIS Hindcast	1956-75	11-12		15-16		(1)
	SOWM Hind.	1956-75			17-18		(1)
Labrador Shelf	METOC	1970-80	9.3(normal yr) 12.5		16-17		(2)
North Sea							
Northern	Buoy	1973-75	9-10		16-18		(1)
Central	Shipborne Wave recorder	1969-76	11-12		11-14		(1)
Southern	Shipborne Wave recorder	1970-79	6-7		9-11		(1)

Table 5. Percent exceedance of peak period.

Location	Time period	Peak period (sec)									Source
		>4	>6	>8	>10	>12	>14	>16	>18	>20	
Queen Charlotte Snd.											
MEDS Stn.216	Oct82-May84	100%	99.0	85.8	60.8	35.8	20.4	9.5	2.3		Juszko et al.(1985) (1)
Stn.503	Aug86-Jan89	100	98.3	89.3	70.0	42.3	19.8	8.6	1.9	0.2	This study
Hecate Strait											
MEDS Stn.215	Oct82-Nov84	99.8	93.1	80.8	61.4	40.0	27.0	12.1	2.5		(1)
Dixon Entrance											
MEDS Stn.211	Nov82-May84	99.8	96.5	82.7	51.3	26.7	14.8	6.0	1.9		(1)
	Mar85-Jan89	99.9	95.0	78.0	45.8	31.5	7.0	7.0	1.3		This study
Tofino											
MEDS Stn.103	Nov84-Jan89	99.9	97.4	85.1	66.0	43.1	19.9	7.0	1.5	0.4	This study
46004	Feb85-Jan88	99.99	96.4	82.3	65.7	35.9	18.0	6.2	0.9	0.9	This study
46005	Jan84-Jan89	99.9	96.5	80.5	64.0	38.8	23.2	9.2	1.7	1.7	This study
Hibernia	1980-83	99	98	85	50	21	5	1			Baird (1984) (2) (estimated from plots)
Sable Island	1981-83	99	90	63	22	7	3	1			(2)
North Sea											
Northern	1973-75	100	97	75	22	3					(2)
Central	1969-76	100	98	81	32	7	<1				(2)
Southern	1970-79	95	55	6	<1						(2)

Table 6. Seasonal percent occurrence of scanned spectral types.

Stn.		No. of Obs.	Type Category 11	12	13	21	22	23	31	32	33	41	42	43	51	52	53
503	W	1100	0.5	1.3	0.4	4.0	10.2	2.0	1.6	2.6	0.2	7.2	15.8	4.2	17.7	29.0	3.5
	S	642	0.0	0.9	0.0	8.6	6.1	0.5	12.2	3.6	0.0	6.2	9.2	0.5	36.6	15.3	0.5
	S	874	0.6	0.1	0.0	6.1	0.8	0.0	28.0	1.7	0.0	7.3	0.3	0.0	52.8	2.3	0.0
	A	1252	0.6	0.6	0.0	8.2	6.7	0.8	12.2	4.5	0.0	5.7	8.0	0.2	37.5	14.6	0.4
	ALL	3868	0.5	0.7	0.1	6.6	6.3	0.9	12.8	3.2	0.1	6.6	8.7	1.3	35.2	16.0	1.2
211	W	973	0.2	4.5	1.6	9.3	28.2	2.4	3.4	4.9	0.0	11.2	9.7	0.6	16.4	7.5	0.1
	S	884	0.1	1.2	0.5	12.9	17.2	1.0	19.1	8.6	0.0	4.6	2.2	0.0	27.7	4.9	0.0
	S	1909	0.2	0.0	0.0	4.6	0.4	0.0	29.6	0.4	0.0	7.5	0.0	0.0	56.9	0.3	0.0
	A	1619	0.2	0.8	0.6	11.9	13.3	0.9	22.2	4.8	0.0	3.3	1.5	0.0	36.8	3.5	0.0
	ALL	5385	0.2	1.3	0.6	9.0	12.1	0.9	20.9	3.9	0.0	6.4	2.6	0.1	38.8	3.3	0.02
103	W	3392	3.3	5.9	0.4	15.9	9.1	0.9	3.0	1.5	0.0	18.5	8.1	0.3	23.5	9.4	0.2
	S	2955	2.3	3.1	0.2	15.0	5.6	0.2	7.7	1.3	0.0	12.7	4.7	0.1	43.6	3.7	0.0
	S	2726	0.4	0.1	0.1	6.6	0.7	0.0	10.2	0.2	0.0	15.7	0.1	0.0	65.9	0.2	0.0
	A	3044	2.3	1.9	0.3	15.9	5.2	0.1	7.6	1.8	0.0	14.5	3.5	0.3	43.0	3.5	0.1
	ALL	12117	2.2	2.9	0.3	13.6	5.4	0.3	6.9	1.2	0.0	15.4	4.3	0.2	42.8	4.5	0.1
46004	W	2315	1.1	11.7	5.4	6.5	32.1	5.4	2.3	4.7	0.1	4.5	6.7	0.3	10.0	8.9	0.2
	S	2451	0.6	8.2	1.8	11.4	22.6	1.6	14.4	4.9	0.0	2.9	3.3	0.04	21.6	6.6	0.04
	S	1949	0.5	0.6	0.1	9.0	5.9	0.1	21.8	2.0	0.0	6.0	0.3	0.0	51.9	2.0	0.0
	A	2093	1.3	4.3	2.3	10.1	21.9	2.0	13.6	5.0	0.0	3.2	3.0	0.1	27.5	5.8	0.0
	ALL	8808	0.9	6.5	2.5	9.3	21.2	2.3	12.7	4.2	0.02	4.1	3.4	0.1	26.7	6.0	0.07
46005	W	2787	2.5	15.8	4.8	5.7	28.7	2.7	3.1	5.4	0.0	7.1	5.1	0.3	11.0	7.6	0.1
	S	2658	1.7	8.7	2.3	15.2	19.2	0.8	11.9	4.4	0.0	4.4	2.8	0.04	24.7	4.0	0.0
	S	2779	0.5	0.6	0.04	7.2	3.0	0.1	21.3	1.2	0.0	6.9	0.1	0.04	58.3	0.7	0.0
	A	2384	2.1	7.1	1.7	15.0	12.5	1.0	14.7	3.1	0.0	6.3	2.4	0.0	30.9	3.2	0.0
	ALL	10608	1.7	8.1	2.2	10.5	15.0	1.2	12.7	3.5	0.0	6.2	2.6	0.1	31.3	3.9	0.03

In order to obtain an idea of the inter-annual variability of the wave climate during the period 1984 to Jan 1989, a comparison can be made against extreme conditions previously reported as well as probability predictions of wave extremes. It is also interesting to examine extremes from other geographic areas as a "severity" reference. This information is included in Table 4 which is a reproduction of Table 8.6 of Juszko et al. (1985) with the addition of extremal predictions made by Hodgins et al. (1985) and extremes observed in this study. A combined data type represents data from various sources (e.g. buoy, hindcast) used for extremal predictions. The wave heights in parentheses are the actual measured maximum individual wave heights (HMAX) from the surface displacement time series corresponding to the listed HSIG. The mean ratio (calculated for selected storms during the period 1982-84) of HMAX to HSIG were estimated at 1.6, 1.64 and 1.83 for Queen Charlotte Snd, Langara and Hecate Strait, respectively. The single most extreme observation was 20m HSIG (30m maximum individual wave) in Hecate Strait and reported by James (1969). Though a visual estimate may be less reliable than buoy measurements, large wave conditions may occur in Hecate Strait, possibly supporting the larger HMAX/HSIG ratio, due to the presence of sometimes strong currents travelling in a direction opposite to the waves. The maximums observed in this study were approximately equal to those observed between 1982 and 84. The maximum 14.1m HSIG observed at NDBO Stn. 46004 exceeded the predicted 100 year wave by Hodgins et al. (1985) which was based on only seven years of data. Table 5 contains information on peak period exceedances. This table is a reproduction of Table 8.7 of Juszko et al.(1985) with the addition of results from this study. The conditions appear to be similar between 1982-84 and 84-89 given consideration of gaps in temporal coverage. The West Coast shows more severe long period wave conditions than Hibernia, Sable Island or the North Sea.

The calculated spectral statistics were also summarized as a function of spectral Type 1 class (as discussed in Section 3.1). Table 6 details the percent occurrence of each class as a function of location and season, and the associated summary statistics are included in Appendix 1. At the three inshore stations, low energy, multiple peak spectra (class 51) tend to dominate on an annual and, with the exception of 211, seasonal basis. The offshore stations and Stn. 211 show a greater occurrence of class 22 spectra during the winter, if one considers classes 11, 12 and 21 to represent swell dominant spectra, then the five stations, in similar order as Table 5 , experience a pure swell 7.8, 10.5, 18.7, 16.7 and 20.3 percent of the time. The total percentage of mixed sea and swell, classes 41, 42, and 52, occurrences are 31.3, 12.3, 24.2, 13.5 and 12.7%. Classes 43, 51 and 53, which represent 37.7, 38.9, 43.1, 26.9 and 31.4% of the

records from each station, are also indicative of multiple peak conditions however it is not clear whether they are mixed sea and swell or multiple sea peaks, particularly for low energy class 51. The large percentage of swell and multiple peak spectra does support a requirement for proper swell modelling and the inclusion, in some form, of swell in a parametric representation.

When examining the statistical tables in Appendix 1. It should be noted that for multiple peak situations, as mentioned in Section 3.1 , that TP does not necessarily agree with the class definition which is determined by the peak explaining the majority of the variance. Because of the grouping, statistics on HSIG and period have to be interpreted in light of the bounds set. The trends in the period statistics (APER, AAP, ACP) follow the grouping criteria for single peaks (i.e. APER 11>21>31) and show an increase with energy within a period grouping(i.e. APER 11<12<13). They generally have lower values (at equivalent energy levels) for groups 51, 52, and 53 than 41, 42 and 43. There is a tendency for the data, particularly at Stns. 211, 46004 and 46005, to show a slight increase in QP (for single peaks) and a decrease in SPW with decreasing TP group (i.e. QP 12<22<32). There were lower QP values for spectra scanned as multiple peaks. QP tended to increase within a period grouping with energy, but the behavior was not consistent.

4. PARAMETERIZATION OF THE HEAVE SPECTRA

This chapter will detail the procedure used to fit a parametric model to the recorded data spectra, it will provide as assessment of the goodness-of-fit of the model, and describe the summary distribution and behavior of the model parameters.

4.1 Methodology

The parameterization of energy density spectra serves two purposes. First, it allows for the representation of a spectrum using a limited number of stored or predicted variables. The model equation may have any form, though one based on theory can provide insight into geophysical processes. Second, the parameters can be related to each other or to environmental measurements (e.g. wind speed, fetch, "wave age") to allow for predictive modelling of the wave climate. The parametric models proposed in the literature have been developed to represent wind wave (i.e. "sea") and can be grouped into three classes based on the formulation for the high frequency "tail", or equilibrium range, described by ω**(-m): 1) m=5 e.g. Pierson-Moskowitz, Bretschneider and JONSWAP spectra (see Pierson and Moskowitz, 1984; Bretschneider, 1959; Hasselmann, et al. 1973); 2) m=4 e.g. Donelan and Toba spectra (see Donelan et al., 1985; Battjes et al., 1987); and 3) m = variable e.g. Wallops and Ochi and Hubble spectra (see Huang et

al., 1981; Ochi and Hubble, 1976). The choice of m=5 was based on theoretical work by Phillips (1958). An m=4 relationship is supported by Toba (1972,1973)0 Kitaigorodskii (1983), Phillips (1985)(after a revised analysis of his results), and through empirical evidence. Both Ochi and Hubble (1976) and Huang et al, (1981) base their formulation on an m=5 equilibrium range. Through statistical arguments, they relax the fixed -5 power law to allow for a variable m value. Ochi and Hubble (1976) add two sets of spectral formulations in order to represent a separate sea and swell. Though developed independently, it can be shown that the deep water Wallops spectrum and Ochi and Hubble spectrum (hereafter referred to as OH spectrum) are equivalent under certain assumptions. As the above mentioned models were all developed to account for the growth of sea waves, none of the parameterizations strictly apply when modelling swell. The extension in the OH formula to account for swell would provide an appropriate functional form as it addresses the three primary features which need to be modelled: 1) the peak frequency; 2) the variance in the peak; and 3) the peak shape. Prior application of this model to wave data collected on the East coast showed that it was capable of properly reproducing the majority of wave spectra encountered. Given the large percentage of occurrences of multiple peak spectra indicated in the previous section, a model that cannot handle more than one spectral peak would not be useful in representing the day-to-day wave climate.

The OH spectrum is given as:

$$S(\omega) = \frac{1}{4} \sum_{i=1}^{2} \frac{\left(\frac{4\lambda_i + 1}{4}\ \omega m_i^4\right)^{\lambda_i}\ \delta_i^2\ e^{-\frac{(4\lambda_i+1)}{4}\left(\frac{\omega m_i}{\omega}\right)^4}}{\Gamma(\lambda_i)\omega^{4\lambda_i+1}}$$

where ωm is the modal or peak frequency, δ the significant wave height or variance parameter and λ a spectral shape parameter. This model was fit to the data spectrum by means of a non-linear, iterative, least-squares technique which calculates a fit residual following slight modification of the parameter values. This modification is determined through a combined Newton and steepest descent method (i.e. Levenberg-Marquardt method), requiring a first guess to the parameters and the first derivatives of the function to be fit. The first guesses for $\omega m1$ and $\omega m2$ were taken as the associated frequency of the two major scanned peaks in the data spectrum, if only one peak was scanned, then $\omega m2$ was set to $\omega m1+.314$. The variance associated with frequencies below and above $0.5*(\omega m1 + \omega m2)$ was determined and the corresponding significant wave heights calculated which were then used

as the first guess for δ1 and 2. The first guesses for the shape parameters were taken as 2.5 and 1.0, respectively. The fit residual was calculated as:

$$\sum_{i=1}^{N} [E(\omega_i) - S(\omega_i)]^2 WT_i^2$$

where E(ωi) is the data spectrum, S(ωi) the model spectrum, the sum is performed over all frequencies N and frequency weighting (WTi) can be applied if the input spectrum contained variable band-averaging or if one would like to force the model fit to emphasize certain frequency regions. With the exception of Stn. 503W data, no weighting (or, equivalently, a weighting of 1) was required. The frequency weighting for Stn. 503W data was given by:

$$WTi = \frac{\text{NO. OF BANDS AVERAGED AT FREQ. i}}{\text{TOTAL NO. OF AVAILABLE FREQ. BANDS}}$$

and reflects the degree of confidence one would have in the given spectral density estimate.

During the fit iterations, limits on the parameters were set to ensure convergence. These limits were:

$0 < \delta 1, \delta 2, \lambda 1, \lambda 2 < 20$
$\omega m1 < \omega m2$
$0.25 < \omega m1 \qquad \omega m2 < 1.9$

The fit was terminated after 100 iterations, if 10 iterations in a row resulted in a relative change in the fit residual of less than 2E-5, or if 15 iterations in a row resulted in an increase in the fit residual. An optional second processing occurred if ωm2 was greater than 1.69 rps or if ωm1 and ωm2 were approximately equal, in order to ensure that a swell peak was not missed. Further details on the fit procedure and behavior can be found in Juszko (1989,1990).

To evaluate the goodness-of-fit, a residual error statistic, RESH, was calculated as:

$$RESH = \frac{\sum_{i=1}^{N} [E(\omega_i) - S(\omega_i)]^2 WT_i^2}{\sum_{i=1}^{N} [E(\omega_i)]^2 WT_i^2}$$

This statistic allowed for an acceptance level to be set for record rejection prior to performing any statistical or predictive calculations.

The spectral typing discussed in section 3.1 works well when analyses are being performed on the data spectra; however, when examining model fit parameters, the behavior of the fit should also be addressed. The fit procedure provides values for the six parameters which reduces the residual error to a minimum. The six parameters were designed to model two separate peaks or one broad peak and this proved particularly useful in examining storm development when both sea and swell were present. However, in cases of single peaks, the variance may be split between the two sets of parameters, or the first set will describe the majority of the variance while the second set handles the high-frequency "tail". In order to help in derivation of predictive relationships, the spectra were further classified according to the amount of variance explained by each set of parameters and the frequency separation between $\omega m1$ and $\omega m2$. Twelve Type 2 categories were established with number codes set to:

	A	B	C	D
O< HSIG ⩽3m	1	2	3	4
3< HSIG <6m	5	6	7	8
HSIG ⩾6m	9	10	11	12

Column A represents records which were scanned as having one peak and which satisfied the following criteria:

- One set of three fit parameters (usually the lower in frequency) accounted for more than 80% of the total variance and the modal frequencies were separated by $\omega m2 > 1.78*\omega m1$ (established through observation of numerous spectra); or

- One set of three fit parameters explained more than 90% of the total variance and the modal frequencies were separated by less than twice the frequency resolution.

These criteria were selected as observations of fit behavior for distinct single peak spectra indicated that the two modal frequencies were either almost identical or widely separate with one set of parameters explaining little variance. Column B also represents records which were scanned as one peak with the modal frequency separation lying between the limits set for column A and with similar variance ratios. Column C are records that were scanned as two (or more peaks) and fitted as two peaks as indicated by both the frequency separation ($\omega m2 > 1.78*\omega m1$) and the variance ratio of both sets of parameters being less than 80%. The frequency separation and variance criteria were relaxed for certain combinations of HSIG and TP in order to include spectra with minor swell/sea peaks. Column D includes all spectra for which no clear single peak or separate sea/swell designation can be made.

4.2 Fit Assessment

The behavior of the model fit was similar to that observed by Juszko (1989). Examples of the fit can be seen as the short dashed line in Figs. 3 and 4 for Stns. 46005 and 103, respectively. The long dashed line in Fig. 4 is the smoothed data spectrum to which the fit for 103 data was performed. The model reproduces single peaks with very low residuals and slightly higher residuals for multiple peak cases. The overall percent occurrence of RESH, for each station, is shown in Figs. 10 A to F . The seasonal distributions are included by station in Appendix 2. The distribution varies between buoy types and season due to the relative smoothness of the input spectra and the dominance of low energy or multiple peak spectra, more prevalent at inshore stations and during the summer for any given location. Hence, the lowest residuals were observed for fits to the NDBO stations and Stn. 211 (largest number of degrees of freedom associated with the spectrum) and the highest for Stn. 503W and 103 due to the large number of multiple peak spectra. The highest residuals for any given station occur during the summer. An acceptance threshold of 5% was established for all stations, except 503W. for later analyses. A threshold of 10% was used for the 503W data as it generally showed higher average RESH values. This resulted in the acceptance of the fit for over 90% of all records.

4.3 Summary Statistics on Fit Parameters

Summary statistics on the fit parameters were calculated as a function of season, spectral Type 1 and Type 2 (as discussed in Sections 3.1 and 4.1) and are included as tables in Appendix 1. Certain fit records were excluded from the summary statistics if one or more of the six parameters was considered an outlier. These include records with $\lambda 1$ or $\lambda 2$ (at times referred to as SH1 and SH2) greater than 7.0 or less than 0.1, and $\delta 1$ or $\delta 2$ (also referred to as HS1 and HS2) greater than 1.2*HSIG. The latter condition can occur occasionally as the best functional fit may require a large variance parameter value while the frequency summation used in the calculation of HSIG is bounded. Even with these restrictions, there was considerable scatter seen in the parameters. The seasonal summaries average over many spectral shapes and fit behavior types which will influence the mean and distribution statistics. The behavior of the two modal frequencies and variance parameters reflect the seasonal behavior of HSIG and TP. There is also a tendency for SH1 to be smallest in the winter and largest in the summer and the reverse seen for SH2. The seasonal "mean" spectra can be produced using the six mean parameters values. These are shown in Fig 11 . The averaging results in spectra of similar shape though varying in overall energy level with the season.

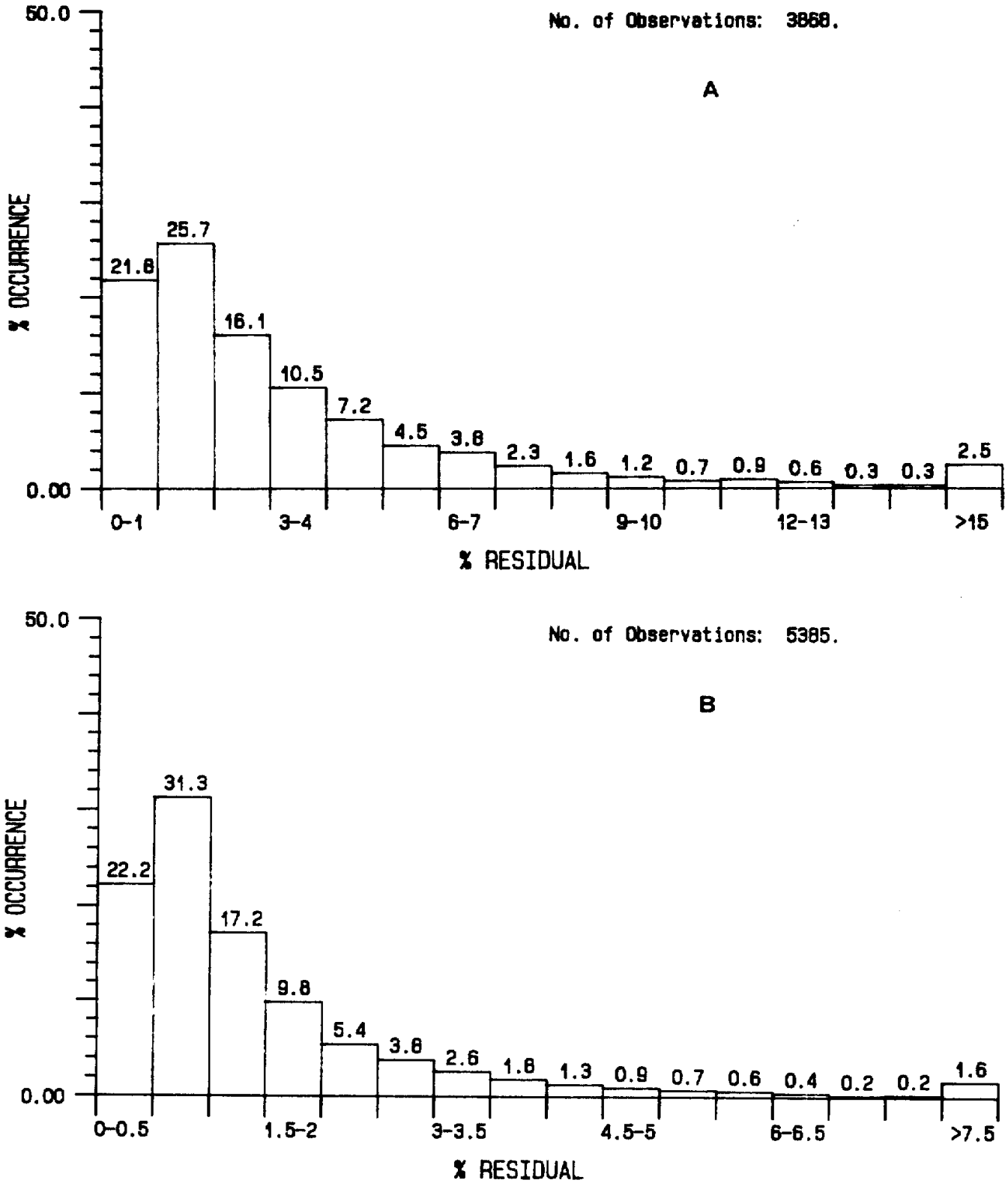

Fig. 10 Total percent occurrence of RESH value.
A) Stn. 503W; B) Stn. 211;

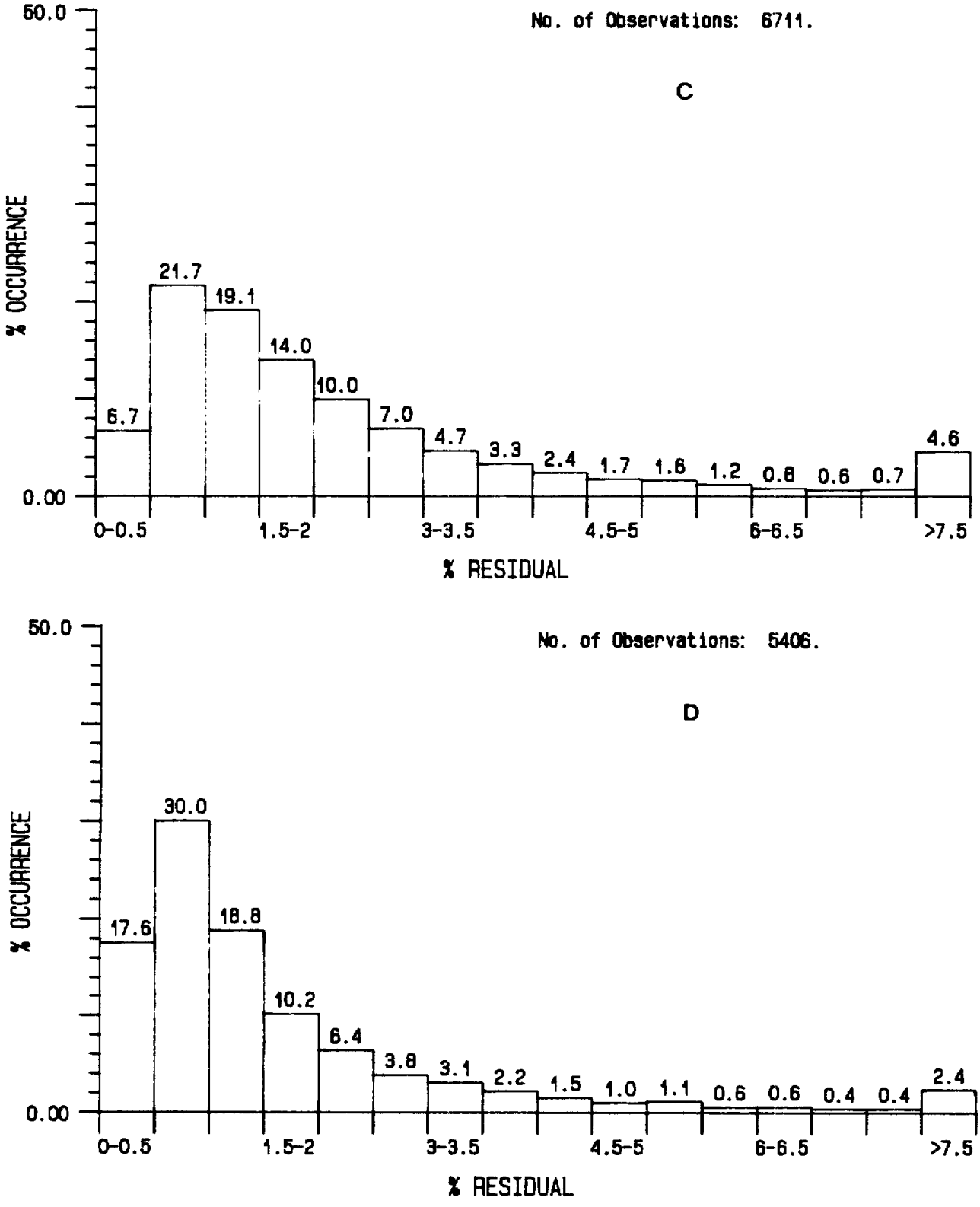

Fig. 10 Total percent occurrence of RESH value.
C) Stn. 103 before Feb. 1987; D) after Feb. 1987.

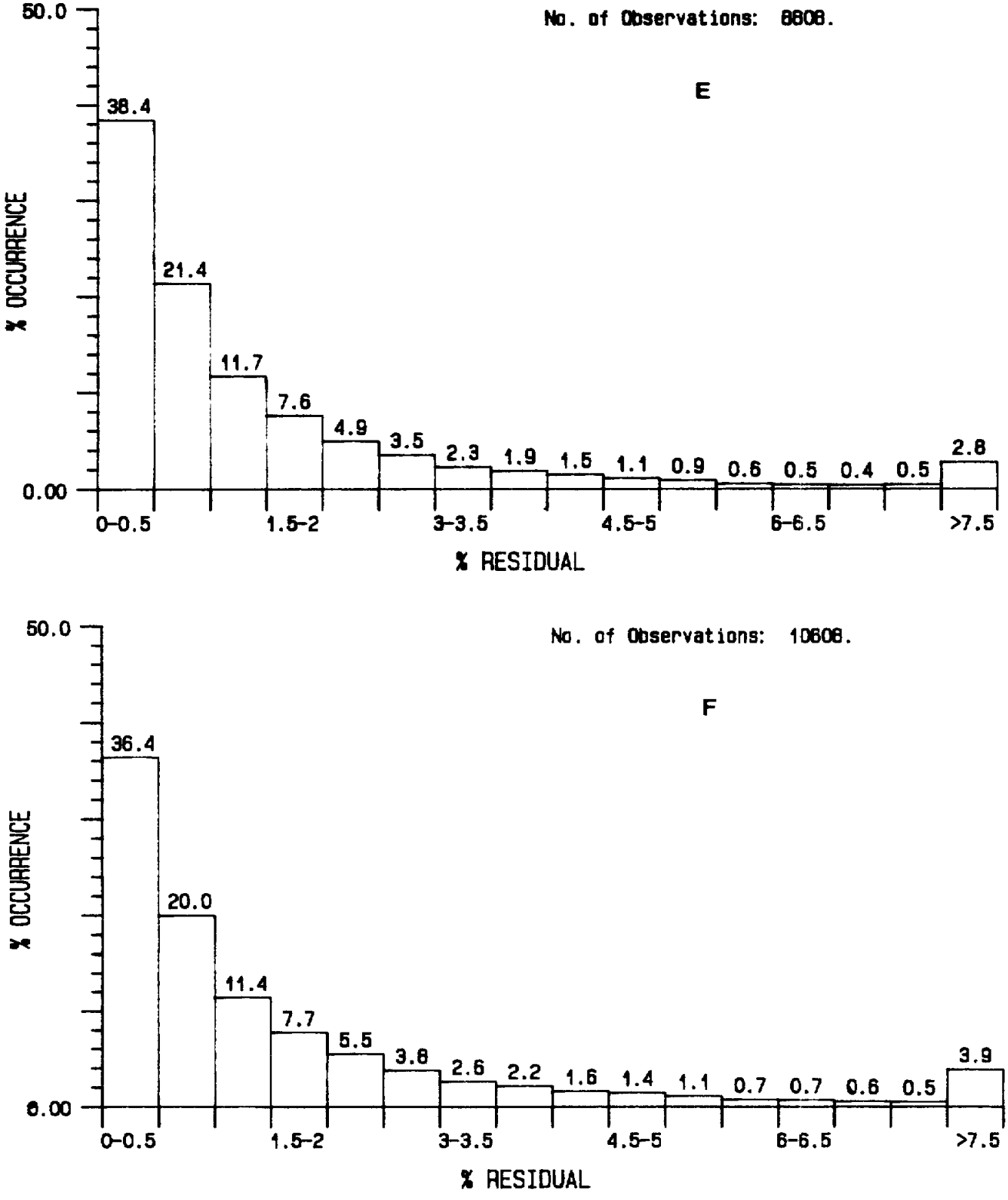

Fig. 10 Total percent occurrence of RESH value.
E) Stn. 46004; and F) Stn. 46005.

Certain trends can be seen by examining the mean behavior indicated in the summary tables of the fit parameters as a function of spectral type. The general feature of increasing TP with increasing HSIG is reflected in the behavior of ωm1, ωm2, HS1, HS2 for single peak groups. Both ωm1 and ωm2 decrease with increasing energy within a period grouping (i.e. ωm1(21) > ωm1(22) > ωm1(23)) and increase with decreasing TP in corresponding energy grouped values (i.e. ωm1(12) < ωm1(22) < ωm1(32)) behave in the opposite manner to the modal frequencies (i.e. HS1(21) < HS1(22) < HS1(23); HS1(11) > HS1(21) > HS1(31)). The same behavior is generally also true for multiple peak groups. The shape parameter, SH1, generally appears to decrease with energy, within a period grouping (i.e. SH1(21) > SH1(22) > SH1(23)) and possibly increases with decreasing period at a given energy level (i.e. similar to ωm1). The shape parameter acts to some extent like the peak enhancement parameter of a JONSWAP type spectra (as will be discussed in Section 6.2) which was used to reconcile the observed peak energy with that predicted by a Pierson-Moskowitz spectrum. As the spectra approaches a fully-developed (fetch unlimited) state, there has been some evidence (e.g. Ewing, 1980) that it more closely resembles a Pierson-Moskowitz type spectra (i.e. the peak enhancement parameter decreases approaching 1) and one may expect a decrease in SH1 with energy for a given period and lower mean values in winter than summer as mentioned above. The shape parameter, SH2, however appears to increase with energy level within a period grouping and also to increase with decreasing TP group (i.e. SH2(21) < SH2(22) < SH2(23); SH2(12) < SH2(22) < SH2(32)). This observed behavior provides some incentive to attempt to establish a predictive relationship with HSIG and TP. As with the seasonal means, the "mean" OH spectra for each spectral type class, can be generated and may be useful as "design" spectra. These are shown in Figs 12 , 13 and 14 grouped according to energy. Note that the average spectra, particularly for low energy cases, may not necessarily correspond to the spectral type from which it is derived due to the linearly averaging of parameters which form part of a complex non-linear expression.

The grouping of the spectra as a function of fit behavior was performed for the later predictive analysis. The summary statistic tables are also included in Appendix 1 for reference. The grouping, though maintaining the same energy criteria, loses its distinction in terms of peak period. The same trends with energy levels can be seen in the means. One can best compare the behavior of the parameters between groups 1, 5, and 9 (single peaks) and the double peak groups 3, 7, and 11. For single peaks, ωm1, HS1, ωm2 and SH2 are generally larger, at a given energy level, while HS2 and SH1 are smaller than their corresponding double peak group means.

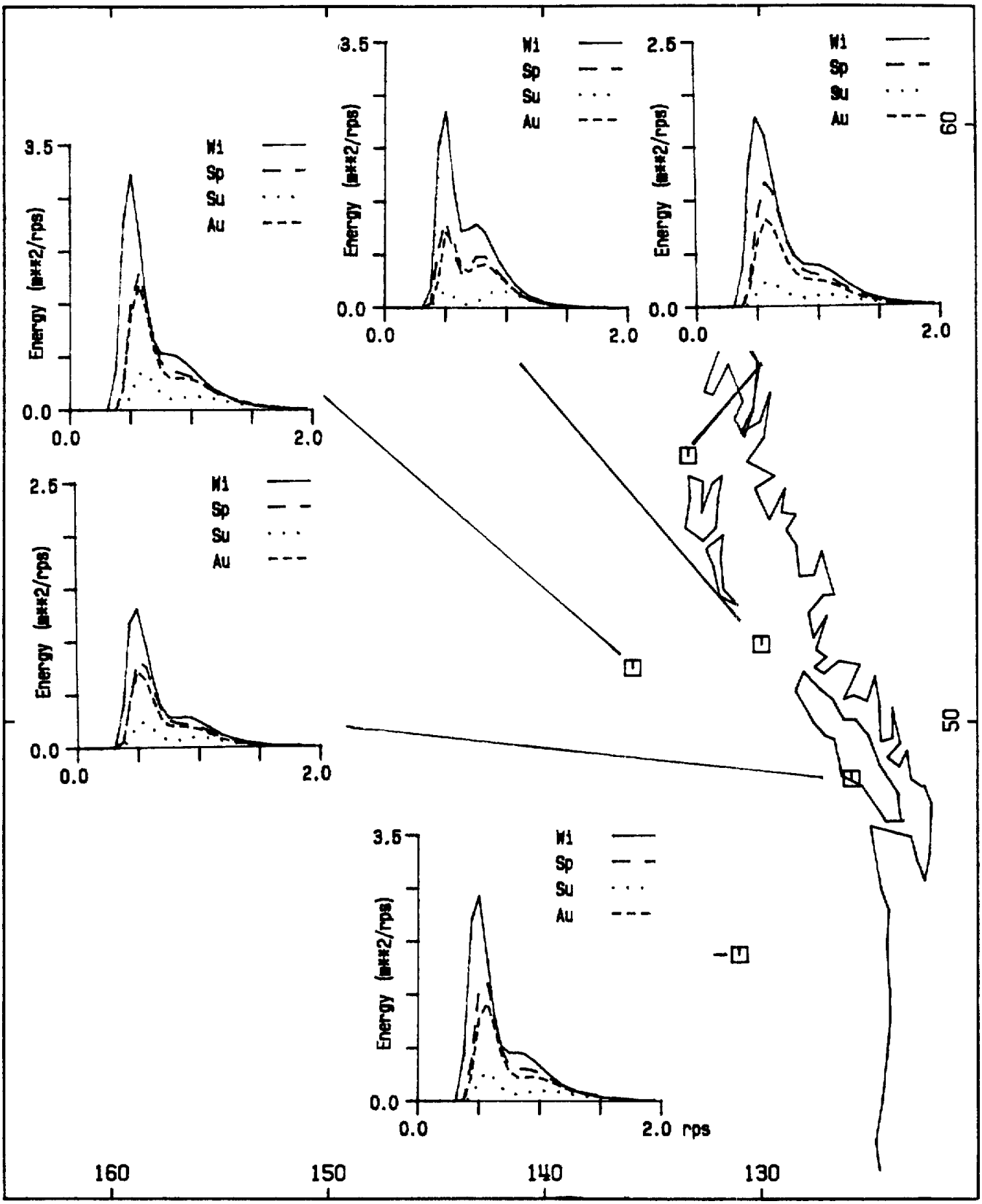

Fig. 11 Seasonal mean OH spectra.

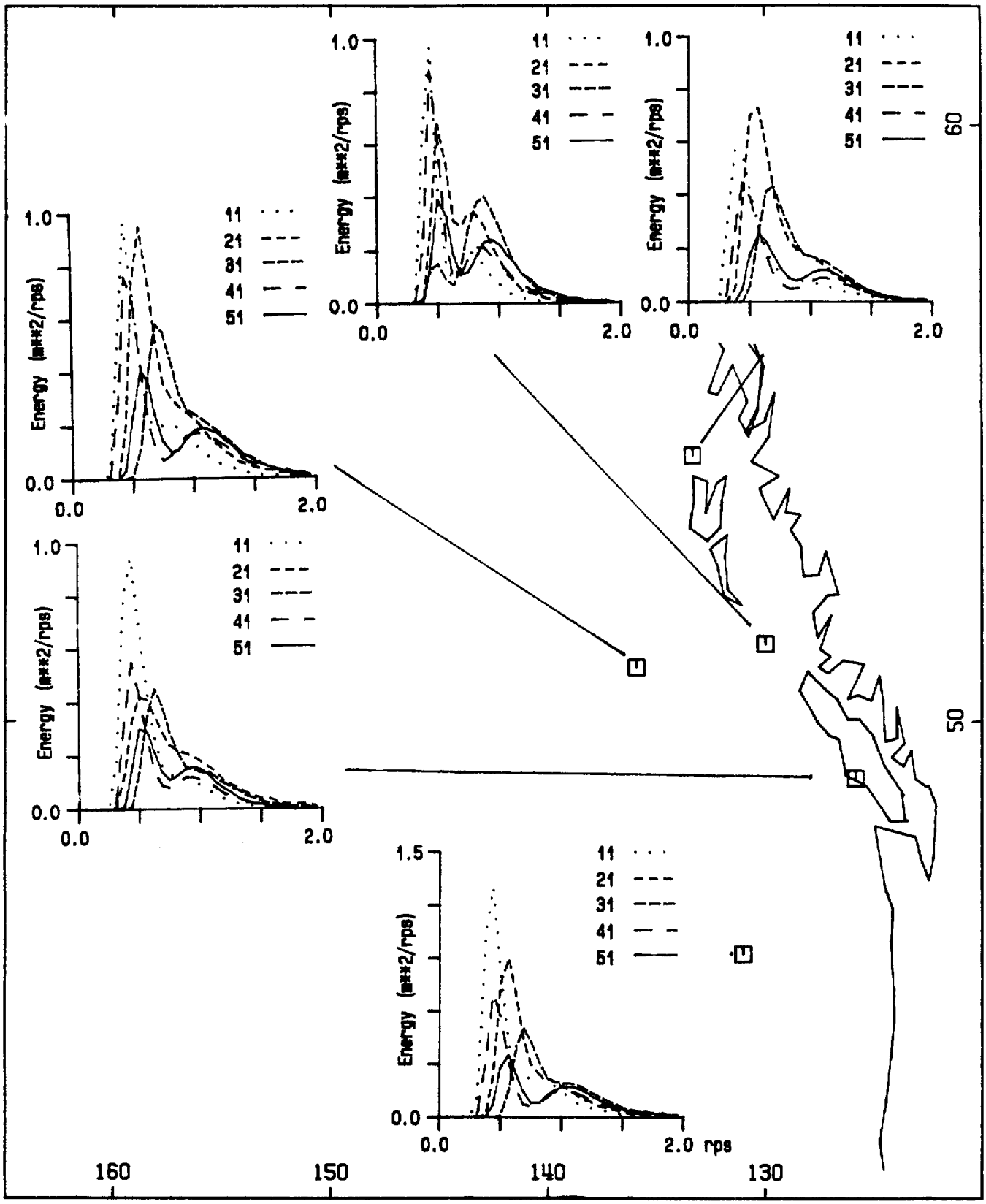

Fig. 12 Mean OH spectra for Type 1 classes: 11,21,31,41,51.

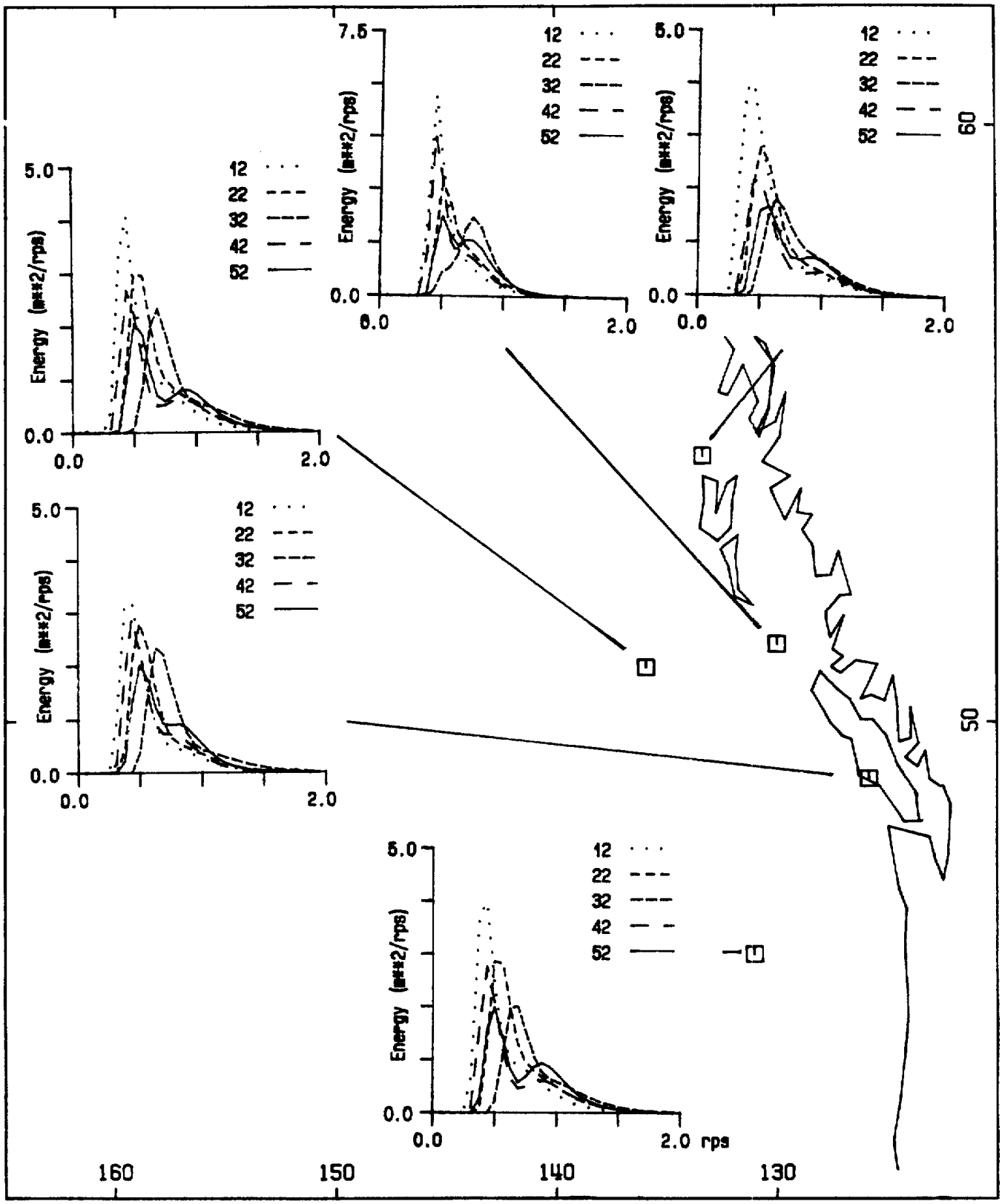

Fig. 13 Mean OH spectra for Type 1 classes: 12,22,32,42,52.

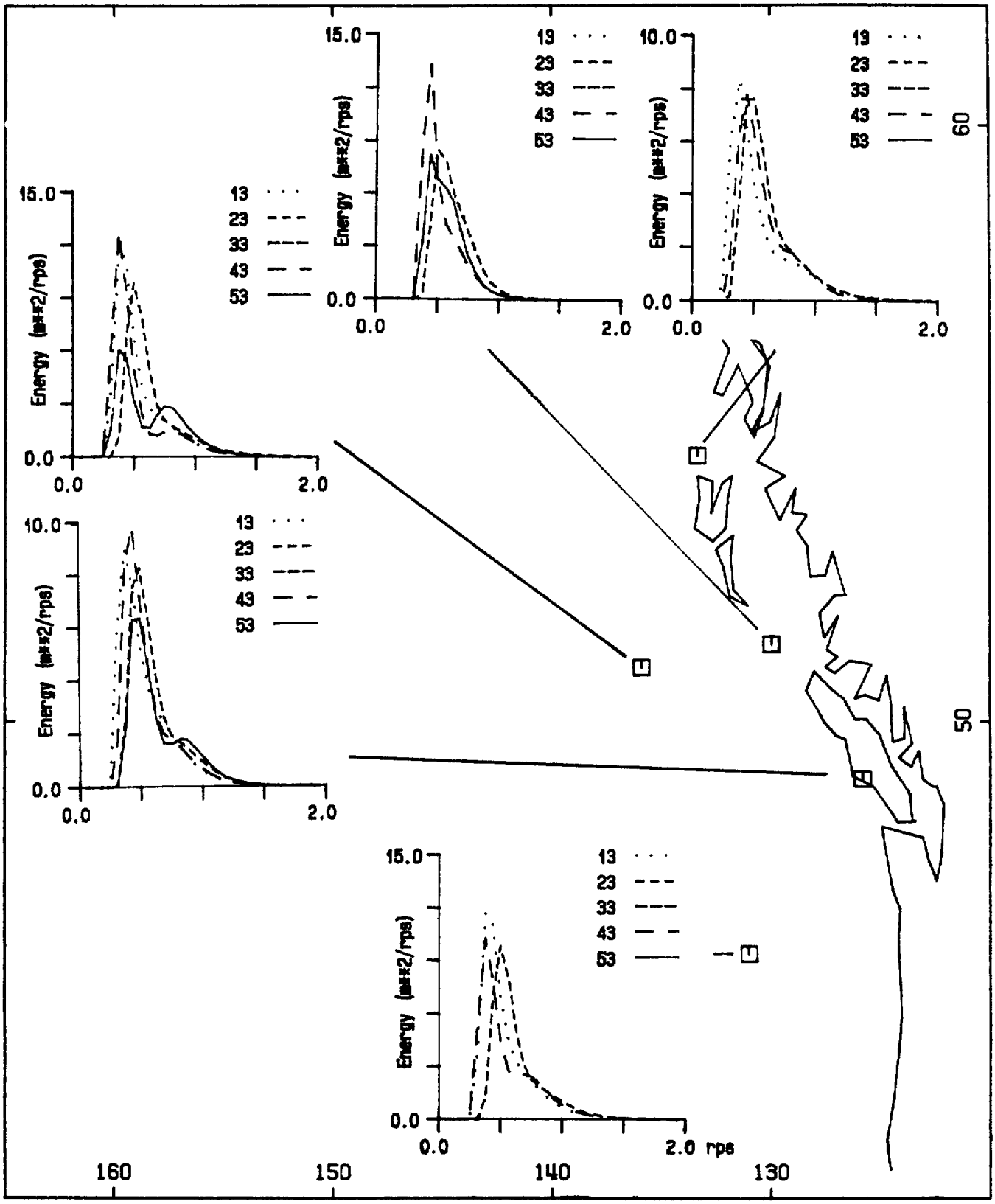

Fig. 14 Mean OH spectra for Type 1 classes: 13,23,33,43,53.

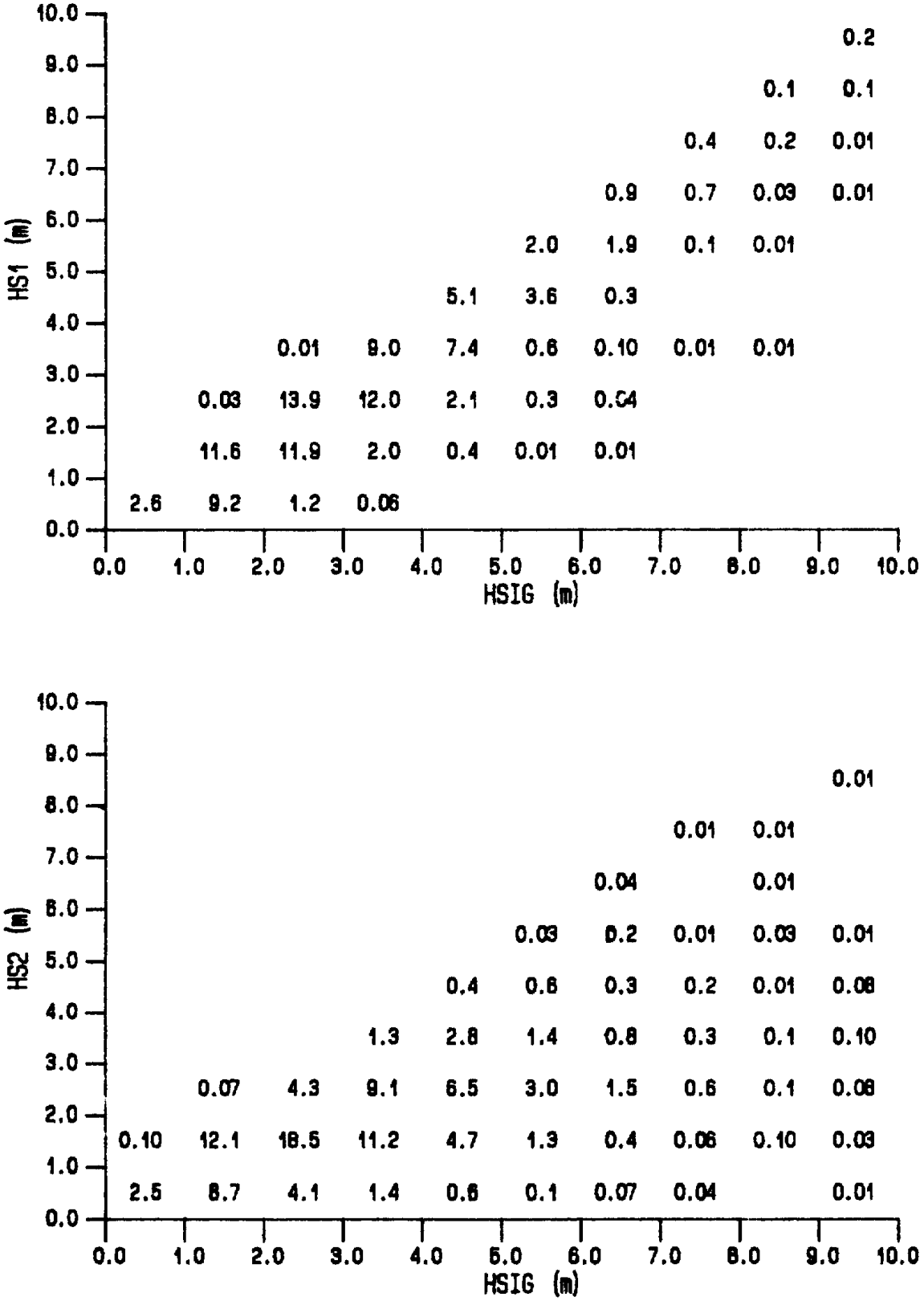

Fig. 15 Joint distribution of fit parameters for Stn. 46004.
a) HS1, HS2 and HSIG

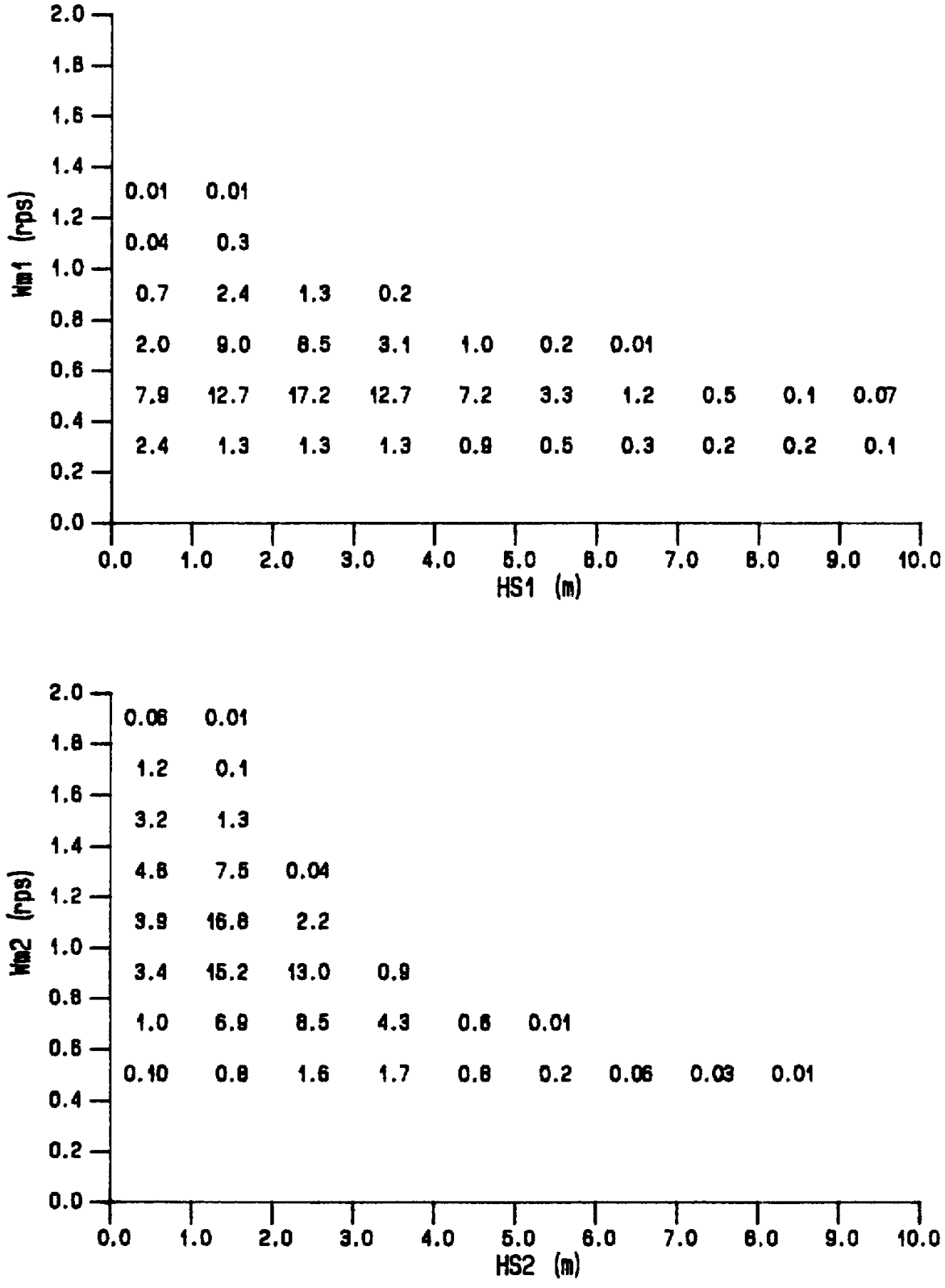

Fig. 15 Joint distribution of fit parameters for Stn. 46004.
b) Wm1 and Hs1; Wm2 and HS2

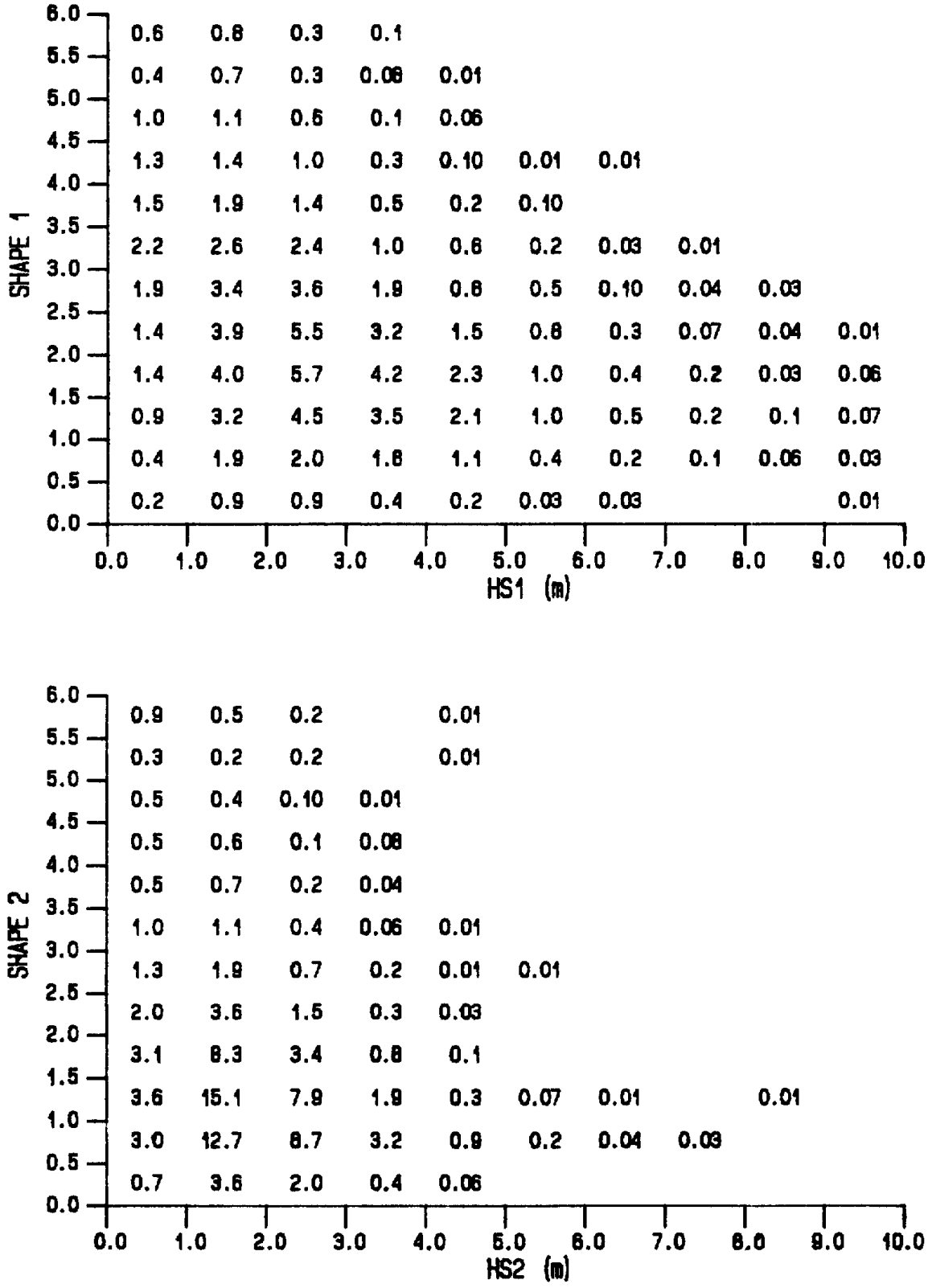

Fig. 15 Joint distribution of fit parameters for Stn. 46004.
c) SH1 and HS1; SH2 and HS2

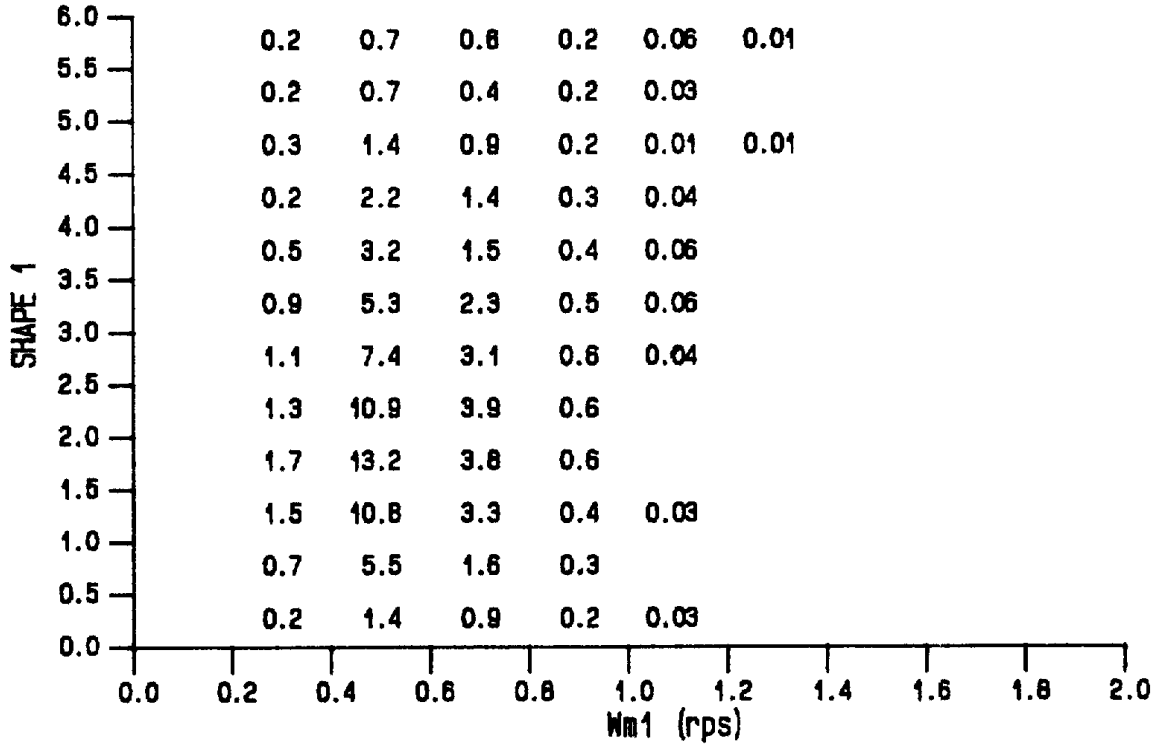

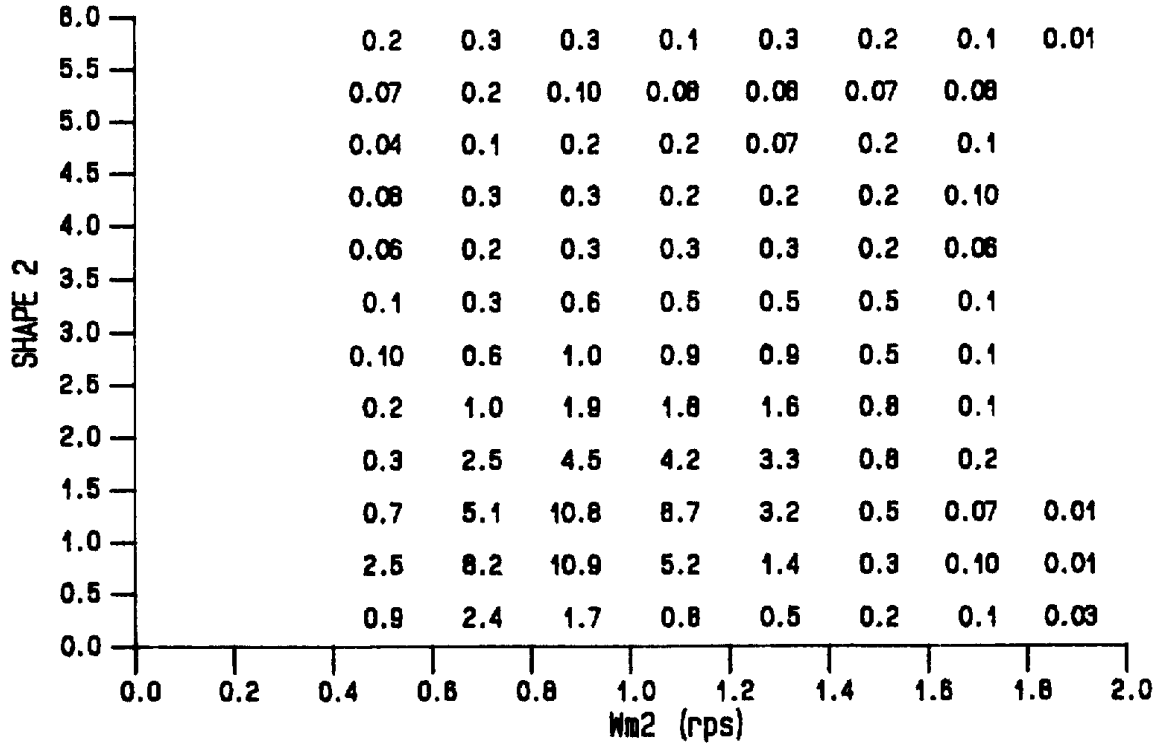

Fig. 15 Joint distribution of fit parameters for Stn. 46004.
d) SH1 and Wm1; SH2 and Wm2

Table 7. Joint occurrence of fit parameters.

	503W	211	103	46004		46005	
					all	single	double
%	20.3	22.9	26.5	13.9	16.8	21.0	26.0
HS1,HSIG	0-1,1-2	1-2,1-2	1-2,1-2	2-3,2-3	1-2,1-2	3-4,3-4	0-1,1-2
%	21.8	23.7	27.1	18.5	17.0	18.4	28.4
HS2,HSIG	1-2,1-2	0-1,1-2	0-1,1-2	1-2,2-3	1-2,2-3	0-1,2-3	1-2,1-2
%	19.6	14.0	24.7	17.2	16.1	18.2	22.7
Wm1,HS1	.4-.6,1-2	.4-.6,0-1	.4-.6,1-2	.4-.6,2-3	.4-.6,2-3	.4-.6,3-4	.4-.6,0-1
%	15.8	17.5	16.5	16.8	17.8	15.3	17.7
Wm2,HS2	.6-.8,1-2	1-1.2,1-2	.8-1.,1-2	1-1.2,1-2	.8-1.,1-2	.8-1.,1-2	.8-1.,1-2
%	4.1	7.7	8.3	5.7	5.3	10.4	7.2
SH1,HS1	2-2.5,0-1	1.5-2,1-2	1-1.5,1-2	1.5-2,2-3	1.5-2,1-2	1-1.5,3-4	1.5-2,1-2
%	9.7	12.0	11.2	15.1	14.4	14.1	27.4
SH2,HS2	1-1.5,1-2	1-1.5,1-2	1-1.5,0-1	1-1.5,1-2	1-1.5,1-2	1-1.5,1-2	.5-1.5,1-2
%	8.8	17.8	17.5	13.2	12.7	26.7	9.7
SH1,Wm1	2.5-3,.4-.6	1-1.5,.4,.6	1-1.5,.4-.6	1.5-2,.4-.6	1.5-2,.4-.6	1-1.5,.4-.6	2-2.5,.4-.6
%	9.5	9.1	9.7	10.9	10.2	9.1	9.1
SH2,Wm2	1-1.5,.6-.8	1-1.5,1-1.2	1-1.5,.8-1.	.5-1.,.8-1.	1-1.5,.8-1.	1-1.5,1-1.2	.5-1.,.8-1.

Figures 15 a to d contain examples of the percent joint occurrence of the fit parameters for Stn. 46004. Similar plots for the other stations are included in Appendix 2, in addition, for Stn. 46005 data, chosen due to completeness and lack of noise in the spectra, similar distributions are provided separately for single (class 1, 5 and 9) and double (class 3, 7 and 11) peak classes. Table 7 details the percentage and parameter range associated with the maximum joint occurrence bin. All stations show a linear relationship between HS1, HS2 and HSIG. $\omega m1$ has maximum occurrence between 0.4 and 0.6 rps for all stations. There is some indication of a decrease in $\omega m2$ with increasing HS2. There is considerable scatter in the shape parameters with SH1 (Fig. 15c) possibly decreasing with HS1 and being skewed to slightly larger values than SH2. The majority of occurrences, for both shape parameters, is between 0.5 and 3.0. Some of the scatter would result from the variability associated with different fit behavior and spectral types and inclusion of joint occurrence plots for the different Type 1 and Type 2 classes would be an inefficient means of assessing inter-relationships between the parameters. A statistical analysis will be conducted in Section 6 which will indicate any

joint behavior (i.e. to allow for possible prediction of the parameters).

5. STORM ANALYSIS

The large scale meteorology of the West Coast is controlled by the relative strength and location of two pressure systems: the Aleutian Low, centered over the Gulf of Alaska, and the North Pacific High, located West of California. There is a strong seasonal pattern with the Aleutian Low dominating in the winter, providing generally southwest to southeast winds, and generating the most severe storms, in the summer, the North Pacific High tends to prevail resulting in weaker north to northwest winds. Topographic steering of the winds occur near shore due to the coastal mountain ranges.

The low pressure systems generating storms are generally of two types. The first consists of a large scale system (order of 1000 kms.) which tends to have the lowest central pressures and to travel relatively slowly eastward along approximately 50 deg. N Latitude. This type of system generated the most severe conditions observed during this study. The second type of system results from a wave or "eddy" off of the main low circulation pattern, is of smaller scale (approx. 500 kms) with slightly higher central pressures and travels rapidly. These small scale systems tend to form locally in the Gulf of Alaska and are able to generate severe sea states if they become "stalled" or travel at a speed (at the approximate group velocity of low frequency surface gravity waves) which allows for continuous re-enforcement of the sea state. The associated winds, of both centers, often intensify as the centers travel East due to deepening of the central pressure possibly gaining heat from the ocean or due to constriction of the isobars under the influence of the coastal mountains. Fig. 16 is a reproduction of the METOC chart for 0600 GMT on December 8, 1987 illustrating both types of pressure systems.

Fifteen storms were selected through examination of the time series of significant wave height and peak period from each station. As geographic representation was desired, the storms with the three largest HSIG values measured at each station were chosen. There was some overlap in storm selection as extreme conditions at different stations may have been produced by the same storm system. Also included were storms in November 1984 which generated considerable damage, September 1986 which was the only storm occurrence when all five stations were operating, and June 1988 which represented a summer storm. Maps of the storm tracks (taken off of METOC charts supplied by AES) and selected energy density spectra are included in Appendix 3 and the reader should refer to these in the following discussion.

Characteristics of the selected storms are summarized in Tables 8 and 9 . Table 8 indicates the storm time period examined, the

minimum central pressure recorded and its position, and the significant wave height, peak period and time of the maximum HSIG record observed for each recording site. Table 9 includes estimates, when possible, of the rate of spectral growth (positive) and decay (negative) obtained through a calculation of the hourly rate of change in significant wave height (dHS/dT) and peak period (dTP/dT), swell properties (estimate of height and period from the model parameters fit to the spectra) when observed, response lag between inshore and offshore stations (positive if given station storm peak lags that observed at stations 46004 or 46005) and the duration of conditions with HSIG > 5m and HSIG > 10m. The growth and decay rates, which provide some idea on the growth response and relaxation time of the seas, should not be considered as absolute rates as there may be contamination by the presence of swell and incomplete relaxation of the seas between build-up periods. They are also representing linear time averages of a property which varies non-linearly with sea state (e.g. rate of peak progression down frequency decreases with frequency). Multiple entries in Table 9 reflect, on occasion, multiple build-up or decay periods due to numerous low pressure centers influencing the region over the selected time interval.

The information in Tables 8 and 9 support some general features of the wave climate. Swell waves were often present with modal periods, as given by the six-parameter fit results, longer than 20 seconds (up to 25 seconds) observed at all locations. The most extreme conditions, in terms of both absolute HSIG and TP and in duration, were observed at the offshore stations and were associated with large scale centers having minimum pressures less than or equal to 960 mbars. During storm 11, however, wave conditions on December 5 and 8 (1987) were more severe in Queen Charlotte Sound than offshore. The surface atmospheric pressure chart for Dec, 8 was shown in Fig. 16 and consisted of both a large and small scale low pressure system with the latter possibly reinforcing existing sea conditions (HSIG 3-5m, TP 12-14s) in Queen Charlotte Snd. The maximum sea growth rate observed at 503W during this period was 1m/hr. The strength of the storm signature at inshore and offshore stations and the lag in response are dependent on the stations position relative to the storm track, in general, Stns, 46004 and 503W and Stns. 46005 and 103 behave in tandem with the inshore station lagging the offshore one and 46004 leading 46005 if the storm track passes from West to East over Queen Charlotte islands.

If the track is to the North of these islands, Stn. 103 may lead 46005 due to its more northerly position while Stn. 211 leads all other stations (e.g. storm 6). The ratio of maximum HSIG between stations, for the limited number of selected storms, ranged from 0.6 (storm 7) to 1.6 (storm 11) for 503W compared to 46004 with a mean of 1.06, from

0.4 (storm 5) to 0.9 (storm 9) for 103 compared to 46005 with a mean of 0.72 and from 0.58 to 1.0 for 211 compared to 46004 with a mean also of 0.72.

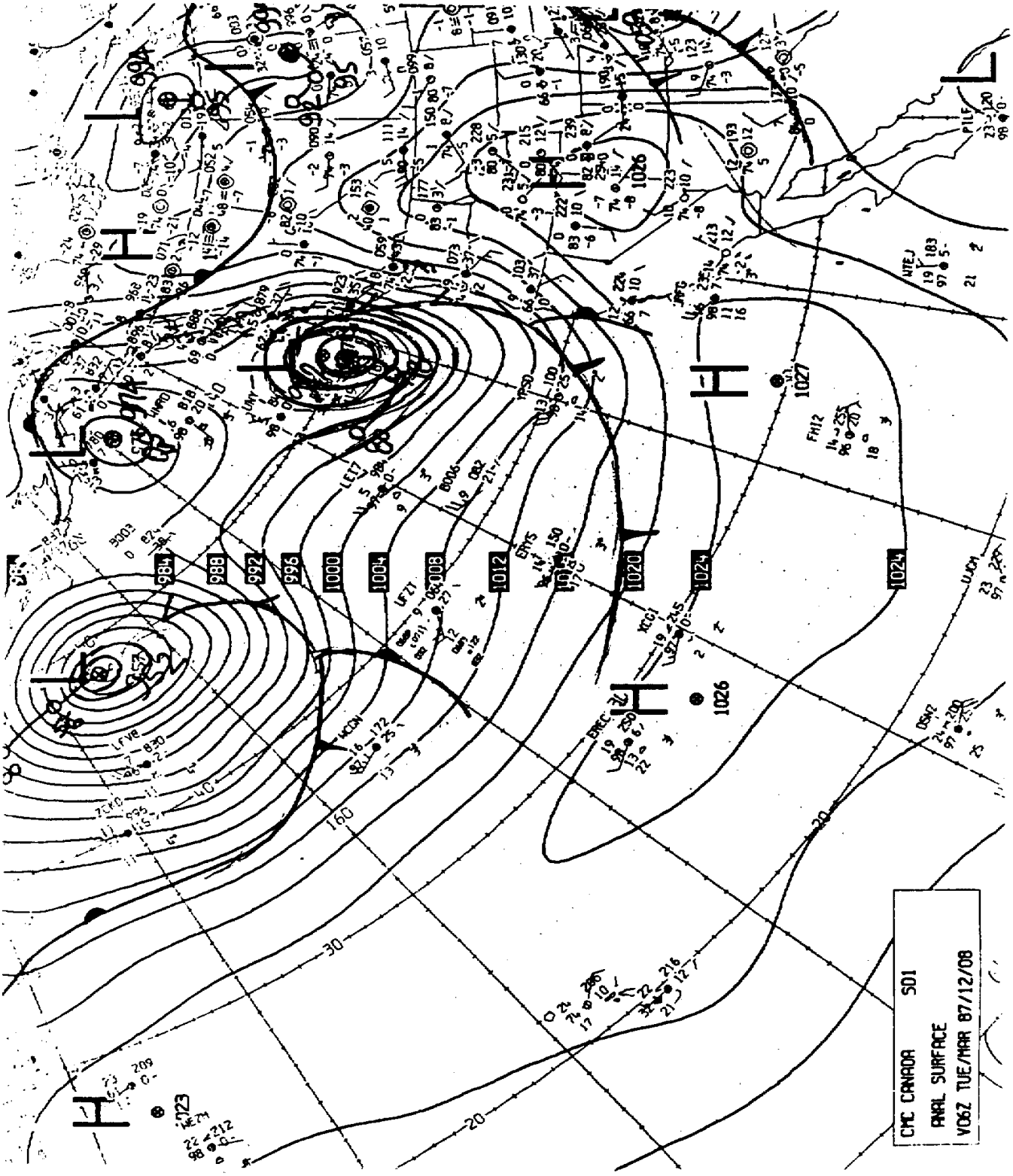

Fig. 16 Reproduction of surface analysis METOC chart for 87/12/08/0600Z (supplied by AES).

Table 8. Storm summary information I.

No.	Date	Min. Pres.	Location Lat. N	Long. W	Wave Information 46005 HS	TP	TIME D/HR	46004 HS	TP	TIME D/HR	103 HS	TP	TIME D/HR	503 HS	TP	TIME D/HR	211 HS	TP	TIME D/HR
1	84/10/12-14	958	52	133	10.7	16.7	12/18												
2	84/11/01-03	966	48	135	9.4	14.3	2/18				7.6	12.4	3/0						
	04-06	984	54.5	152	9.0	20.0	3/15				7.2	13.6	3/18						
3	84/11/26-28	976	46.5	137.5	7.9	12.5	27/0				6.9	13.6	27/12						
					7.6	12.5	28/12				4.5	11.4	28/21						
4	85/03/02-06	993	54.5	135				11.1	16.7	4/9	5.4	17.1	4/18						
5	86/04/11-12	999	42	114	10.2	14.3	12/9	8.0	12.5	11/18	4.1	15.2	12/12				4.7	13.8	12/6
	12-14	1000	46	131															
6	86/04/24-29	980	52	136	7.9	16.7	25/15	8.7	14.3	25/3	5.5	13.6	25/12				5.0	8.9	24/15
		980	54	140				6.4	12.5	27/0							6.4	13.8	27/9
										27/21									
7	86/09/21-25	978	58	137	8.4	16.7	25/3	10.0	14.3	24/6	4.4	12.4	24/9	5.9	15.1	24/14	6.7	13.8	24/6
8	86/11/16-19	958	51	136				7.7	11.1	18/18	8.5	17.1	19/0				4.5	8.9	18/6
	18-20	972	52.5	138				6.2	14.3	20/18	5.4	12.4	21/3						
	21-23	960	55	142				14.1	16.7	23/15	6.3	15.2	24/6				9.2	19.1	24/0
	23-26	963	58.5	144				8.3	14.3	25/9	6.3	13.6	26/3				6.7	13.8	25/18
	26-28	972	50	132				7.1	12.5	27/12	6.9	17.1	29/15						
9	86/12/23-24	978	54	135															
	23-27	954	51.5	156	7.3	16.7	26/9	9.4	16.7	26/9	6.6	17.1	26/21				6.9	12.1	25/9
	27-28	952	53	148.5				7.2	11.1	28/21							8.0	19.1	26/9
10	86/12/31-	944	48.5	169															
	87/1/2	972	48.5	134	9.2	12.5	3/0	8.8	16.7	2/6	8.2	10.5	3/6						
11	87/11/29-	952	51	138	13.6	20.0	1/21	9.1	12.5	2/3	8.7	17.1	2/3	7.6	12.8	1/5			
	12/02													8.8	17.1	2/2			
	12/03-07	952	49	153	7.7	12.5	5/12	9.2	14.3	5/12	6.1	12.9	6/3	10.4	11.6	5/20			
		952	50	146															
	07-10	955	49	154	8.4	11.1	8/6	6.9	12.5	7/12	7.4	11.4	8/9	11.3	13.5	8/8			
					10.4	14.3	10/3	9.1	12.5	10/9	7.6	12.9	10/12	7.8	14.2	10/17			
12	88/01/07-10	978	52	130	8.3	14.3	10/0	5.6	10.0	9/21	6.6	14.8	10/9	7.3	12.8	10/8			
	11-13	954	51.5	151	6.5	12.5	13/3	8.5	16.7	13/15				8.8	11.6	12/23			
	13-15	964	52.5	136	9.4	16.7	14/0				6.6	14.8	14/3	8.1	11.6	13/23			
					10.2	14.3	15/3				7.0	12.9	15/9	6.8	12.8	15/17			
13	88/03/03-05	972	56.5	142.5	7.7	14.3	4/21	8.6	14.3	5/3									
	04-06	978	51	134.5	9.3	16.7	5/21				8.2	14.8	6/6						
	06-08	964	54	156															
14	88/06/01-05	968	47	132	8.8	14.3	2/21	5.0	14.3	3/15	7.8	14.8	3/6						
								5.0	10.0	4/9									
15	88/12/19-21	980	51.5	134	11.6	16.7	21/3				5.2	14.8	21/6	5.5	8.7	20/20	5.0	16.0	20/0
	20-23	978	54.5	162	7.2	14.3	23/0				4.7	14.8	23/9	5.7	16.0	22/20	4.9	16.0	22/15
	23-24	1004	39	127										5.5	14.2	23/11			

Table 9. Storm summary information II.

Storm	46005						46004						103					
	dHS/dT	dTP/dT	Swell H	Swell TP	Duration HS>5	Duration >10	dHS/dT	dTP/dT	Swell H	Swell TP	Duration HS>5	Duration >10	Lag5	dHS/dT	dTP/dT	Swell H	Swell TP	Durat. HS>5	Lag5	Lag4
	(m/hr)	(s/hr)	(m)	(s)	(hr)	(hr)	(m/hr)	(s/hr)	(m)	(s)	(hr)	(hr)	(hr)	(m/hr)	(s/hr)	(m)	(s)	(hr)	(hr)	(hr)
1	0.5	1.1	2-3	12.5	45	3														
	-0.2	-0.14	2-3	11-12																
2	0.2	0.2	3-4	14	57									0.14	0.17	2-3	13-15	33	6	
														-0.11						
3	0.45	0.6	3-4	17-20	20									0.43	0.5	1	11	15	12	
	-0.2	-0.25												-0.13	-0.08	2	17			
4							0.5	0.48	1-2	14	51	15		0.43	1.05	1.5	13-14	6		9
							-0.12	-0.12						-0.07	-0.21	2	17			
5	0.3	0.25	<1	17	27	3	0.42	0.7	1-2	10-11	27		-27	0.16	0.5	1-1.5	9-11	-	3	18
	-0.3	-0.2	2	10-11												<1	17			
6	0.26	0.45	1-2	9	24		0.25	0.35			24		-12	0.20	0.42	1	9	6	-3	9
	-0.24	-0.26					-0.23	-0.22						-0.13	-0.14	2-3	13-15			
							0.24	0.42								2-3	13-14			
							-0.06	-0.06												
7	0.24	0.36	.5-1.	8	48		0.19	0.21			48	3	-21	0.14	0.40	<1	9		-18	3
	0.09	0.15					-0.12	-0.12						-0.05						
	-0.12	-0.15																		
8							0.19	0.23	2	12	21			0.32	0.57	1-2	13-15	18		9,18
							0.54	0.46			105	12				2-3	13-15			
9	-0.11	0.0	3-6	16-20	33		0.11	0.37	2	16	54		0	-0.10	-0.12	>3	17-19	18	12	12
							-0.12	-0.12												
10			3-4	16-20	81				3-6	20	66		-18			2-3	17-19	30	6	24
11	0.41	0.36	4	12-14	60	12	-0.27	-0.1	3-4	12	24,72		6	0.40	0.50	3-4	12-14	57	6	0
	-0.24	-0.19	2-3	12-14	159	3	-0.12	-0.08	3-6	20	57,33		0	-0.22	-0.11			36	15	15
	.3-.4	.4-.5											6	0.21	0.35			39	9	3
	0.3	0.2												-0.11	0.00					
	-0.16	-0.08																		
12	0.33	0.8	1-1.5	25	24		0.18	0.33	2	25	51		-3			2-2.5	21-17	57	6	
	-0.19	-0.17	2-3.5	20	90	3			2-3	20			12			2-3	11-12			
	0.34	0.35							2-3	12-14										
13	0.34	0.48	2	11	64		0.25	0.21			24		-18	0.37	0.5	2-2.5	13	18	9	27
	0.59	0.40												-0.18	-0.18	2	11			
	-0.20	-0.20																		
14	0.55	0.80	2-3	11	18						3			0.65	0.94	1-2	10-11	15	9	-9
	-0.17	-0.13	2	9-10										-0.17	-0.17					
15	0.44	0.36	2-3	16-17	33	15										<1-2	17-14	6	3	
	-0.28	-0.20			24														9	
	0.22	0.28																		
	-0.13	-0.14																		

Table 9. Storm summary information II(continued).

Storm	503W							211						
	dHS/dT	dTP/dT	Swell H	Swell TP	Durat. HS>5	Lag5	Lag4	dHS/dT	dTP/dT	Swell H	Swell TP	Durat. HS>5	Lag5	Lag4
	(m/hr)	(s/hr)	(m)	(s)	(hr)	(hr)	(hr)	(m/hr)	(s/hr)	(m)	(s)	(hr)	(hr)	(hr)
5								0.09	0.27	<1	11-12		-3	18
								-0.09	0.00	1-2	12			
6								0.33	0.47	<1	25	3	-24	-12
								0.23	0.46	1-2	8-10	12		
								-0.10	-0.08					
7	0.15	0.26			24	-13	8	0.20	0.23			24	-21	0
	-0.07	-0.08												
8								0.27	0.45	2	10-11	30		9
								-0.23	-0.33	2-3	12-14	27		
								-0.06	-0.05					
9								-0.14	-0.06		18.5	63	0	0
11	0.54	0.35	2-3	11-13	57	5	-1							
	0.46				48	8	8							
	-0.11	-0.07			84	3	-1							
						14	8							
12	-0.19	-0.08	1-1.5	21	18	8	11							
	0.5	0.59	2-2.5	18	51	14								
15	0.15	0.33	2	15-16	15	-7				4-5	16		-27	
						-4				2-3	13-14		-9	

The growth and decay rates listed in Table 9 could not always be calculated due to confused sea conditions. They also reflect an integration of a variety of environmental conditions including wind speed, fetch, duration, previous wave history, background swell, etc. However, given these limitations, general statements may be made. The extreme sea states were associated with an average dHS/dT rate greater than 0.4 m/hr with an increase in the period of the spectral peak at a rate as high as 1.1 s/hr though on average between 0.2 and 0.5 s/hr. During storm 8, the maximum rate of change at Stn. 46004, the largest for any station, was 4m in 3 hours (1,3 m/hr) with the peak period increasing from 12.5 to 16.7 over this same period (1.4 s/hr). The decay rates for HSIG, which tend to be more uniform over time than the growth rates, ranged from a very slow decay of -.06 m/hr to -.3 m/hr.

Peak period may or may not decrease with decay depending on whether or not swell is present.

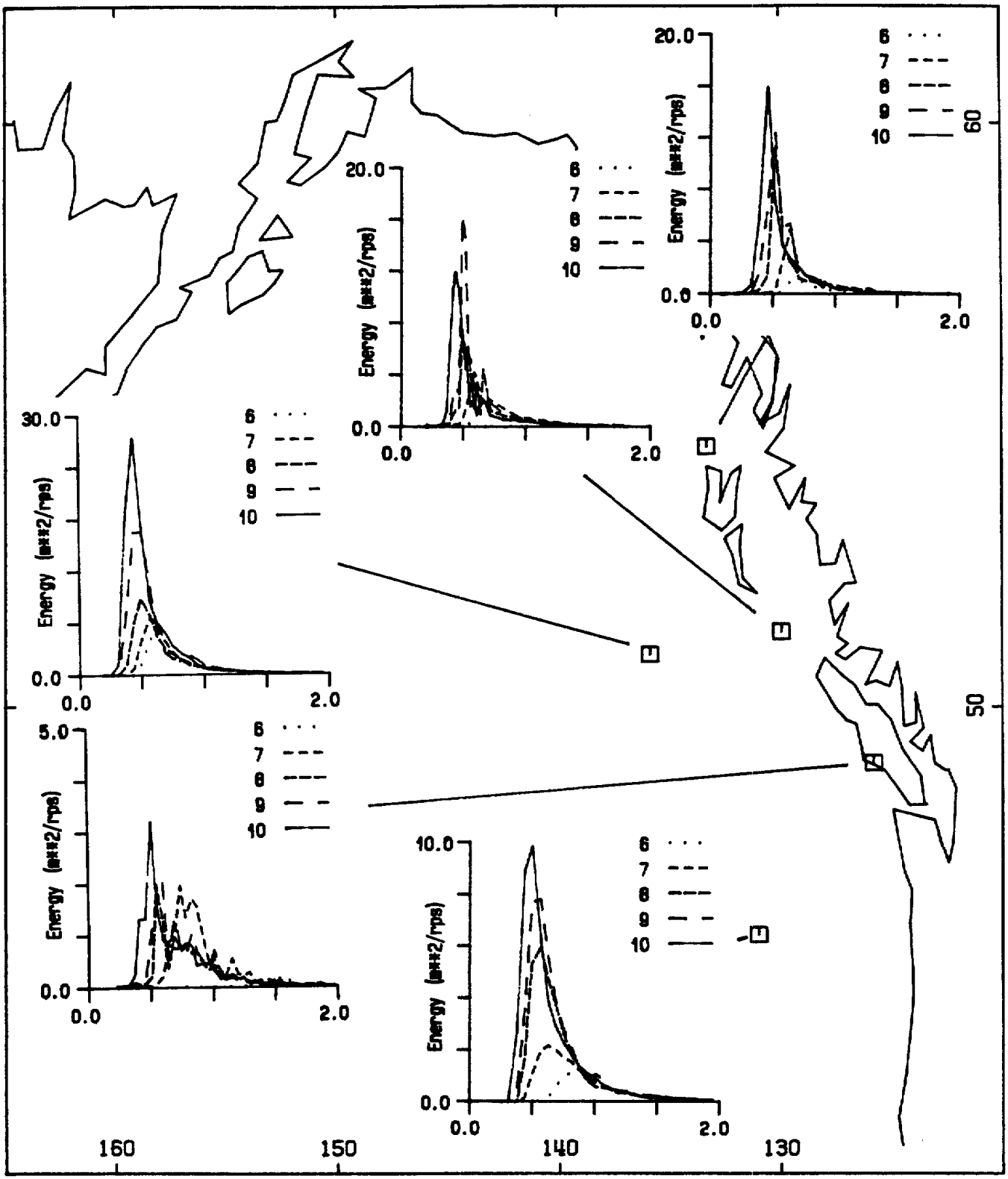

86/9/23/900:6, 23/1500:7, 23/2100:8, 24/0:9, 24/600:10

Fig. 17 Sample spectra from Storm 7 - sea growth.

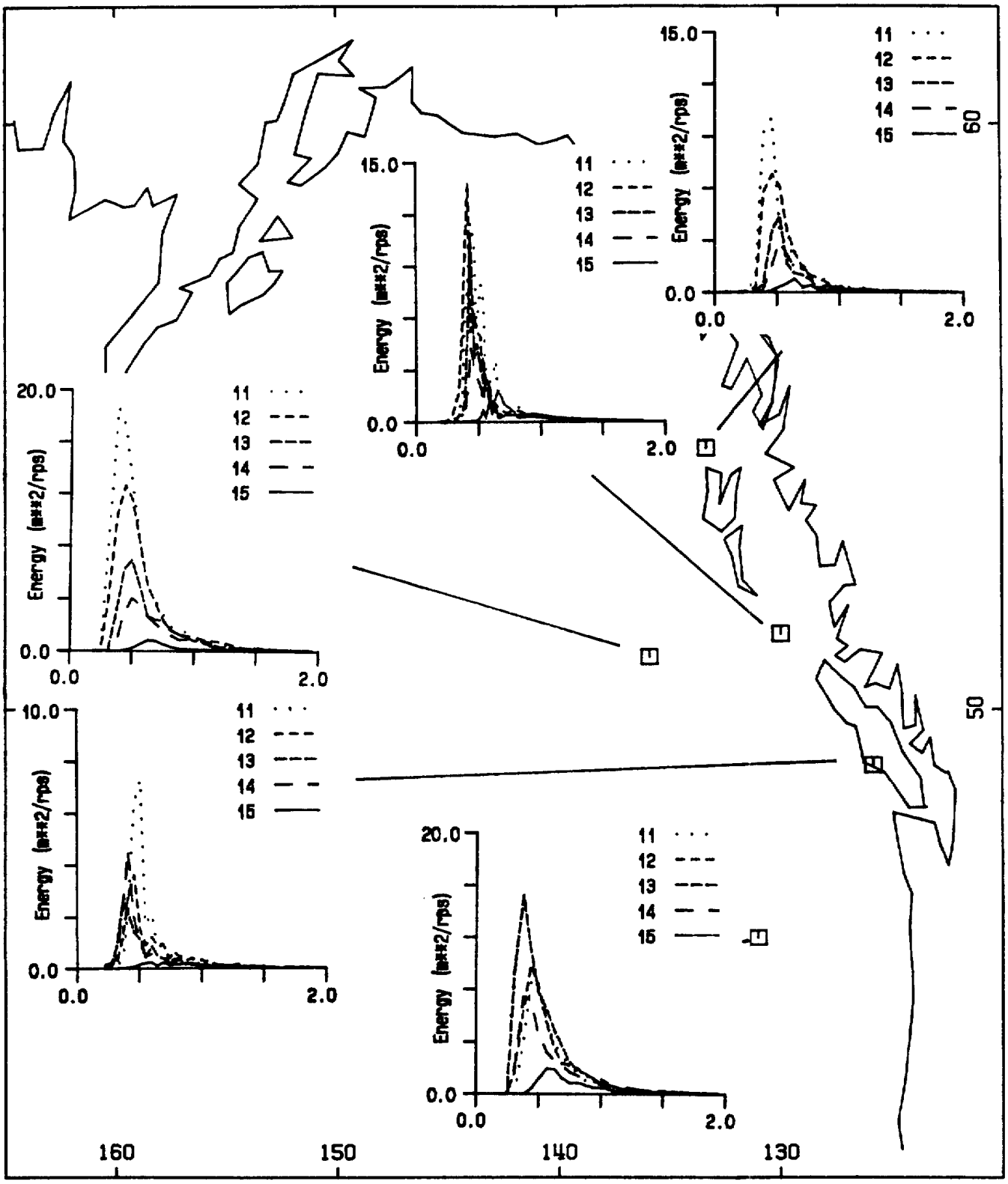

86/9/24/900:11, 24/1800:12, 25/300:13, 25/900:14, 26/2100:15

Fig. 18 Sample spectra from Storm 7 - sea decay.

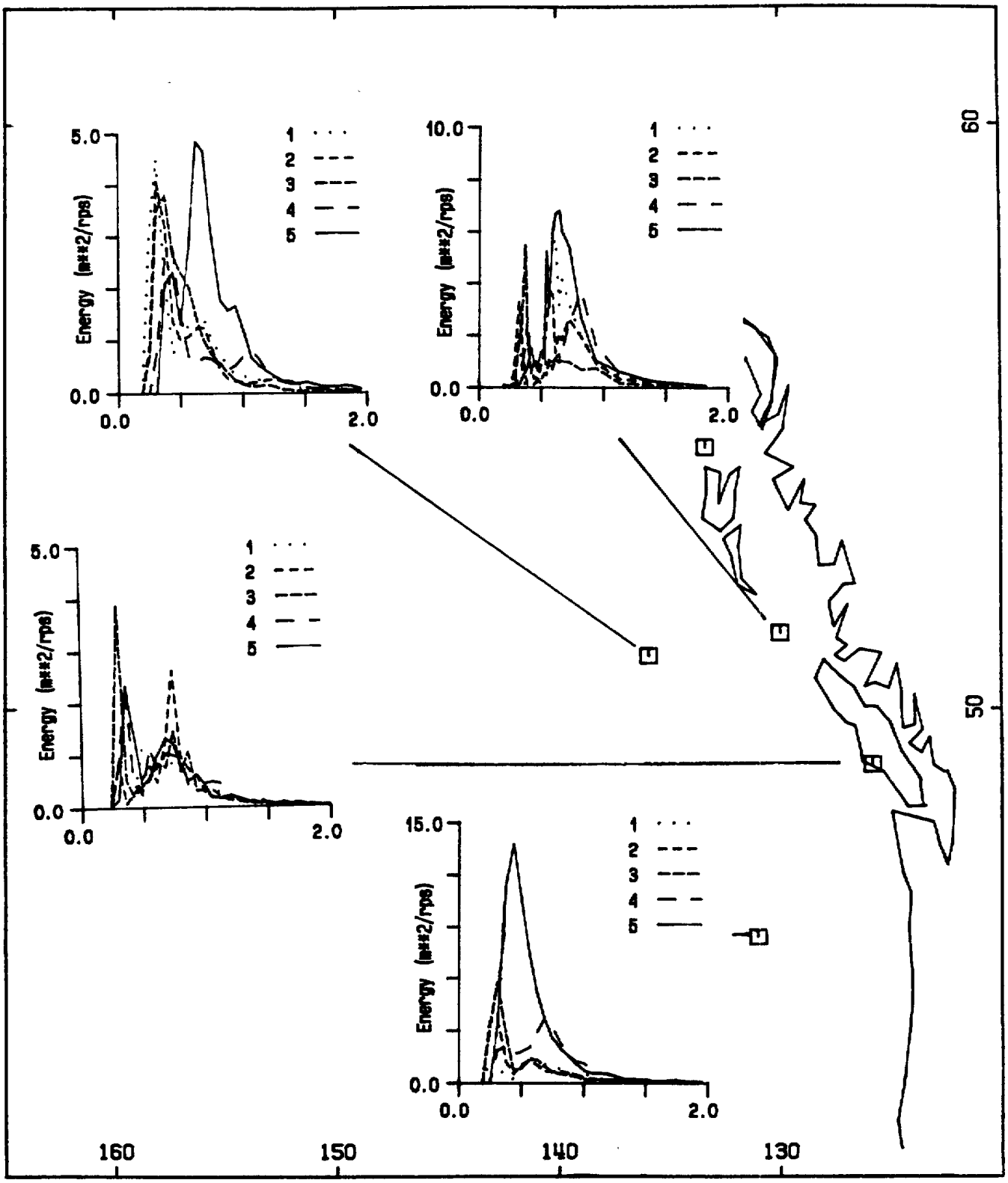

88/1/8/2100:1, 9/0:2, 9/600:3, 9/1500:4, 9/2100:5

Fig. 19 Sample spectra from Storm 12 - mixed sea and swell

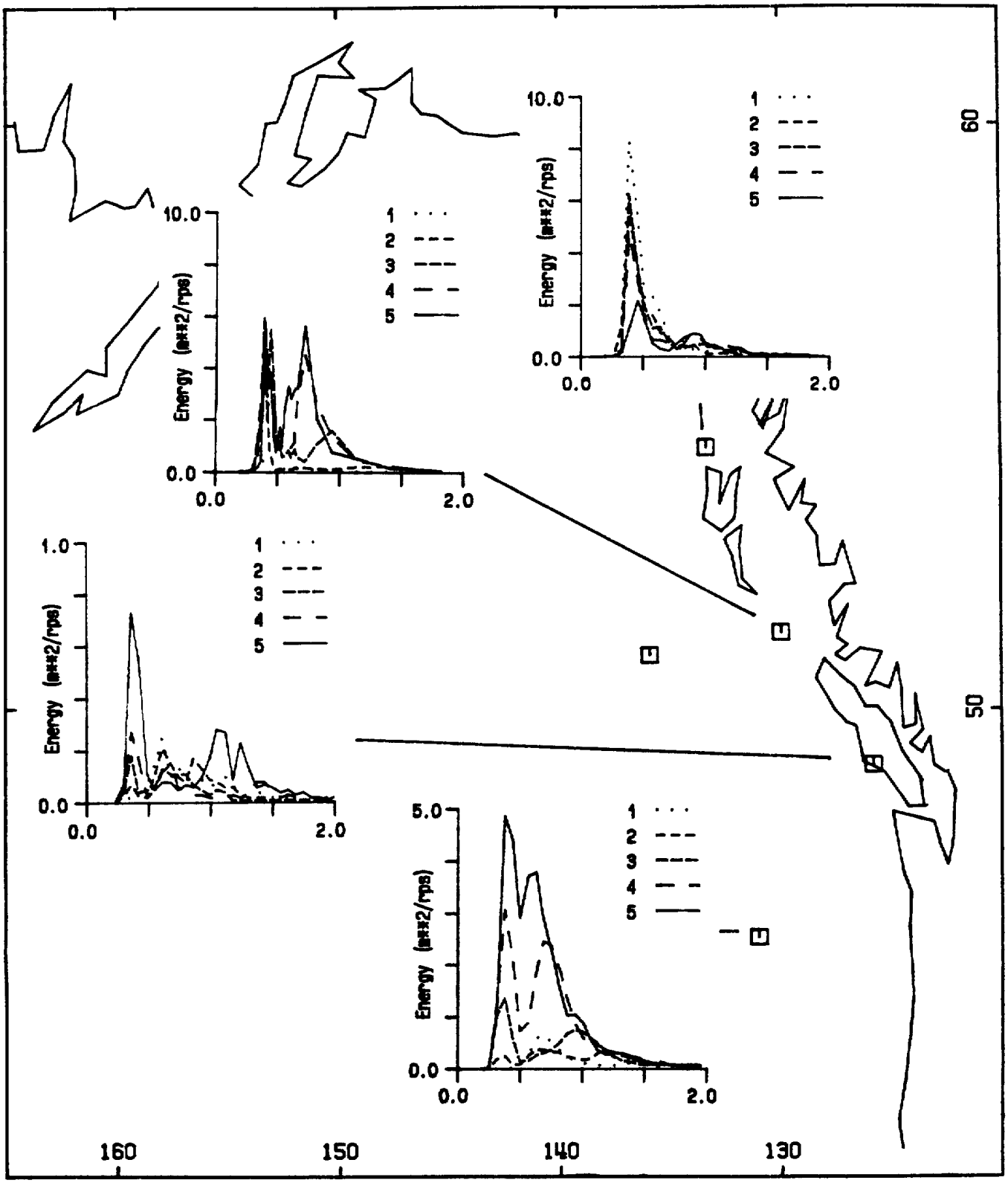

88/12/20/0:1, 20/600:2, 20/900:3, 20/1200:4, 20/1500:5

Fig. 20 Sample spectra from Storm 15 - precursor swell and sea

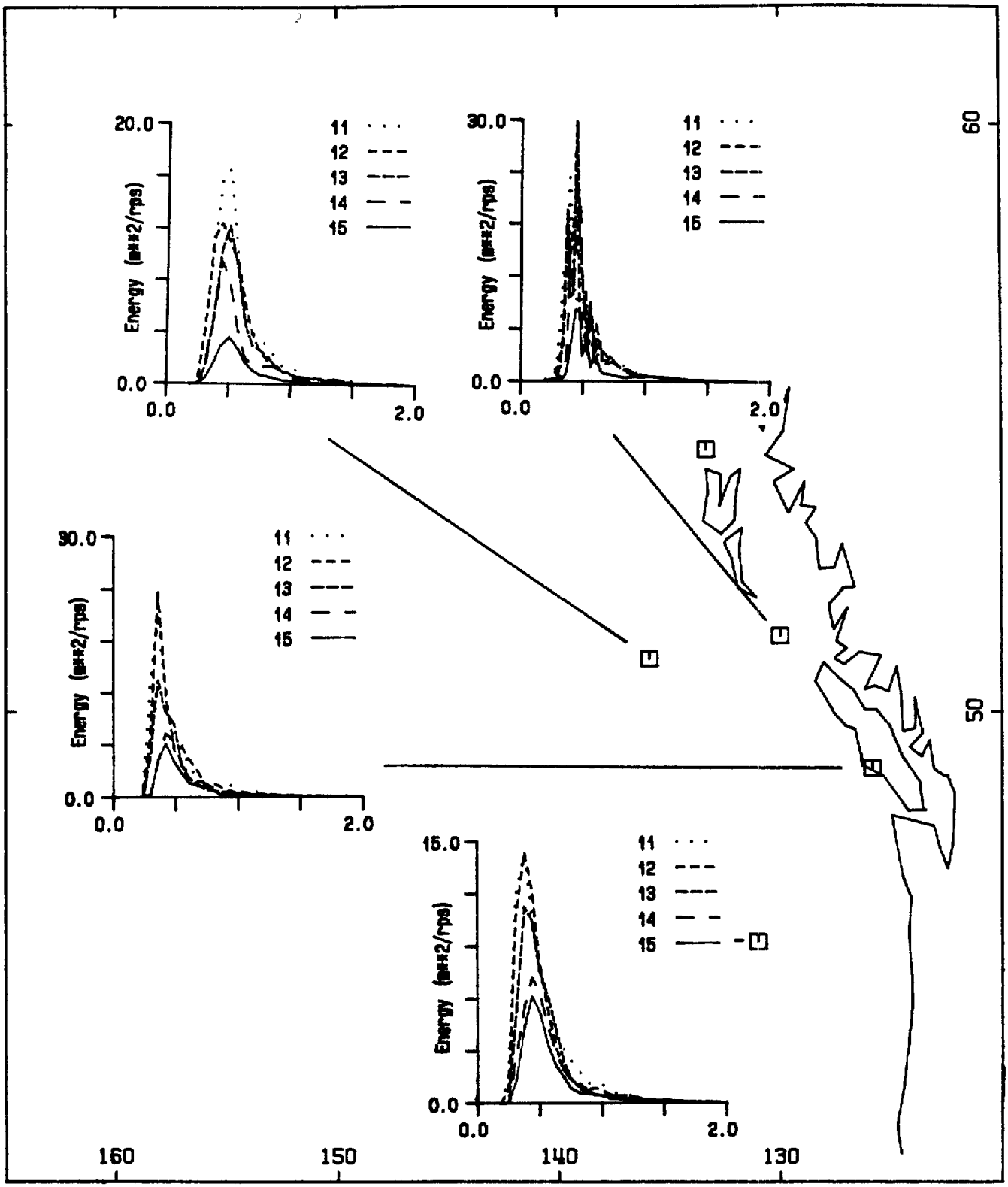

87/12/2/300:11, 2/600:12, 2/900:13, 2/1500:14, 2/2100:15

Fig. 21 Sample spectra from Storm 11. a) sea decay.

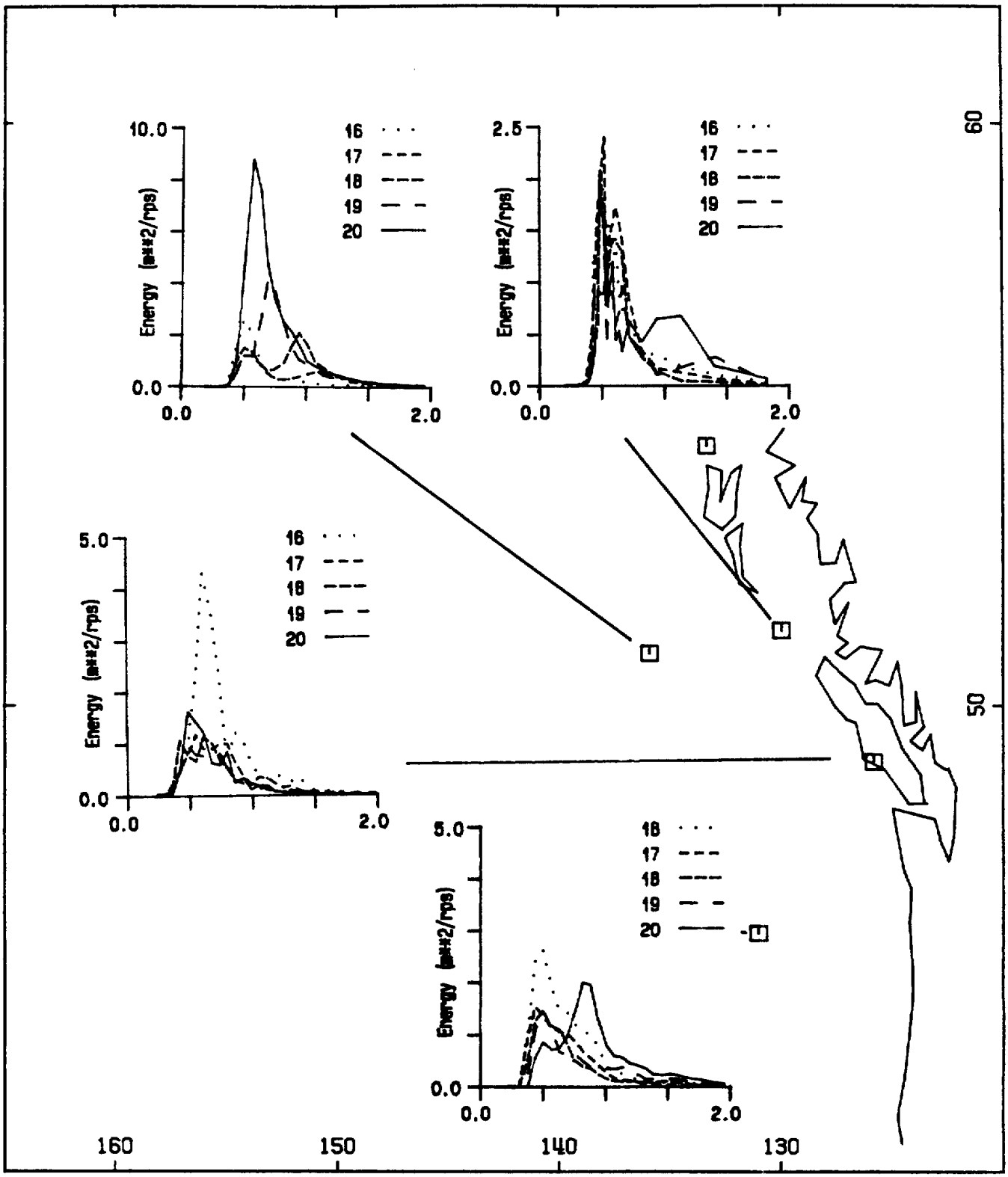

87/12/4/1500:16, 4/2100:17, 5/0:18, 5/300:19, 5/600:20

Fig. 21 Sample spectra from Storm 11. b) remnant "swell".

The wave spectra, included in Appendix 3. contain examples of varied spectral behavior. The classic picture of sea peak development, showing increasing energy with migration of the peak towards low frequencies, can be observed, for example, at all stations during Storm 7 (Fig. 17) and, clearly, for the NDBO buoys during storms 1, 2 and 6. The decay of this peak can be seen in Fig. 18 to be almost a reflection of the peak growth. In this storm, there was essentially no swell present however, the presence of both a sea and swell is a common occurrence in early sea peak development. This is shown in Fig. 19 for the early sea development of Storm 12. In many cases the swell that is present is a "remnant" sea from a previous build-up. A good example of forerunner swell can be seen during the early stages of Storm 15 (Fig. 20), particularly at Stns. 103 and 46005 where the swell period dropped from 17 to 14 seconds over 15 hours, with increasing energy (unlike remnant seas which tend to decrease in energy with time), as the early sea peak developed. A single sea peak is the most common spectral form associated with the maximum HSIG record. The decay of the storm peak can appear as either the reverse of sea peak growth as mentioned previously (e.g. Stn. 46004 - Storm 4) or, in the majority of the cases, the energy decreases but there is relatively little migration of the peak towards higher frequencies as the seas do not have sufficient time to relax prior to a second build-up. An example of this occurred during Storm 11 (Fig. 21a) at all stations. These peaks can be interpreted as swell (strictly defined as waves whose phase speed is greater than local wind speed or whose direction of travel is not aligned with the local wind) as they can be seen, in the spectral plots 16-20 of Fig. 21b , to still be present as background energy during the new sea build-up.

As the storm observations indicate, the wave climate on the West Coast is quite varied. A proper modelling of this region would have to account for the differences in scales of the storm generating pressure centers, the influence of land masses and bathymetry, the presence of swell, the often rapid sea growth, details of which would be missed if the time step is too long, and the complex interaction, particularly in Queen Charlotte Sound and Hecate Strait, of sea and generating winds which can lead to intensification of the wave climate in these areas.

6. PREDICTION OF FIT PARAMETERS

The prediction of model parameters from their probability distribution, environmental measurements, spectral statistics or other model parameters, has practical and theoretical applications. It can provide bounds on possible spectral shapes (i.e. "design spectra") for input into engineering models. It can supplement information for areas where direct field measurement of wave spectra are not

available. It may allow for improvement in fit procedure by supplying first guesses, bounds on the fit parameters or reduce the number of parameters which need to be fit. Finally, it may also provide empirical evidence to support theoretical relationships.

The feasibility of predicting the OH model fit parameters from limited field information or from internal relationships between the parameters will be examined and discussed in Section 6.1 . In Section 6.2 , a statistical approach will provide a family of model wave spectra, based on the probability distributions of the fit parameters, for single and double peak spectra from three significant wave height classes. In Section 6.3 , an analytical approach will examine the relationship between the OH model and other parametric models discussed in the literature.

6.1 Numerical Prediction

There are two separate requirements for predicting model parameters. First, one must be able to determine a relationship with independently measured, routinely reported synoptic information such as wind speed and direction, and directly observed estimates of significant wave height and peak period so that the prediction equations can be used to supplement existing wave climate information. Second, one must examine any inter-dependence in the model parameters (i.e. internal variables) in order to improve these predictive equations. The "goodness" of a predictive relationship is determined by the amount of variance, present in the predicted parameter, that can be explained by the other variates.

It was assumed, for this analysis, that the only available external variables were HSIG and ωp (i,e. peak frequency). Excluding swell contributions, these may be calculated from wind information using established engineering relationships. Both sea and swell properties may be available from visual reports (e.g. MANMAR records include estimates of wave height, period and direction for both swell and sea which could be used as predictors for $\omega m1$, $\delta 1$, $\omega m2$ and $\delta 2$). The internal variables include the remaining five fit parameters and the ratios of modal frequency to peak frequency and variance parameter to significant wave height. The ratios were used for the prediction of the shape parameters as an initial correlation analysis showed little dependence on these ratios by ωm or δ. The spectral Type 1 and Type 2 classes (as described in Sections 3.1 and 4.1 .) were treated independently though the distinction based on energy was removed as a dependence on HSIG appears in the predictive equation (i.e. Type 1 classes 11, 12 and 13; 21, 22, 23; etc. were grouped together).

The prediction procedure consisted of a preliminary calculation of the linear correlation matrix for the 12 channels (i.e. HSIG, TP, six

fit parameters, four ratios). The correlation matrices for the non-linear relationships PAR=VAR**X and PAR=EXP(VAR) were also calculated on test cases of Stn. 46005 data, and they did not show any significant improvement over the linear values. For each predicted parameter, the variables were ordered (in decreasing order) according to their correlation value, it was determined whether they were useful predictors given the standard deviation in their distribution, and were then sequentially added to the prediction equation. The significance of the added variate was determined in the following manner. Let

$$\hat{y}_p = f(\lambda_1,\ldots,\lambda_p) \quad \hat{y}_{p-1} = f(\lambda_1,\ldots,\lambda_{p-1})$$

be the regression estimate with p variates and p-1 variates, respectively. The ratio

$$F(1,N-P) = \frac{\sum_{I=1}^{N}(\hat{y}_{Ip} - \bar{\hat{y}}_{Ip})^2 - \sum_{I=1}^{N}(\hat{y}_{Ip-1} - \bar{\hat{y}}_{Ip-1})^2}{\sigma_e^2}$$

was then calculated. The summation is taken over N data points, the overbar represents the mean of the estimated parameter and σ_e^2 is the residual variance given by

$$\sigma_e^2 = 1/(N-(p+1))^* \sum_{I=1}^{N}(y_I - \hat{y}_I)^2$$

This is the ratio of increase in explained variance to residual variance and, assuming that the residual series has an underlying Gaussian distribution, this ratio follows an F distribution with 1 and N-P degrees of freedom, if the ratio is large, then there is good probability that the added variate significantly decreases the explained variance. In practice, if the ratio exceeded the 95% confidence limit, the variate was kept in the regression. After this F test, the standard error of the regression coefficients was calculated and if any coefficient lay within three standard deviations of 0, it was also dropped from the model. Finally, the residual from the reduced regression model was compared to the residual error of the model incorporating all possible variates to ensure that the deletion process had not sacrificed too much explained variance. The residual variance generally increased by less than 5% (less than 1% for the prediction of HS1 or HS2). The procedure proved effective in determining the underlying inter-relationships in the variates.

This analysis was performed for all stations, on the Type 1 and Type 2 groups discussed above. The procedure, as it is based on the measured correlation values, may result in the inclusion of a variable showing correlation with the parameter but which does not reduce the residual variance appreciably. This can occur if the variable is self-correlated with predictors already included in the regression. The analysis results were examined for consistent variable/parameter relationships, which explain the majority of the variance, and then specific variable regressions were performed on all the data.

The preliminary results indicated that $\delta 1$ and $\delta 2$ were the best predicted, followed by $\omega m1$ and $\omega m2$. The shape parameters consistently had large residual variances which reflect the scatter observed in these parameters in the joint occurrence plots included in Appendix 2. The common variable/parameter predictive groupings were:

$\omega m1$: ωp, ($\omega m2$, HSIG)
HS1: HSIG, (HS2)
SH1: HS1/HSIG, $\omega m1$, ($\omega m1/\omega p$)

$\omega m2$: $\omega m1$, HS2, HSIG
HS2: HSIG, HS1
SH2: HS2/HSIG, HS1/HSIG (ωp, $\omega m2/\omega p$)

The order in which the parameters would be predicted is influenced by the available information and the amount of variance accounted for by the respective prediction equations. A proper ordering allows for a previously predicted parameter to act as a variable in later predictions. A suggested order would be HS1, HS2, $\omega m1$, $\omega m2$, SH1 and SH2. The variables in parentheses listed above resulted in either lesser reduction of the variance than the others or would normally be predicted after the current parameter. It was interesting to note that the shape parameters were better correlated with variance ratios than with total variance. Tables 10 a to c and 11 a to e contain the percent residual variance, regression coefficients and their standard deviation for predictions based on Type 2 and Type 1 groups, respectively. The constant in the table represents the linear regression constant which is always included in the prediction equation, if a given set of coefficients did not reduce the residual variance, these were omitted from the tables. One would expect lower residual variances in the Type 2 analyses as the fit behavior is being addressed but this was not always the case for a given fit parameter. The prediction equations were generally similar between locations with the possible exception of Stn. 503w. For this station the frequency resolution may have influenced both the fits and subsequent analyses or physically different processes may be occurring.

By definition, the single peak spectral classes 1, 5 and 9 (table 10a) consisted of spectra scanned as one peak with the fit resulting

in over 80% of the variance being explained by the first set of parameters, it is not surprising, therefore, that ωm1 is well predicted by ωp. Knowing both HSIG and HS2 will allow for accurate determination of HS1. This is a consistent picture for all spectral types which is to be expected as the total heave variance must be conserved by the model. The slope of the HS1-HSIG equation indicates that over 90% of the total heave variance is being explained which is evidence that the prediction procedure is working properly. The relatively large residual variance in HS1 prediction by HSIG alone is a reflection of the fit behavior, in order for the peak to be modelled properly for very sharp spectra, proportionally more variance present in the high frequency "tail" must be explained by HS2. Hence high variability in HS1 is linked to variability in the spectral shape further indicated by the inverse relationship between SH1 and HS1/HSIG. The prediction equation for ωm2 is also consistent with a single peak picture as there is a constant high frequency offset which is proportionally reduced as HS2 increases. There was very little variance explained in the prediction of SH2.

The residual variance in SH1 is consistently high (greater than 60%). However, it is possible that a basic underlying trend is being accounted for and the variance is a result of the large "experimental" scatter in the statistic. The SH1 values will tend to a limit, for a given ωm1, as HS1 approaches HSIG and ωm1=ωp. For ωm1 = 0.314rps (i.e. TP of 20s), SH1 would have values of 0.86, 0.69, 0.81 0.7 and 2.56 for Stns. 46005, 46004, 103, 211 and 503W, respectively. The large SH1 value for Stn. 503W is consistent with the large peakedness parameter values also seen for these records. As discussed in Section 4.1 , different parametric models contain different formulations of the equilibrium range of the wave spectrum requiring either an ω**-4 or ω**-5 power law relationship. The limits of 0.7 to 0.86 support a -4 power law if these records are considered as swell waves or fully-developed, fetch unlimited seas, with little or no peak enhancement. For ωm1 = .628rps (i.e. TP of 10s), SH1 would have values of 1,07, 1.0. 1.09, 1.04 and 1,12, which is a more peaked spectra and would tend to imply a -5 power law relationship. These records would most likely represent wind-driven sea and the larger SH1 value may be required to handle the peak enhancement as opposed to the high frequency "tail". In which case, the frequency relationship may be considered as ω**(-4 -Δλ) where Δλ (the difference between λ and 4) is an implicit peak enhancement while still maintaining a -4 power law. This illustrates some of the difficulty encountered in trying to justify either a -4 or -5 relationship from experimental evidence.

It can be seen in Table 10b , representing double peaked spectra, that Wm1 is not well predicted by either ωp or ωm2. In contrast to single peak spectra, the two sets of fit parameters are essentially

independent and there are numerous energy/frequency combinations possible for double peaked spectra. For example, if one visualizes sea peak growth with concurrent swell decay, the relative dominance of the peaks as well as their position, are changing with time, HSIG is a somewhat better predictor of both HS1 and HS2 for double peaks than for single peaks (Table 10a), if one substitutes the prediction equation for HS2 into that for HS1, then the equations imply an approximate 60-40% distribution of the total heave variance between the Set 1 and Set 2 parameters. The shape parameter predictions are more complex than for single peaks and can go to negative, physically unrealistic values, for certain combinations of predictors (this feature may be useful for setting bounds on possible combinations of parameters in the production of model design spectra). An example for the use of the SH2 equations, for Stn. 46005, is as follows. Let HS2/HS = 0.6, then the first prediction equation results in SH2 = 1.97. If one takes, for example, $\omega m2 = \omega p = 0.628$rps and HS1/HS = 0.8 (when HS2/HS = 0.6 and all the heave variance is being accounted for), then the second prediction equation yields SH2 = 1.66. If one sets $\omega m2 = 0.628$rps and $\omega p = 0.45$, with similar HS1 and HS2 relationships, SH2 would be reduced to 1.42.

Table 10c contains the predictive equations for spectra which were classified as having their heave variance split between the two sets of parameters, if one compares this table with Table 10b , there appeared to be a stronger inter-dependence between $\omega m1$ and $\omega m2$, while the ability to predict HS1 and HS2, SH1 and SH2 were similar with HS1 containing a marginally greater percentage of the total variance and SH2 expected to be slightly smaller. There was approximately 65-35% distribution of the total heave variance between HS1 and HS2. The shape parameters were the best predicted of the Type 2 spectral classes.

Tables 11 a to e contain the prediction equations and residual variances for spectra Type 1 classes. For the single peak classes, Tables 11 a , b and c , the prediction of $\omega m1$ and $\omega m2$ are poorer than that seen in Table 10a as peak "splitting" may be occurring. This may be more severe for the higher frequency classes (31,32,33) of generally lower energy as these tend to be broad and more likely to require both sets of parameters for proper representation. In fact, all the regression coefficients will be influenced to some extent by varied fit behavior. There is better prediction, however, of HS1 from HSIG (poorer for HS2) and for both shape parameters. For the low frequency, Type 1 classes Table 11a , there was no improvement of the prediction of SH1 from period information for the two NDBO buoys. The indicated limit for SH1 (i.e, when HS1=HSIG) was 1.1 for both 46005 and 46004. For SH2, if HS2/HS remains the same, then the prediction

equations indicate that its value would increase with decreasing period class (Tables 10 a to c) which was previously suggested by the summary statistics discussed in Section 4.3 and further confirms that the predictive analysis is behaving properly.

Table 10a. Coefficients for prediction equations
Spectral TYPE2 - Classes 1,5,9.

		Station													
		46005			46004			103			211			503W		
	Npts:	1073			915			2244			949			63		
Par.	Var.	Coef	Std	%Res	Coef	Std	%Res	Coef	Std	%Res	Coef	Std	%Res	Coef	Std	%Res
Wm1	Const.	.015	.003	3.1	.014	.003	3.0	.013	.002	3.2	.013	.003	3.4	-.005	.007	1.1
	Wp	.967	.005		.970	.006		.971	.004		.972	.006		1.01	.014	
Hs1	Const.	.020	.008	.43	.009	.010	.47	.003	.004	.38	-.019	.008	.43	.010	.019	.23
	HSIG	.952	.002		.953	.002		.959	.001		.968	.002		.943	.006	
	Const.	.019	.002	.03	.022	.003	.05	.013	.001	.05	.014	.002	.04	.011	.004	.007
	HSIG	1.03	.001		1.03	.002		1.03	.001		1.02	.001		1.06	.003	
	Hs2	-.266	.002		-.263	.003		-.249	.002		-.241	.002		-.338	.008	
Sh1	Const.	10.90	.488	71.9	11.8	.49	62.8	10.40	.366	75.5	8.41	.439	69.9	10.67	4.8	83.2
	Hs1/Hs	-10.24	.509		-11.4	.51		-9.89	.381		-8.03	.451		-6.66	5.3	
	Wm1	.648	.129		.935	.127		.919	.103		1.06	.110		-4.58	1.6	
Wm2	Const.	.368	.029	61.2	.388	.031	59.9	.425	.025	72.6	.591	.035	74.2	.001	.137	50.1
	Wm1	1.44	.055		1.41	.057		1.40	.048		1.13	.062		2.09	.263	
	Const.	.722	.033	47.8	.770	.035	44.9	.735	.026	58.2	.973	.036	53.8	.280	.169	45.2
	Wm1	1.09	.053		1.05	.053		1.13	.045		.825	.056		1.76	.281	
	Hs2	-.151	.009		-.152	.009		-.225	.01		-.230	.012		-.104	.040	
	Const.	.593	.037	45.7	.617	.04	42.6	.649	.028	56.2						
	Wm1	1.22	.054		1.21	.056		1.21	.045							
	Hs2	-.219	.013		-.216	.012		-.319	.014							
	HSIG	.036	.005		.035	.005		.044	.005							
Hs2	Const.	-.006	.029	37.1	.052	.036	40.1	.040	.014	40.9	.137	.030	54.1	.003	.056	13.3
	HSIG	.292	.007		.286	.008		.268	.005		.233	.008		.333	.016	
	Const.	.065	.008	2.9	.081	.012	4.6	.050	.005	5.2	.066	.009	4.9	.032	.010	.42
	HSIG	3.60	.029		3.49	.038		3.64	.027		3.89	.037		3.03	.062	
	Hs1	-3.47	.031		-3.37	.040		-3.51	.028		-3.78	.039		-2.86	.065	
Sh2	Const.	2.96	.120	91.9	2.91	.130	92.3	2.55	.094	98.5	2.54	.135	98.8	3.92	1.07	97.9
	Hs2/Hs	-3.83	.393		-3.62	.416		-1.82	.313		-1.54	.459		-3.66	3.17	

Table 10b. Coefficients for prediction equations
Spectral TYPE2 - Classes 3,7,11

		Station											
		46005			46004			103			211			503W		
	Npts:	3546			2716			4629			1621			1075		
Par.	Var .	Coef	Std	%Res	Coef	Std	%Res	Coef	Std	%Res	Coef	Std	%Res	Coef	Std	%Res
Wm1	Const.	.316	.006	75.0	.317	.007	70.3	.325	.005	81.6	.395	.011	87.4	.329	.009	73.0
	Wp	.331	.010		.359	.011		.280	.009		.222	.015		.285	.014	
	Const.	.042	.007	43.0	.073	.008	43.9	.089	.007	55.7	.013	.014	53.6	.209	.010	56.5
	Wp	.220	.008		.236	.009		.208	.007		.173	.011		.218	.013	
	Wm2	.338	.007		.309	.008		.298	.006		.376	.012		.176	.01	
Hs1	Const.	-.216	.014	16.	-.257	.018	16.	-.181	.009	11.	-.206	.014	11.6	-.195	.023	15.1
	HSIG	.819	.006		.841	.007		.865	.005		.887	.008		.766	.010	
	Const.	.009	.005	1.8	.031	.006	1.8	.0[illegible]	.0[illegible]	1.2	.031	.006	1.5	.018	.007	1.4
	HSIG	1.29	.003		1.27	.004		1.3[illegible]	.00[illegible]		1.32	.005		1.39	.007	
	Hs2	-.853	.005		-.824	.006		-.877	.004		-.904	.009		-.995	.010	
Sh1	Const.	3.84	.092	62.2	3.31	.11	57.7	.611	.071	67.8	.508	.071	59.9	5.70	.306	76.4
	Hs1/Hs	-5.98	.134		-6.30	.14		-4.17	.111		-2.83	.127		-5.07	.375	
	Wm1	2.04	.135		2.46	.14		3.75	.116		2.95	.111		-3.83	.456	
	Wm1/Wp	2.01	.113		2.51	.13		2.75	.117		1.66	.089		3.32	.381	
Wm2	Const.	.392	.011	53.1	.396	.014	55.3	.432	.010	65.4	.566	.017	61.1	.259	.031	71.0
	Wm1	1.20	.021		1.18	.025		1.03	.021		.973	.030		1.30	.062	
	Const.	.673	.013	40.2	.742	.016	40.5	.584	.012	59.8	.673	.020	58.2	.564	.037	60.7
	Wm1	1.01	.019		.943	.023		.944	.020		.935	.030		1.03	.061	
	Hs2	-.132	.004		-.138	.004		-.102	.005		-.084	.009		-.114	.009	
	Const.	.686	.012	35.4	.745	.015	36.3									
	Wm1	.930	.019		.878	.022										
	Hs2	-.245	.006		-.231	.007										
	HSIG	.092	.004		.075	.004										
Hs2	Const.	.264	.015	34.4	.350	.020	39.0	.215	.009	30.4	.263	.015	32.7	.214	.022	19.7
	HSIG	.552	.007		.516	.008		.508	.005		.475	.008		.624	.009	
	Const.	.038	.005	3.8	.074	.007	4.6	.029	.003	3.2	.064	.006	4.3	.036	.007	1.8
	HSIG	1.41	.005		1.42	.007		1.39	.005		1.33	.009		1.32	.007	
	Hs1	-1.04	.006		-1.08	.007		-1.02	.005		-.975	.009		-.913	.009	
Sh2	Const.	3.50	.070	83.4	3.47	.075	81.2	3.59	.065	85.0	3.65	.111	86.6	3.11	.186	95.0
	Hs2/Hs	-2.55	.096		-2.62	.104		-2.72	.095		-2.50	.158		-1.84	.244	
	Const.	6.85	.381	68.8	6.61	.383	67.6	7.60	.391	74.5	5.40	.549	75.4	8.75	.879	83.7
	Hs2/Hs	-6.05	.246		-5.83	.245		-6.22	.271		-5.04	.379		-6.12	.655	
	Hs1/Hs	-4.05	.273		-4.11	.287		-3.37	.296		-2.43	.424		-3.78	.643	
	Wm2/Wp	.369	.047		.441	.054		-.047	.040		.227	.071		-.264	.079	
	Wp	2.05	.114		1.97	.122		1.48	.113		1.94	.180		.825	.221	

Table 10c. Coefficients for prediction equations
Spectral TYPE2 - Classes 4,8,12

		Station													
		46005			46004			103			211			503W		
	Npts:	3124			2936			1985			736			1024		
Par.	Var.	Coef	Std	%Res	Coef	Std	%Res	Coef	Std	%Res	Coef	Std	%Res	Coef	Std	%Res
Wm1	Const.	.096	.005	26.5	.079	.005	22.5	.114	.009	45.2	.160	.018	56.9	.343	.012	81.4
	Wp	.788	.008		.826	.008		.716	.015		.654	.028		.293	.019	
	Const.	.051	.004	16.8	.033	.004	14.0	.037	.007	23.7	.087	.016	42.1	.214	.012	62.2
	Wp	.488	.010		.551	.009		.441	.012		.456	.027		.138	.019	
	Wm2	.266	.006		.244	.006		.302	.007		.242	.015		.299	.017	
Hs1	Const.	-.139	.023	14.6	-.201	.026	15.	-.121	.027	19.	-.177	.059	22.4	-.554	.059	24.9
	HSIG	.836	.006		.847	.007		.850	.009		.868	.017		.839	.015	
	Const.	.060	.007	1.3	.077	.008	1.4	[illegible]		1.9	.006	.021	2.7	-.047	.022	3.2
	HSIG	1.27	.003		1.27	.007		1.[illegible]	[illegible]		1.26	.017		1.42	.009	
	Hs2	-.842	.005		-.849	.005		-.842	.006		-.823	.011		-1.03	.012	
Sh1	Const.	1.06	.191	57.4	.631	.207	60.	-1.88	.183	63.	-.920	.191	60.7	3.94	.383	89.8
	Hs1/Hs	-6.45	.138		-6.27	.146		-4.33	.176		-2.85	.191		-2.21	.363	
	Wm1	2.46	.142		2.68	.147		3.22	.231		2.90	.251		-5.11	.630	
	Wm1/Wp	5.40	.220		5.51	.236		5.98	.242		3.14	.299		4.06	.507	
Wm2	Const.	.044	.010	30.3	.055	.010	31.2	.038	.014	38.9	.158	.030	58.6	.233	.022	65.4
	Wm1	1.42	.017		1.41	.017		1.41	.025		1.15	.051		.972	.042	
	Const.	.219	.015	28.1	.279	.016	28.2	.127	.018	37.8	.327	.042	56.1	.427	.026	56.9
	Wm1	1.25	.019		1.20	.020		1.33	.027		1.01	.056		.806	.041	
	Hs2	-.042	.003		-.050	.003		-.031	.004		-.048	.008		-.058	.003	
	Const.	.133	.014	24.9	.186	.015	24.3	.065	.170	32.4	.204	.042	51.0			
	Wm1	1.31	.019		1.26	.019		1.32	.025		1.05	.053				
	Hs2	-.092	.004		-.105	.004		-.099	.005		-.100	.010				
	HSIG	.045	.002		.049	.002		.063	.003		.059	.007				
Hs2	Const.	.237	.026	36.5	.327	.029	39.1	.175	.031	46.2	.223	.068	55.0	.491	.053	38.0
	HSIG	.515	.007		.504	.007		.497	.010		.480	.020		.558	.014	
	Const.	.086	.008	3.3	.112	.009	3.6	.047	.010	4.8	.033	.024	6.6	.024	.020	4.9
	HSIG	1.42	.006		1.41	.006		1.40	.008		1.41	.014		1.27	.010	
	Hs1	-1.08	.006		-1.07	.007		-1.07	.008		-1.07	.015		-.843	.010	
Sh2	Const.	3.25	.070	80.5	2.96	.068	83.0	3.81	.096	83.3	4.07	.146	78.9	2.28	.173	99.6
	Hs2/Hs	-2.99	.108		-2.64	.108		-3.18	.159		-3.41	.243		-.456	.237	
	Const.	12.05	.400	57.0	11.0	.410	59.	12.46	.645	59.	11.12	.945	59.9	9.17	.947	85.7
	Hs2/Hs	-8.43	.262		-7.71	.270		-8.78	.428		-8.32	.627		-6.27	.658	
	Hs1/Hs	-4.28	.280		-3.87	.288		-2.98	.445		-2.70	.610		-3.33	.533	
	Wm2/Wp	-1.98	.075		-1.86	.074		-2.80	.110		-2.35	.166		-1.33	.218	
	Wp	1.18	.109		1.25	.110		1.28	.220		1.46	.342		2.03	.372	

Table 11a. Coefficients for prediction equations
Spectral TYPE1 - Classes 11,12,13

		Station											
		46005			46004			103			211		
	Npts:	1132			768			550			82		
Par.	Var.	Coef	Std	%Res	Coef	Std	%Res	Coef	Std	%Res	Coef	Std	%Res
Wm1	Const.	.055	.006	26.5	.067	.009	32.7	.160	.013	59.9	.219	.038	78.3
	Wp	.858	.015		.830	.021		.598	.031		.637	.091	
	Const.	.044	.006	23.4	.050	.009	29.7	.123	.013	51.7	.130	.035	54.6
	Wp	.824	.015		.814	.020		.618	.029		.527	.078	
	Wm2	.033	.003		.030	.003		.032	.003		.054	.009	
Hs1	Const.	-.230	.054	14.4	-.465	.075	15.	-.025	.042	7.7	.506	.276	25.3
	HSIG	.898	.011		.937	.014		.928	.011		.824	.053	
	Const.	.064	.019	1.7	.084	.027	1.9	.014	.019	1.6	.292	.103	3.5
	HSIG	1.15	.005		1.15	.006		1.10	.006		1.03	.022	
	Hs2	-.655	.007		-.664	.009		-.530	.011		-.560	.025	
Sh1	Const.	6.32	.123	46.4	6.02	.129	42.9	-.916	.389	84.8	1.39	.519	74.8
	Hs1/Hs	-5.18	.143		-4.89	.152		-2.19	.275		-1.66	.449	
	Wm1							-.155	.764		-1.18	1.49	
	Wm1/Wp							4.38	.471		1.59	.555	
Wm2	Const.	.022	.062	88.9	.148	.086	93.9	.025	.153	94.	-.457	.374	85.0
	Wm1	1.77	.015		1.47	.207		2.10	.369		3.56	.934	
	Const.	.590	.056	59.4	.841	.075	58.4	.916	.139	65.3	1.78	.385	46.2
	Wm1	.968	.126		.471	.170		.558	.322		-1.42	.914	
	Hs2	-.105	.004		-.114	.005		-.216	.014		-.171	.021	
	Const.	.373	.054	50.6	.496	.074	48.5	.898	.133	58.5			
	Wm1	1.20	.118		.952	.160		1.42	.305				
	Hs2	-.143	.005		-.145	.005		-.269	.016				
	HSIG	.045	.005		.045	.004		.069	.009				
Hs2	Const.	.449	.078	64.5	.827	.105	74.5	.074	.070	65.	-.383	.457	82.5
	HSIG	.391	.016		.325	.020		.329	.019		.366	.088	
	Const.	.140	.027	7.6	.215	.038	9.4	.036	.032	13.2	.396	.174	11.5
	HSIG	1.60	.014		1.56	.018		1.73	.031		1.63	.065	
	Hs1	-1.35	.015		-1.32	.018		-1.51	.032		-1.54	.068	
Sh2	Const.	2.46	.082	84.8	2.36	.093	83.8	2.65	.126	89.8	2.31	.239	93.6
	Hs2/Hs	-2.21	.155		-2.07	.170		-2.50	.316		-1.57	.664	
	Const.	9.38	.869	75.5	8.15	.984	80.1	9.70	1.25	78.3			
	Hs2/Hs	-6.68	.475		-5.04	.553		-6.90	.720				
	Hs1/Hs	-4.87	.627		-3.70	.684		-4.10	1.06				
	Wm2/Wp	-.697	.080		-.272	.094		-.802	.095				
	Wp	1.63	.713		-1.68	.965							

Table 11b. Coefficients for prediction equations
Spectral TYPE1 - Classes 21,22,23

		Station													
		46005			46004			103			211			503W		
	Npts:	2488			2495			2046			1044			288		
Par.	Var.	Coef	Std	%Res	Coef	Std	%Res	Coef	Std	%Res	Coef	Std	%Res	Coef	Std	%Res
Wa1	Const.	.084	.007	40.1	.083	.007	34.0	.140	.009	56.2	.121	.012	49.1	.475	.034	99.7
	Wp	.823	.014		.827	.012		.702	.018		.744	.023		.060	.060	
	Const.	.043	.007	31.9	.049	.006	27.4	.078	.008	41.2	.040	.011	36.5	.343	.032	74.8
	Wp	.766	.012		.771	.011		.670	.015		.754	.020		-.039	.052	
	Wa2	.079	.003		.072	.003		.081	.003		.075	.004		.243	.025	
Hs1	Const.	-.197	.026	13.1	-.318	.028	12.3	-.048	.023	10.6	-.106	.034	9.4	-.481	.107	25.2
	HSIG	.906	.007		.827	.007		.916	.007		.942	.009		.884	.030	
	Const.	.035	.009	1.7	.032	.010	1.5	.020	.008	1.8	.025	.014	1.6	-.069	.042	3.7
	HSIG	1.17	.003		1.17	.003		1.13	.004		1.12	.005		1.37	.017	
	Hs2	-.657	.005		-.650	.005		-.610	.006		-.582	.008		-.993	.024	
Sh1	Const.	1.70	.247	53.7	.965	.276	55.	-2.11	.204	76.	-1.83	.169	73.4	3.46	.593	96.8
	Hs1/Hs	-6.30	.138		-6.13	.140		-3.66	.182		-.832	.150		.142	.512	
	Wa1	2.42	.313		3.24	.306		.679	.322		2.55	.234		-.105	1.54	
	Wa1/Wp	4.45	.291		4.70	.310		6.83	.295		2.60	.255				
Wa2	Const.	.069	.036	82.1	.082	.036	82.	-.095	.049	80.8	.182	.072	88.8	.237	.055	74.9
	Wa1	1.57	.067		1.53	.066		2.10	.095		1.58	.138		1.05	.107	
	Const.	.662	.035	57.1	.664	.033	54.2	.571	.473	57.5	.921	.067	58.9	.566	.053	50.3
	Wa1	.910	.060		.962	.056		1.25	.086		.704	.119		.765	.091	
	Hs2	-.139	.004		-.139	.004		-.222	.008		-.221	.010		-.092	.008	
	Const.	.407	.032	43.4	.370	.031	40.7	.476	.044	49.7	.679	.068	53.0	.613	.049	43.0
	Wa1	1.11	.052		1.22	.049		1.17	.080		.890	.114		.578	.088	
	Hs2	-.211	.004		-.203	.004		-.315	.009		-.277	.011		-.149	.011	
	HSIG	.079	.003		.073	.003		.089	.005		.063	.006		.050	.007	
Hs2	Const.	.353	.037	61.5	.539	.041	64.5	.111	.029	63.5	.226	.053	70.5	.415	.010	48.5
	HSIG	.395	.010		.372	.010		.356	.010		.307	.015		.492	.028	
	Const.	.092	.013	7.8	.109	.015	7.8	.046	.012	10.9	.074	.022	11.8	.002	.039	7.1
	HSIG	1.60	.010		1.63	.010		1.60	.013		1.65	.020		1.25	.021	
	Hs1	-1.33	.010		-1.35	.010		-1.36	.014		-1.43	.020		-.860	.021	
Sh2	Const.	2.56	.055	84.2	2.53	.055	83.0	2.22	.058	94.9	2.39	.083	94.2	1.52	.257	98.9
	Hs2/Hs	-2.22	.103		-2.27	.100		-1.36	.130		-1.57	.196		-.456	.237	
	Const.	10.46	.488	71.9	11.3	.489	69.9	7.49	.542	83.4	7.06	.775	85.2	12.0	1.76	87.9
	Hs2/Hs	-6.90	.294		-7.44	.294		-4.84	.328		-4.67	.477		-6.79	1.30	
	Hs1/Hs	-4.27	.375		-5.09	.377		-2.20	.441		-2.10	.631		-4.62	.906	
	Wa2/Wp	-1.15	.062		-1.10	.061		-1.01	.062		-.833	.166		-1.72	.411	

Table 11c. Coefficients for prediction equations
Spectral TYPE1 - Classes 31,32,33

		Station													
		46005			46004			103			211			503W		
	Npts:	1119			1013			663			1038			298		
Par.	Var.	Coef	Std	%Res	Coef	Std	%Res	Coef	Std	%Res	Coef	Std	%Res	Coef	Std	%Res
Wm1	Const.	.571	.028	98.6	.351	.028	86.5	.418	.035	94.4	.364	.026	88.4	.597	.042	97.8
	Wp	.146	.036		.459	.037		.307	.049		.410	.035		-.134	.052	
	Const.	.242	.026	61.6	.077	.024	53.2	.103	.031	56.5	.093	.023	54.5	.420	.041	74.4
	Wp	.081	.029		.365	.029		.344	.038		.361	.035		-.369	.052	
	Wm2	.345	.013		.308	.012		.262	.012		.278	.011		.430	.044	
Hs1	Const.	-.414	.038	21.6	-.352	.042	21.3	-.290	.037	14.7	-.167	.034	20.9	-.200	.090	65.5
	HSIG	.972	.015		.952	.016		.986	.016		.916	.015		.488	.039	
	Const.	-.026	.017	3.9	.020	.019	4.2	-.048	.017	3.1	-.028	.015	3.8	-.037	.027	6.0
	HSIG	1.26	.008		1.24	.008		1.19	.008		1.23	.008		1.70	.025	
	Hs2	-.810	.011		-.796	.012		-.689	.014		-.773	.011		-1.46	.027	
Sh1	Const.	1.23	.192	56.6	.946	.235	62.	-1.24	.234	57.	-1.02	.135	61.7	3.14	.456	93.6
	Hs1/Hs	-7.77	.269		-7.29	.293		-6.58	.338		-3.75	.199		-2.29	.706	
	Wm1	2.36	.411		1.71	.411		3.28	.472		2.08	.250		-2.32	1.47	
	Wm1/Wp	6.34	.408		6.69	.444		7.19	.491		4.80	.279		2.74	1.01	

Table IIc. Continued.

		Station											
		46005			46004			103			211			503W		
	Npts:	1119			1013			663			1038			298		
Par.	Var.	Coef	Std	%Res	Coef	Std	%Res	Coef	Std	%Res	Coef	Std	%Res	Coef	Std	%Res
Wm2	Const.	.351	.029	62.0	.297	.033	61.6	.195	.047	63.6	.261	.035	63.5	.619	.035	87.2
	Wm1	1.09	.042		1.17	.047		1.42	.073		1.27	.052		.456	.069	
	Const.	.755	.033	47.4	.744	.040	48.0	.688	.051	46.0	.740	.039	46.2	.774	.038	73.4
	Wm1	.819	.039		.860	.045		1.02	.067		.879	.048		.404	.064	
	Hs2	-.167	.009		-.164	.010		-.241	.015		-.206	.010		-.069	.009	
	Const.	.738	.031	41.8	.573	.036	38.5	.722	.045	35.6	.711	.036	40.0	.819	.046	72.6
	Wm1	.713	.038		.696	.041		.738	.062		.755	.046		.285	.093	
	Hs2	-.236	.010		-.266	.010		-.368	.016		-.303	.012		-.115	.028	
	HSIG	.077	.006		.112	.006		.127	.009		.099	.008		.047	.027	
	Const.													.271	.046	37.5
	Wm1													.031	.068	
	Hs2													-.253	.022	
	HSIG													.198	.021	
	Wp													.772	.046	
Hs2	Const.	.479	.042	72.3	.467	.047	70.2	.352	.048	75.7	.180	.040	64.3	.111	.059	22.0
	HSIG	.353	.017		.363	.018		.300	.021		.411	.017		.826	.025	
	Const.	.059	.019	13.0	.112	.022	13.8	.019	.023	15.8	.003	.017	11.6	-.013	.018	2.0
	HSIG	1.34	.016		1.32	.017		1.43	.024		1.38	.016		1.13	.010	
	Hs1	-1.01	.014		-1.01	.016		-.896	.026		-1.06	.015		-.621	.011	
Sh2	Const.	3.00	.093	86.4	2.67	.098	91.0	2.45	.115	98.4	2.66	.091	93.8	1.65	.362	99.4
	Hs2/Hs	-1.96	.148		-1.62	.162		-.704	.211		-1.38	.166		-.519	.400	
	Const.	11.85	.565	65.3	11.1	.570	64.0	9.80	.956	79.2	10.3	.671	69.3	8.40	2.18	89.6
	Hs2/Hs	-7.48	.393		-6.70	.387		-5.71	.665		-6.37	.462		-3.19	1.62	
	Hs1/Hs	-2.85	.334		-1.99	.345		-1.64	.570		-1.59	.415		-.254	.932	
	Wm2/Wp	-2.37	.130		-2.65	.129		-2.26	.182		-2.49	.130		-3.10	.567	

Table IId. Coefficients for prediction equations
Spectral TYPE1 - Classes 41,42,43

		Station													
		46005			46004			103			211			503W		
	Npts:	868			606			2119			434			439		
Par.	Var.	Coef	Std	%Res	Coef	Std	%Res	Coef	Std	%Res	Coef	Std	%Res	Coef	Std	%Res
Wm1	Const.	.064	.006	16.8	.022	.007	13.8	.109	.005	32.7	.044	.010	20.6	.018	.005	6.0
	Wp	.850	.013		.944	.015		.743	.011		.894	.022		.954	.011	
	Const.	.053	.006	15.6	.015	.007	13.1	.078	.005	30.0	.011	.011	18.6	.016	.005	5.6
	Wp	.816	.013		.914	.016		.721	.011		.867	.021		-.928	.012	
	Wm2	.027	.003		.021	.004		.045	.003		.041	.006		.018	.003	
Hs1	Const.	-.090	.023	8.0	-.127	.040	12.1	-.130	.011	4.7	-.099	.020	3.0	-.149	.043	7.0
	HSIG	.842	.008		.847	.013		.903	.004		.921	.008		.831	.011	
	Const.	.037	.008	0.9	.109	.015	1.6	.025	.004	0.6	.030	.008	0.4	.034	.012	0.5
	HSIG	1.17	.005		1.17	.013		1.16	.003		1.12	.005		1.24	.006	
	Hs2	-.635	.008		-.689	.011		-.620	.005		-.539	.010		-.753	.010	
Sh1	Const.	6.54	.213	67.6	7.08	.197	48.3	.809	.290	84.3	.422	.347	78.2	8.44	.521	85.8
	Hs1/Hs	-5.41	.265		-6.26	.245		-3.17	.166		-2.30	.242		-5.64	.662	
	Wm1							1.77	.310		2.16	.340				
	Wm1/Wp							2.81	.291		1.85	.354				
Wm2	Const.	.244	.058	84.3	.225	.074	85.5	.450	.034	91.9	.603	.074	90.7	-.009	.078	82.1
	Wm1	1.64	.129		1.65	.163		1.06	.077		1.07	.160		1.69	.173	
	Const.	.596	.051	58.0	.748	.064	53.0	.614	.032	74.8	.684	.070	78.3	.349	.072	58.7
	Wm1	1.41	.107		1.20	.130		1.05	.070		1.20	.150		1.35	.148	
	Hs2	-.173	.009		-.186	.010		-.141	.006		-.130	.016		-.095	.007	
	Const.	.604	.049	52.6	.707	.060	46.6									
	Wm1	1.29	.103		1.05	.122										
	Hs2	-.282	.014		-.278	.014										
	HSIG	.084	.014		.078	.009										
Hs2	Const.	.198	.034	34.2	.342	.055	44.5	.249	.016	35.2	.239	.035	36.4	.243	.055	22.9
	HSIG	.512	.012		.479	.017		.412	.007		.369	.013		.536	.014	
	Const.	.074	.012	3.9	.183	.020	6.0	.066	.006	4.3	.081	.013	5.0	.059	.015	1.6
	HSIG	1.69	.015		1.54	.018		1.69	.011		1.84	.029		1.56	.014	
	Hs1	-1.40	.017		-1.26	.020		-1.41	.012		-1.60	.031		-1.23	.016	
Sh2	Const.	3.86	.130	70.9	3.62	.139	69.2	3.96	.089	76.5	3.66	.180	82.3	4.20	.254	81.9
	Hs2/Hs	-3.88	.206		-3.59	.218		-3.93	.154		-3.17	.328		-3.95	.401	
	Const.	9.77	.967	65.5	7.22	.809	62.6							10.6	1.92	77.7
	Hs2/Hs	-7.06	.536		-5.50	.456								-7.39	1.19	
	Hs1/Hs	-6.21	.856		-4.67	.748								-4.64	1.63	
	Wm2/Wp	-.446	.070		.602	.085								-.368	.142	

Table 11e. Coefficients for prediction equations
Spectral TYPE1 - Classes 51,52,53

		Station													
		46005			46004			103			211			503W		
	Npts:	2754			2192			3790			1608			1292		
Par.	Var.	Coef	Std	%Res	Coef	Std	%Res	Coef	Std	%Res	Coef	Std	%Res	Coef	Std	%Res
Wm1	Const.	.350	.009	82.9	.350	.009	77.7	.375	.008	90.6	.458	.013	94.6	.361	.009	81.6
	Wp	.292	.012		.324	.013		.235	.012		.163	.017		.249	.015	
	Const.	.027	.009	41.8	.070	.010	44.5	.108	.008	55.1	.077	.015	56.0	.256	.010	67.7
	Wp	.155	.009		.180	.010		.141	.009		.116	.013		.186	.014	
	Wm2	.406	.008		.359	.009		.344	.007		.374	.011		.158	.010	
Hs1	Const.	-.180	.016	21.5	-.216	.021	20.2	-.188	.012	16.3	-.236	.017	13.4	-.080	.029	22.9
	HSIG	.770	.008		.803	.009		.858	.006		.909	.009		.671	.010	
	Const.	.019	.006	2.4	.033	.007	2.4	.002	.004	1.7	.005	.007	1.9	.028	.011	3.1
	HSIG	1.29	.004		1.25	.009		1.27	.003		1.27	.005		1.43	.009	
	Hs2	-.878	.006		-.818	.006		-.833	.005		-.818	.008		-1.07	.012	
Sh1	Const.	3.69	.095	58.2	3.13	.113	55.6	.706	.070	55.	.530	.072	57.1	5.03	.266	74.9
	Hs1/Hs	-7.13	.164		-7.08	.170		-5.33	.111		-3.26	.124		-5.64	.323	
	Wm1	3.32	.166		3.40	.175		5.14	.135		3.42	.130		-2.12	.455	
	Wm1/Wp	2.19	.176		2.69	.134		2.64	.092		1.63	.095		3.28	.286	
Wm2	Const.	.361	.012	46.2	.367	.015	50.6	.351	.012	58.3	.492	.019	58.7	.290	.031	78.5
	Wm1	1.21	.021		1.20	.026		1.14	.022		1.07	.032		1.13	.060	
	Const.	.627	.014	36.0	.699	.018	37.5	.565	.014	49.2	.685	.022	51.4	.651	.031	56.9
	Wm1	1.03	.020		.972	.024		1.01	.021		.985	.030		.839	.053	
	Hs2	-.122	.004		-.133	.005		-.128	.005		-.138	.009		-.112	.005	
	Const.	.670	.014	32.2	.723	.017	34.3	.588	.014	48.0						
	Wm1	.904	.020		.872	.024		.929	.022							
	Hs2	-.235	.008		-.216	.007		-.190	.008							
	HSIG	.094	.005		.072	.005		.050	.005							
Hs2	Const.	.227	.018	34.3	.304	.024	41.5	.228	.014	42.7	.295	.019	46.4	.101	.025	16.6
	HSIG	.599	.008		.551	.010		.498	.007		.437	.010		.712	.009	
	Const.	.044	.006	3.8	.071	.008	4.8	.026	.005	4.5	.046	.008	6.4	.036	.009	2.3
	HSIG	1.38	.006		1.42	.008		1.42	.006		1.39	.010		1.25	.007	
	Hs1	-1.01	.007		-1.08	.008		-1.07	.006		-1.05	.011		-.807	.009	
Sh2	Const.	3.86	.082	79.5	3.70	.084	78.2	3.97	.064	78.8	3.92	.100	80.8	3.69	.175	91.8
	Hs2/Hs	-2.86	.107		-2.80	.113		-3.00	.094		-2.78	.142		-2.42	.225	
	Const.	9.46	.392	72.6	8.44	.404	72.8	6.86	.401	73.7	6.74	.542	77.3	9.42	.722	83.4
	Hs2/Hs	-6.57	.286		-5.77	.282		-4.68	.281		-4.45	.377		-6.28	.561	
	Hs1/Hs	-3.77	.308		-3.36	.327		-1.20	.310		-1.53	.435		-3.20	.523	
	Wm2/Wp	-.234	.043		-.184	.050		-.586	.040		-.370	.079		-.446	.066	

For the multiple peak groups, Table 11d and e , ωm1 showed better prediction by ωp for Classes 41,42,43 while ωm2 had lower residual variances for Classes 51,52,53. As with the single peak classes, HS1 was well predicted by HSIG with a steeper slope in Table 11d indicating that the first set of parameters were generally representing the major peak of the spectra. There was an approximately 77-23% split of the total heave variance. For Stn. 46005, this implies that SH1 = 1.78 and SH2 = 2.0 (using the first set of prediction equations). For Type 1 classes 51,52,53, the total heave variance split was close to 50-50%. There was a stronger dependence on the period for SH1 prediction while SH2 = 1.8 using the first set of prediction equations and HS2/HS of 71 (i.e. 50% variance ratio). For these and, in general, any previous calculation of the shape parameters, the prediction equations suggest a parameter value less than the means in the summary tables and closer to the modal distribution values included in Table 7 . This suggests that the scatter in the parameter values may be biasing the mean calculations and may be resulting from experimental variability as opposed to geophysical variability.

6.2 Statistical Probability Spectra

A second conclusion that may be drawn from the instances of very high residual variances listed in Tables 10 and 11 , is that no underlying relationship between the fit parameters exists or has sufficient confidence associated with it to be used for prediction. This is particularly true for the shape parameters. However, one can obtain a statistical description of the most probable and extreme model spectra based on the probability distributions of the individual fit parameters. Following the procedure outlined in Ochi and Hubble (1976), families of model spectra were generated for scanned single and double peak spectra in three significant wave height groups (i.e. a total of six groups 1: TYPE 1 classes 11, 21, 31; 2: 12, 22, 32; 3: 13, 23, 33; 4: 41 and 51; 5: 42 and 52; and 6: 43 and 53). Briefly, the procedure consisted of first determining the probability distribution of one of the six fit parameters (i.e. target parameter). From the fitted probability density function, the modal and 90% confidence limit values (i.e. associated with a 5% and 95% probability) of the target parameter were obtained. The recorded model parameters were then scanned for occurrences of a target parameter falling within 5% of the modal and 90% confidence limits and the average value for each of the remaining five co-occurring parameters would be calculated. This process was then repeated for each of the six fit parameters and resulted in a family of 18 spectra for each spectral group examined. Both a bounded normal and gamma probability distribution were fitted to the histogram of the probability density distribution, by means of a non-linear procedure similar to that in

Section 4 , and the residual error was calculated. The fit residual errors indicated that the frequency and variance parameters were best represented by the bounded normal distribution. This was also generally true for the shape parameters, Ochi and Hubble (1976) fit a gamma function to the probability density distribution of the two shape parameters. Examples of the probability histogram and fitted distributions for the six fit parameters are shown in Figs. 22 a to c for Stn. 46005 single peak spectra. The gamma function will fit the mode of the shape parameter distribution well and handle the behavior of the larger parameter values while underestimating the probability associated with the lower parameter values. The resulting parameter values are listed in Tables 12a to e . Results were omitted when there were fewer than 50 data values associated with any of the six spectral groups. The highlighted entries correspond to the 5% (L) probability value, mode (M) and 95% (U) probability value obtained from the analytical probability density functions for the target parameter. Reading across the row provides the average values for the remaining five fit parameters. Entries of zero are possible as there may have been no observations of the target parameter falling within the 5% range of the statistically predicted value. Both the bounded normal and gamma probability values are included for the SH1 and SH2 parameters as the mode and confidence limit values are different for the two distributions. The relative behavior of the fit parameters in Tables 12a to e , between spectral groups for the same target parameter, is similar to the overall behavior discussed in Section 4.3 (e.g. ωm1 varies inversely with HS1, HS2 and directly with ωm2, SH1 and SH2). Examples of the 5%, mode and 95% statistically predicted spectra are included in Fig. 23 for Group 2 (plot 1, 3, 5, 7, 9 and 11) and Group 4 (plot 2, 4, 6, 81 10 and 12) spectra associated with the target parameters ωm1, HS1, SH1, ωm2, HS2 and SH2, respectively. As can be seen in Fig. 23 , there is a considerable difference in spectral shape, particularly for the double peak Group 4 spectra, when different target parameters are used. These statistical spectra would be useful as design spectra for various applications as they represent a wide variety of spectral types using a relatively limited number of parameter sets.

6.3 Analytical Analysis

In this section, relationships between a three-parameter Ochi and Hubble model given as:

$$E_{OH}(\omega) = \frac{1}{4} \frac{\left(\frac{4\lambda+1}{4} \omega m^4\right)^{\lambda} Hs^2 \cdot e^{-\frac{(4\lambda+1)}{4}\left(\frac{\omega m}{\omega}\right)^4}}{\Gamma(\lambda)\ \omega^{4\lambda+1}}$$

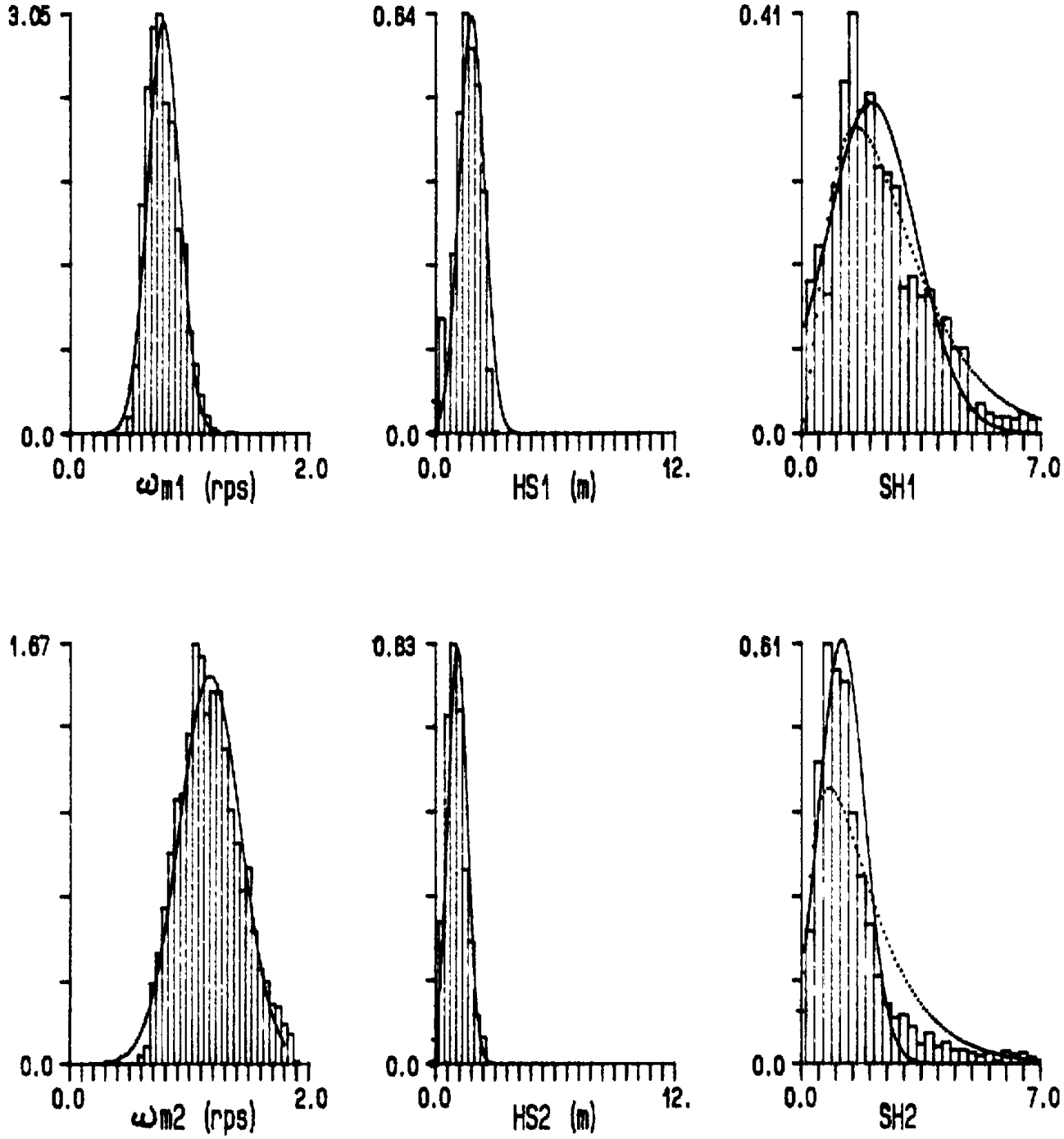

Fig. 22a Probability density histogram, fitted bounded normal distribution (solid line) and gamma distribution (dashed line) for the six fit parameters. Group 1 spectra (Type 1 classes 11, 21 and 31).

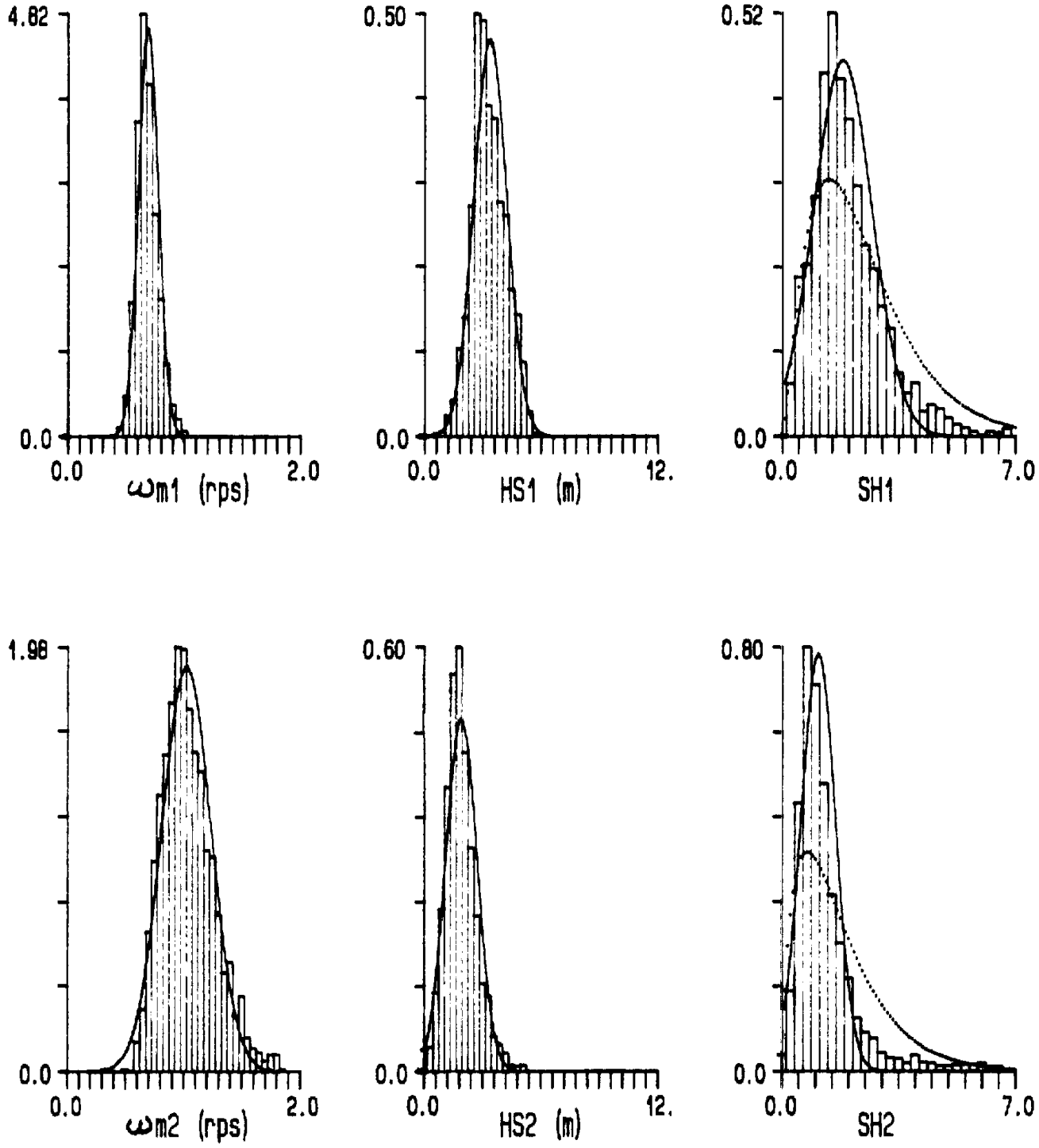

Fig. 22b Probability density histogram, fitted bounded normal distribution (solid line) and gamma distribution (dashed line) for the six fit parameters. Group 2 spectra (Type 1 classes 12, 22 and 32).

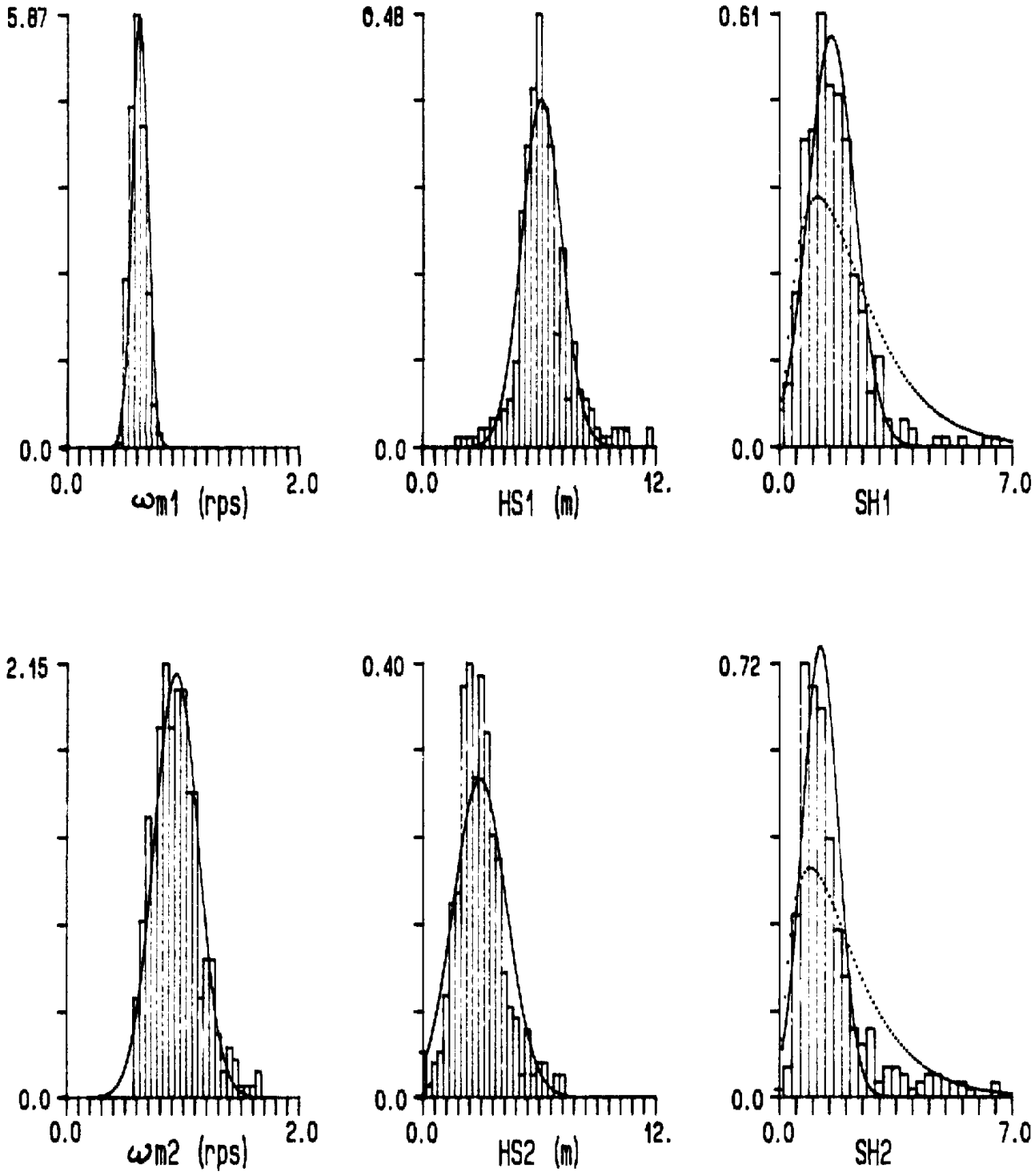

Fig. 22c Probability density histogram, fitted bounded normal distribution (solid line) and gamma distribution (dashed line) for the six fit parameters. Group 3 spectra (Type 1 classes 13, 23 and 33).

Table 12a. Fit parameter values for the modal and 90% confidence spectra. Stn. 46005.
L = 5% prob. value; M = Mode; U = 95% prob. value
1: TYPE1 class 11,21,31; 2: 12,22,32; 3: 13,23,33; 4: 41,51; 5: 42,52; 6: 43,53

		Wm1			HS1			SH1			Wm2			HS2			SH2		
		L	M	U	L	M	U	L	M	U	L	M	U	L	M	U	L	M	U
	1	0.56	0.78	0.99	1.91	1.70	1.46	2.19	2.61	2.68	0.96	1.19	1.39	1.14	1.10	0.87	1.46	1.80	2.67
	2	0.54	0.69	0.82	3.46	3.23	2.96	2.07	2.67	3.07	0.91	1.11	1.37	1.99	1.73	1.36	1.51	1.77	2.04
Wm1	3	0.51	0.62	0.73	6.20	5.62	0.00	2.00	2.26	0.00	0.91	1.14	0.00	2.66	2.06	0.00	1.72	1.93	0.00
	4	0.47	0.68	0.87	1.19	1.36	1.36	2.69	2.63	2.78	1.00	1.19	1.36	1.27	1.16	0.95	1.68	1.73	2.34
	5	0.51	0.66	0.79	2.73	3.34	3.00	2.02	2.67	3.02	0.93	1.11	1.35	2.19	1.68	1.43	1.81	1.52	2.48
	1	0.47	0.61	0.60	0.75	1.81	2.75	3.46	2.72	2.42	0.89	0.98	1.00	1.47	1.19	1.19	1.40	1.48	1.58
	2	0.46	0.51	0.51	1.95	3.37	4.75	3.65	2.31	2.13	0.62	0.84	0.86	3.17	2.10	2.05	0.97	1.33	1.43
HS1	3	0.38	0.44	0.43	4.35	6.11	7.75	3.63	1.88	1.77	0.50	0.74	0.77	5.74	3.25	3.10	0.89	1.54	1.65
	4	0.44	0.49	0.53	0.25	1.06	2.15	4.88	3.12	2.74	0.92	0.97	1.03	0.60	1.10	1.20	1.39	1.48	1.64
	5	0.44	0.46	0.47	1.65	2.70	3.65	3.25	2.54	2.21	0.75	0.82	0.88	2.92	2.54	2.32	1.71	1.53	1.73
	1	0.63	0.60	0.61	1.47	1.91	1.26	0.37	2.03	4.21	0.93	1.02	0.92	1.06	1.16	1.48	3.00	1.35	1.37
	2	0.51	0.50	0.52	3.25	3.58	3.01	0.46	1.81	3.21	0.76	0.88	0.79	1.84	1.90	2.48	2.46	1.30	1.17
SH1	3	0.39	0.41	0.46	6.59	6.63	5.60	0.46	1.55	2.71	0.72	0.75	0.77	2.89	3.33	3.34	3.32	1.48	1.29
	4	0.54	0.51	0.53	1.76	1.17	0.88	0.54	2.42	4.71	1.15	1.00	0.91	1.07	1.27	1.37	2.35	1.57	1.37
	5	0.43	0.49	0.47	3.40	2.81	2.33	0.54	2.01	3.54	0.84	0.88	0.76	1.63	2.41	2.80	5.06	1.67	1.48
	1	0.58	0.59	0.64	1.95	1.87	1.33	0.54	1.58	5.62	0.86	1.08	0.85	0.87	1.04	1.58	3.68	1.33	1.16
	2	0.51	0.49	0.53	3.25	3.68	2.33	0.46	1.42	5.37	0.76	0.93	0.67	1.84	1.73	3.16	2.46	1.26	1.01
SH1	3	0.33	0.42	0.37	4.93	6.58	3.22	0.37	1.17	4.96	0.45	0.84	0.44	6.15	2.53	6.43	0.98	1.63	1.03
G	4	0.57	0.55	0.57	1.56	1.27	0.79	0.71	1.92	6.12	1.25	1.09	0.91	0.88	1.18	1.32	3.06	1.60	1.15
	5	0.43	0.49	0.50	3.40	3.09	2.07	0.54	1.58	5.54	0.84	0.95	0.78	1.63	2.06	2.68	5.06	1.67	0.86
	1	0.52	0.67	0.69	1.69	1.79	2.00	2.54	2.32	1.47	0.74	1.17	1.59	1.48	0.96	0.53	1.43	1.51	2.84
	2	0.46	0.56	0.60	3:27	3.67	3.67	2.16	2.10	1.48	0.68	1.03	1.36	2.52	1.64	1.00	1.52	1.42	1.76
Wm2	3	0.41	0.47	0.52	5.87	6.63	6.41	1.82	1.79	1.36	0.62	0.94	1.24	3.94	2.34	1.34	1.43	1.41	2.19
	4	0.44	0.60	0.73	0.94	1.37	1.39	3.29	2.30	1.62	0.79	1.20	1.59	1.40	1.10	0.70	1.32	1.81	3.37
	5	0.41	0.51	0.61	2.58	3.09	3.29	2.46	1.87	1.74	0.71	1.04	1.36	2.77	1.79	1.13	1.48	1.89	2.68
	1	0.61	0.63	0.55	1.53	1.82	1.58	1.70	2.29	3.01	1.29	1.04	0.79	0.35	1.11	1.85	3.00	1.52	1.01
	2	0.45	0.53	0.47	3.72	3.38	3.13	1.02	2.10	2.75	1.21	0.87	0.67	0.65	1.91	3.15	1.98	1.33	0.97
HS2	3	0.45	0.43	0.43	6.95	6.48	4.89	0.94	1.79	2.79	1.29	0.76	0.58	0.85	2.93	5.15	2.58	1.71	1.00
	4	0.61	0.53	0.50	0.82	1.19	1.41	1.30	2.80	3.16	1.24	1.03	0.87	0.35	1.13	1.85	4.11	1.53	1.31
	5	0.54	0.47	0.41	3.33	2.78	2.45	0.97	2.07	2.78	1.31	0.88	0.70	0.95	2.24	3.45	3.84	1.59	1.64
	1	0.52	0.60	0.65	2.52	1.67	1.68	1.18	2.65	2.36	1.11	0.99	1.14	1.01	1.29	1.03	0.21	1.17	2.29
	2	0.47	0.49	0.53	3.39	3.38	3.61	1.54	2.23	1.90	0.69	0.85	0.95	2.18	2.11	1.72	0.29	1.09	1.87
SH2	3	0.40	0.42	0.48	8.20	6.40	6.84	1.06	1.78	1.58	0.69	0.77	0.92	3.09	3.21	2.42	0.37	1.22	2.04
	4	0.50	0.51	0.55	1.29	1.11	1.31	3.16	2.86	2.34	0.83	1.00	1.09	1.68	1.24	1.07	0.21	1.20	2.71
	5	0.48	0.46	0.47	2.75	2.52	2.81	1.69	2.33	1.82	0.63	0.86	0.94	1.82	2.43	2.22	0.21	1.30	2.79
	1	0.52	0.57	0.61	2.52	1.73	2.19	1.18	2.59	1.32	1.11	0.92	1.12	1.01	1.39	0.73	0.21	0.83	4.37
	2	0.47	0.47	0.53	3.52	3.35	3.71	1.48	2.37	1.04	0.61	0.78	0.93	1.77	2.41	1.29	0.21	0.75	4.37
SH2	3	0.00	0.42	0.43	0.00	6.16	6.06	0.00	2.09	0.75	0.00	0.72	0.76	0.00	3.63	2.14	0.29	0.92	4.62
G	4	0.50	0.50	0.61	1.29	1.14	1.52	3.16	3.00	1.48	0.83	0.96	1.26	1.68	1.29	0.95	0.21	0.83	4.46
	5	0.37	0.45	0.63	2.80	2.63	3.00	1.70	2.37	1.22	0.70	0.82	1.06	1.84	2.64	1.87	0.29	0.92	4.62

Table 12b. Fit parameter values for the modal and 90% confidence spectra. Stn. 46004.
L = 5% prob. value; M = Mode; U = 95% prob. value
1: 11,21,31; 2: 12,22,32; 3: 13,23,33; 4: 41,51; 5: 42,52; 6: 43,53

		Wm1			HS1			SH1			Wm2			HS2			SH2		
		L	M	U	L	M	U	L	M	U	L	M	U	L	M	U	L	M	U
	1	0.57	0.81	1.02	1.94	1.82	1.56	2.10	2.54	3.54	0.96	1.24	1.46	1.30	1.16	0.95	1.42	1.75	2.22
	2	0.57	0.71	0.84	3.45	3.27	3.11	2.35	2.86	3.14	0.95	1.17	1.30	2.08	1.71	1.44	1.36	1.71	2.47
Wm1	3	0.52	0.65	0.76	6.01	5.81	0.00	2.14	2.43	0.00	0.91	1.12	0.00	2.75	2.31	0.00	1.76	1.66	0.00
	4	0.49	0.72	0.94	1.36	1.52	1.57	2.47	2.56	2.47	1.00	1.24	1.51	1.39	1.17	0.89	1.48	1.87	2.44
	5	0.52	0.69	0.82	2.92	3.02	3.04	2.08	2.63	4.69	0.96	1.24	1.24	2.15	1.59	1.88	1.84	2.24	1.67
	1	0.53	0.63	0.63	0.95	1.91	2.75	3.24	2.58	2.36	0.89	1.00	1.03	1.50	1.29	1.29	1.39	1.43	1.50
	2	0.48	0.54	0.53	1.95	3.40	4.75	3.90	2.44	2.22	0.62	0.87	0.88	3.20	2.19	2.15	0.85	1.24	1.35
HS1	3	0.39	0.46	0.46	4.55	5.95	7.25	2.88	2.10	1.95	0.53	0.78	0.81	5.30	3.18	3.01	0.98	1.46	1.55
	4	0.00	0.52	0.56	0.25	1.18	2.35	0.00	3.02	2.64	0.00	1.01	1.06	0.00	1.21	1.30	0.00	1.38	1.59
	5	0.44	0.49	0.49	1.65	2.73	3.65	4.06	2.60	2.30	0.70	0.86	0.91	3.06	2.50	2.32	1.43	1.54	1.66
	1	0.60	0.62	0.68	1.97	1.84	1.52	0.37	2.02	4.12	0.90	1.03	1.02	1.09	1.25	1.56	2.81	1.22	1.31
	2	0.52	0.52	0.56	3.22	3.61	3.03	0.46	1.89	3.37	0.76	0.89	0.85	2.06	2.05	2.64	2.79	1.22	1.26
SH1	3	0.40	0.46	0.50	5.93	6.38	5.74	0.54	1.73	2.96	0.74	0.82	0.82	3.24	3.01	3.41	1.37	1.36	1.54
	4	0.59	0.53	0.54	1.69	1.39	1.01	0.46	2.33	4.62	1.10	1.05	0.88	0.85	1.37	1.53	3.36	1.45	1.11
	5	0.54	0.49	0.47	3.31	2.97	2.20	0.54	1.95	3.46	0.85	0.93	0.80	1.76	2.34	2.82	2.02	1.52	1.30
	1	0.68	0.64	0.65	1.51	1.97	1.42	0.54	1.58	5.62	0.86	1.14	0.89	1.04	1.13	1.76	3.56	1.46	0.98
	2	0.51	0.51	0.55	3.78	3.74	2.28	0.54	1.50	5.46	0.78	0.92	0.70	2.17	1.93	2.98	3.30	1.16	1.01
SH1	3	0.33	0.43	0.37	6.78	6.35	1.99	0.46	1.33	5.21	0.70	0.82	0.48	1.92	2.73	6.46	4.82	1.32	0.98
G	4	0.56	0.53	0.65	1.45	1.36	1.01	0.71	1.83	5.96	1.22	1.07	0.93	0.93	1.34	1.56	3.43	1.55	1.01
	5	0.54	0.47	0.58	3.31	3.12	2.16	0.54	1.50	5.54	0.85	0.94	0.77	1.76	2.22	3.00	2.02	1.71	0.90
	1	0.54	0.69	0.77	1.55	1.97	2.05	2.65	2.28	1.81	0.77	1.20	1.61	1.58	1.05	0.66	1.31	1.55	2.39
	2	0.48	0.57	0.61	3.27	3.72	3.55	2.24	2.14	1.50	0.69	1.06	1.41	2.64	1.72	1.02	1.34	1.36	1.88
Wm2	3	0.40	0.51	0.40	6.67	6.46	7.68	1.77	1.91	0.95	0.69	1.00	1.29	3.22	2.31	0.93	1.22	1.47	2.78
	4	0.45	0.63	0.75	1.02	1.45	1.46	3.27	2.29	1.61	0.81	1.23	1.64	1.47	1.15	0.69	1.17	1.66	3.09
	5	0.45	0.54	0.58	2.70	3.16	3.51	2.35	1.78	1.05	0.76	1.10	1.42	2.75	1.71	0.88	1.70	1.77	2.82
	1	0.61	0.65	0.57	1.65	1.94	1.56	1.03	2.44	2.94	1.38	1.04	0.79	0.35	1.23	2.05	3.48	1.47	0.93
	2	0.48	0.54	0.47	3.59	3.58	3.05	1.05	2.16	2.83	1.31	0.91	0.65	0.65	2.00	3.35	2.57	1.36	0.96
HS2	3	0.40	0.47	0.42	8.40	6.49	6.43	0.90	1.88	1.70	1.03	0.83	0.63	1.35	2.83	4.25	1.52	1.46	1.03
	4	0.89	0.57	0.50	0.84	1.34	1.44	1.71	2.64	3.10	1.67	1.08	0.89	0.35	1.23	2.05	4.35	1.43	1.19
	5	0.62	0.52	0.42	3.55	2.95	2.52	1.11	2.22	3.00	1.43	0.96	0.71	0.85	2.08	3.25	3.55	1.59	1.47
	1	0.66	0.61	0.69	1.71	1.83	1.86	1.87	2.52	2.31	0.86	1.02	1.17	1.24	1.36	1.00	0.29	1.12	2.12
	2	0.46	0.52	0.56	3.75	3.46	3.69	1.26	2.34	2.11	0.96	0.89	1.00	1.56	2.21	1.87	0.29	1.06	1.79
SH2	3	0.00	0.46	0.46	0.00	6.17	6.01	0.00	1.98	1.98	0.00	0.85	0.82	0.00	3.02	2.67	0.37	1.25	2.12
	4	0.55	0.55	0.62	1.14	1.20	1.44	2.06	2.85	2.19	1.28	1.04	1.19	1.27	1.32	1.16	0.21	1.15	2.62
	5	0.47	0.52	0.51	3.06	2.92	2.90	2.58	2.48	2.07	0.71	0.95	0.98	2.84	2.37	2.29	0.29	1.30	2.62
	1	0.59	0.58	0.62	1.81	1.69	2.00	2.01	2.83	1.31	0.90	0.91	0.96	1.89	1.58	0.97	0.21	0.75	4.37
	2	0.53	0.50	0.54	3.94	3.12	4.43	1.05	2.69	1.04	0.84	0.79	0.88	1.92	2.55	1.78	0.21	0.75	4.29
SH2	3	0.51	0.42	0.40	5.44	5.73	6.57	2.16	2.08	0.81	0.64	0.74	0.71	3.82	3.47	1.69	0.29	0.92	4.54
G	4	0.55	0.53	0.70	1.14	1.27	1.59	2.06	2.77	1.59	1.28	0.98	1.41	1.27	1.32	0.87	0.21	0.75	4.37
	5	0.47	0.53	0.57	3.06	2.94	3.05	2.58	2.77	1.16	0.71	0.91	1.05	2.84	2.39	1.71	0.29	0.92	4.54

Table 12c. Fit parameter values for the modal and 90% confidence spectra. Stn. 103.
L = 5% prob. value; M = Mode; U = 95% prob. value
1: 11,21,31; 2: 12,22,32; 3: 13,23,33; 4: 41,51; 5: 42,52; 6: 43,53

		Wa1			HS1			SH1			Wa2			HS2			SH2		
		L	M	U	L	M	U	L	M	U	L	M	U	L	M	U	L	M	U
	1	0.56	0.72	0.86	1.84	1.74	1.57	1.56	1.99	2.18	1.05	1.19	1.41	0.77	0.83	0.57	1.78	2.07	2.87
	2	0.54	0.67	0.77	3.49	3.46	3.09	1.70	2.18	3.19	1.00	1.24	1.26	1.34	1.23	1.40	1.90	1.76	1.62
Wa1	3	0.52	0.64	0.74	6.22	0.00	0.00	1.76	0.00	0.00	0.97	0.00	0.00	2.26	0.00	0.00	1.54	0.00	0.00
	4	0.49	0.67	0.82	1.50	1.41	1.31	1.59	2.06	2.89	0.96	1.12	1.27	1.05	0.88	0.76	2.00	2.24	2.28
	5	0.52	0.66	0.77	3.10	3.13	2.98	1.82	2.26	3.35	0.89	1.14	1.22	1.87	1.45	1.47	2.15	2.11	2.63
	1	0.42	0.54	0.54	0.75	1.81	2.75	1.90	1.65	1.62	0.77	0.99	1.01	1.23	0.84	0.86	1.50	1.75	1.77
	2	0.41	0.50	0.50	2.25	3.33	4.35	1.48	1.62	1.60	0.53	0.91	0.94	3.21	1.44	1.41	0.80	1.65	1.71
HS1	3	0.41	0.44	0.44	5.05	6.09	6.95	1.34	1.32	1.32	0.56	0.81	0.84	4.64	2.48	2.33	1.42	1.94	2.07
	4	0.39	0.47	0.50	0.25	1.09	2.25	2.65	1.86	1.81	0.79	0.93	0.96	0.65	0.87	0.98	0.70	1.69	1.86
	5	0.42	0.48	0.47	1.85	3.01	4.05	2.32	1.74	1.68	0.66	0.82	0.84	3.00	1.98	1.92	1.33	1.94	2.09
	1	0.51	0.55	0.54	1.41	1.89	1.75	0.29	1.37	2.62	0.70	1.14	0.92	1.48	0.72	0.93	2.27	1.67	1.56
	2	0.43	0.49	0.56	2.75	3.56	3.46	0.37	1.32	2.37	0.63	1.01	0.98	2.35	1.23	1.70	1.63	1.64	1.53
SH1	3	0.00	0.40	0.50	0.00	6.50	6.20	0.21	1.11	2.12	0.00	0.85	0.91	0.00	2.06	2.31	0.00	1.86	1.55
	4	0.47	0.49	0.54	1.18	1.23	1.17	0.29	1.43	3.12	0.88	1.02	0.94	0.89	0.96	1.03	2.70	1.75	1.61
	5	0.55	0.47	0.52	2.98	3.22	3.16	0.29	1.48	2.96	0.88	0.92	0.87	2.05	1.78	2.06	3.96	1.68	1.58
	1	0.51	0.51	0.55	1.41	1.92	1.26	0.29	0.92	4.62	0.70	1.11	0.78	1.48	0.77	1.43	2.27	2.11	1.43
	2	0.00	0.46	0.63	0.00	3.62	2.73	0.29	0.92	4.62	0.00	1.03	0.86	0.00	1.08	1.82	0.00	1.81	1.60
SH1	3	0.00	0.00	0.00	0.00	0.00	0.00	0.21	0.75	4.37	0.00	0.00	0.00	0.00	0.00	0.00	0.00	0.00	0.00
G	4	0.47	0.48	0.68	1.18	1.26	1.16	0.29	1.00	4.71	0.88	1.02	1.01	0.89	0.92	1.07	2.70	1.87	1.84
	5	0.55	0.48	0.62	2.98	3.27	2.82	0.29	1.00	4.71	0.88	0.90	0.94	2.05	1.54	2.10	3.96	2.63	1.74
	1	0.47	0.58	0.58	1.42	1.83	1.85	1.17	1.73	1.26	0.64	1.17	1.69	1.22	0.65	0.35	2.31	1.37	2.24
	2	0.44	0.55	0.58	3.56	3.58	3.85	1.86	1.70	1.17	0.74	1.12	1.49	1.71	1.08	0.70	1.98	1.65	2.25
Wa2	3	0.00	0.49	0.00	0.00	6.19	0.00	0.00	1.34	0.00	0.64	1.06	1.46	0.00	1.57	0.00	0.00	2.32	0.00
	4	0.44	0.55	0.66	1.09	1.35	1.39	1.80	1.78	1.72	0.76	1.11	1.46	1.10	0.87	0.65	1.70	1.94	2.48
	5	0.44	0.53	0.64	3.05	3.25	3.16	1.60	1.81	1.62	0.74	1.02	1.29	2.07	1.54	0.98	2.27	2.29	2.70
	1	0.50	0.55	0.50	1.81	1.82	1.70	0.69	1.79	1.57	1.59	1.00	0.74	0.15	0.75	1.45	2.38	1.76	1.61
	2	0.49	0.52	0.46	3.67	3.50	3.57	0.67	1.68	1.80	0.94	0.99	0.75	0.35	1.26	2.15	1.74	1.64	1.48
HS2	3	0.41	0.46	0.32	6.18	6.30	8.06	0.87	1.64	0.50	1.11	0.91	0.39	0.85	2.21	3.45	3.25	1.80	3.04
	4	0.50	0.50	0.49	0.62	1.21	1.56	1.95	1.72	1.85	1.07	0.96	0.87	0.25	0.89	1.55	3.21	1.92	1.49
	5	0.49	0.49	0.40	2.99	3.19	2.76	1.20	1.69	1.76	1.13	0.86	0.67	0.75	1.87	2.95	1.29	2.17	1.53
	1	0.57	0.54	0.55	1.56	1.77	1.85	1.13	1.79	1.39	1.01	1.04	1.02	0.73	0.86	0.77	0.21	1.30	2.71
	2	0.45	0.51	0.52	3.57	3.58	3.60	1.19	1.86	1.52	1.04	0.99	1.02	1.21	1.40	1.19	0.29	1.35	2.54
SH2	3	0.39	0.48	0.59	7.74	6.06	6.49	1.08	1.44	1.49	0.81	0.99	1.17	2.11	1.87	1.58	0.37	1.44	2.54
	4	0.44	0.49	0.53	1.12	1.20	1.36	2.11	1.88	1.67	0.85	0.94	1.03	1.27	1.03	0.89	0.29	1.38	2.96
	5	0.00	0.49	0.49	0.00	3.13	3.05	0.00	1.99	1.79	0.00	0.89	0.88	0.00	1.89	1.80	0.37	1.48	2.79
	1	0.51	0.51	0.56	1.55	1.61	1.75	1.69	1.77	0.86	1.07	0.96	1.06	0.98	1.00	0.55	0.29	0.92	4.62
	2	0.45	0.47	0.48	3.57	3.35	3.61	1.19	1.50	0.93	1.04	0.95	0.82	1.21	1.41	1.54	0.29	1.00	4.62
SH2	3	0.39	0.42	0.00	7.74	5.06	0.00	1.08	1.54	0.00	0.81	0.72	0.00	2.11	3.26	0.00	0.37	1.17	4.96
G	4	0.44	0.47	0.53	1.12	1.17	1.49	2.11	1.95	1.19	0.85	0.89	0.97	1.27	1.12	0.79	0.29	1.00	4.71
	5	0.00	0.46	0.49	0.00	2.87	3.32	0.00	1.82	0.99	0.00	0.81	0.80	0.00	2.07	1.71	0.37	1.17	4.96

Table 12d. Fit parameter values for the modal and 90% confidence spectra. Stn. 211.
L = 5% prob. value; M = Mode; U = 95% prob. value
1: 11,21,31; 2: 12,22,32; 3: 13,23,33; 4: 41,51; 5: 42,52; 6: 43,53

		Wa1			HS1			SH1			Wa2			HS2			SH2		
		L	M	U	L	M	U	L	M	U	L	M	U	L	M	U	L	M	U
	1	0.61	0.83	1.04	1.92	1.65	1.54	1.47	1.99	3.11	1.10	1.24	1.59	0.87	0.92	0.62	1.85	1.99	3.24
	2	0.57	0.72	0.84	3.55	3.28	2.60	1.43	1.79	2.62	1.01	1.14	1.26	1.53	1.51	1.41	1.79	1.95	1.78
Wa1	3	0.52	0.64	0.74	6.46	0.00	0.00	1.47	0.00	0.00	1.00	0.00	0.00	2.02	0.00	0.00	1.83	0.00	0.00
	4	0.47	0.73	0.98	0.98	1.42	1.17	1.33	1.77	2.96	1.05	1.27	1.42	0.86	0.86	0.80	1.87	2.22	2.64
	5	0.57	0.71	0.82	3.19	2.83	3.04	1.47	1.90	1.67	1.01	1.23	1.33	1.69	1.31	1.35	2.59	2.10	3.11
	1	0.42	0.63	0.63	0.55	1.77	2.85	1.45	1.57	1.55	0.81	1.05	1.09	1.44	0.95	0.94	1.34	1.89	1.88
	2	0.46	0.55	0.54	1.95	3.46	4.85	1.36	1.32	1.30	0.63	0.99	1.00	3.17	1.50	1.49	1.00	1.79	1.85
HS1	3	0.38	0.44	0.44	4.95	6.17	7.25	1.14	1.19	1.18	0.48	0.83	0.86	5.66	2.74	2.49	0.84	1.57	1.57
	4	0.00	0.49	0.56	0.15	0.98	2.35	0.00	1.47	1.46	0.00	1.04	1.12	0.00	0.83	0.93	0.00	1.82	2.05
	5	0.41	0.52	0.51	2.15	3.03	3.85	1.13	1.29	1.28	0.79	1.01	1.01	2.75	1.77	1.73	1.32	2.11	2.19
	1	0.47	0.62	0.72	1.16	1.77	1.62	0.29	1.42	2.71	0.74	1.17	1.16	1.16	0.87	1.03	2.07	1.51	1.82
	2	0.54	0.50	0.63	2.83	3.85	3.42	0.29	1.20	2.12	0.79	1.08	1.10	2.27	1.24	1.53	3.65	1.38	1.68
SH1	3	0.00	0.45	0.50	0.00	6.44	6.78	0.29	1.07	1.79	0.00	0.87	0.99	0.00	2.15	1.92	0.00	1.55	1.91
	4	0.50	0.50	0.67	1.25	1.10	1.26	0.29	1.32	2.46	0.84	1.10	1.21	1.12	0.95	0.95	2.65	2.04	1.74
	5	0.00	0.48	0.63	0.00	3.14	2.93	0.29	1.22	2.12	0.00	1.00	1.10	0.00	1.89	1.62	0.00	1.64	2.10
	1	0.47	0.57	0.87	1.16	1.83	1.36	0.29	0.92	4.62	0.74	1.13	1.23	1.16	0.84	1.08	2.07	2.19	1.56
	2	0.00	0.48	0.00	0.00	3.86	0.00	0.21	0.83	4.37	0.00	0.98	0.00	0.00	1.30	0.00	0.00	2.36	0.00
SH1	3	0.00	0.39	0.00	0.00	5.45	0.00	0.21	0.67	4.21	0.00	0.70	0.00	0.00	2.65	0.00	0.00	1.41	0.00
6	4	0.50	0.51	0.78	1.25	1.28	0.93	0.29	0.83	4.46	0.84	1.14	1.16	1.12	0.88	1.32	2.65	2.30	1.21
	5	0.00	0.48	0.00	0.00	3.02	0.00	0.21	0.83	4.37	0.00	0.99	0.00	0.00	1.70	0.00	0.00	2.83	0.00
	1	0.55	0.70	0.69	1.14	1.86	1.87	1.12	1.81	1.39	0.82	1.31	1.77	1.31	0.72	0.60	2.17	1.69	2.64
	2	0.51	0.56	0.53	3.82	3.73	3.65	1.19	1.44	1.05	0.87	1.23	1.58	1.56	1.01	0.60	2.16	1.69	3.18
Wa2	3	0.45	0.43	0.00	6.29	6.53	0.00	1.28	0.97	0.00	0.94	1.15	1.36	1.85	1.18	0.00	1.67	1.91	0.00
	4	0.45	0.62	0.69	0.74	1.34	1.36	1.18	1.64	1.13	0.87	1.30	1.73	0.89	0.90	0.58	1.80	2.09	3.78
	5	0.50	0.54	0.71	3.21	3.11	3.13	1.24	1.33	1.39	0.93	1.21	1.49	2.00	1.29	0.85	2.21	2.42	3.49
	1	0.60	0.65	0.55	1.50	1.83	1.34	1.24	1.69	1.52	1.51	1.11	0.88	0.25	0.86	1.45	2.57	1.79	1.57
	2	0.48	0.54	0.56	3.80	3.65	3.26	1.00	1.43	1.14	1.45	1.01	0.79	0.45	1.32	2.15	2.63	1.76	1.95
HS2	3	0.00	0.45	0.47	0.00	6.55	6.14	0.00	1.18	1.37	0.00	0.96	0.87	0.75	1.74	2.65	0.00	1.61	1.64
	4	0.40	0.61	0.55	0.51	1.27	1.53	0.63	1.57	1.51	0.81	1.20	1.04	0.25	0.86	1.45	1.14	2.13	1.57
	5	0.00	0.52	0.47	0.00	3.21	3.03	0.00	1.42	1.29	0.00	1.01	0.88	0.75	1.62	2.45	0.00	1.95	1.92
	1	0.56	0.61	0.65	2.49	1.71	1.77	1.30	1.64	1.56	1.21	1.11	1.17	0.80	0.99	0.75	0.37	1.47	2.71
	2	0.51	0.53	0.55	3.59	3.78	3.69	0.89	1.47	1.13	1.11	1.04	0.99	0.40	1.44	1.45	0.37	1.46	2.54
SH2	3	0.00	0.49	0.43	0.00	6.24	6.34	0.00	1.49	1.00	0.00	0.98	0.91	0.00	2.13	1.64	0.46	1.51	2.54
	4	0.46	0.57	0.57	0.83	1.24	1.29	0.93	1.51	1.28	1.13	1.11	1.17	1.08	0.95	0.82	0.29	1.60	3.46
	5	0.00	0.49	0.57	0.00	3.17	3.04	0.00	1.09	1.16	0.00	1.00	1.11	0.00	1.73	1.48	0.46	1.72	3.12
	1	0.56	0.58	0.66	2.49	1.52	1.87	1.30	1.57	0.85	1.21	1.06	0.94	0.80	1.11	0.81	0.37	1.08	4.87
	2	0.51	0.52	0.47	3.59	3.43	4.03	0.89	1.34	0.90	1.11	0.97	0.82	0.40	1.78	1.16	0.37	1.08	4.87
SH2	3	0.00	0.44	0.37	0.00	6.38	8.31	0.00	1.10	0.62	0.00	1.00	1.27	0.00	1.73	0.02	0.29	1.08	4.79
6	4	0.55	0.54	0.62	1.50	1.12	1.41	1.28	1.57	0.84	0.84	1.11	1.13	1.25	0.97	0.73	0.37	1.17	5.04
	5	0.00	0.51	0.54	0.00	3.26	3.41	0.00	1.51	0.85	0.00	0.99	0.92	0.00	1.83	1.53	0.46	1.33	5.29

Table 12e. Fit parameter values for the modal and 90% confidence spectra. Stn. 503W.
L = 5% prob. value; M = Mode; U = 95% prob. value
1: 11,21,31; 2: 12,22,32; 3: 13,23,33; 4: 41,51; 5: 42,52; 6: 43,53

		Wa1			HS1			SH1			Wa2			HS2			SH2		
		L	M	U	L	M	U	L	M	U	L	M	U	L	M	U	L	M	U
	1	0.47	0.66	0.84	0.84	1.60	1.26	3.44	2.46	1.18	0.79	0.98	0.97	1.56	1.24	1.76	1.97	1.94	3.92
	2	0.59	0.70	0.81	2.88	2.35	2.43	3.24	2.30	6.50	0.79	0.81	0.81	2.47	2.72	2.60	2.05	2.69	0.91
Wa1	4	0.52	0.69	0.84	1.47	1.10	0.76	3.11	2.83	2.55	0.88	1.12	1.28	1.45	1.16	0.84	1.89	1.78	2.71
	5	0.57	0.69	0.77	2.56	2.36	0.00	3.08	2.58	0.00	0.81	0.94	0.00	2.76	2.22	0.00	2.06	2.55	0.00
	6	0.51	0.62	0.73	5.53	0.00	0.00	4.22	0.00	0.00	0.66	0.00	0.00	3.74	0.00	0.00	3.08	0.00	0.00
	1	0.00	0.00	0.49	0.05	0.11	2.85	0.00	0.00	3.18	0.00	0.00	0.84	0.00	0.00	1.53	0.00	0.00	1.99
	2	0.40	0.51	0.51	1.15	2.91	4.55	2.89	3.35	3.39	0.66	0.72	0.73	3.55	2.76	2.64	2.53	2.05	1.98
HS1	4	0.26	0.49	0.51	0.15	1.01	2.05	1.13	3.62	3.48	0.67	0.95	0.92	2.53	1.11	1.31	0.88	1.72	1.71
	5	0.44	0.48	0.48	1.55	2.74	3.85	3.99	3.75	3.60	0.65	0.73	0.74	3.30	2.76	2.75	1.77	1.80	1.89
	6	0.46	0.42	0.43	3.45	5.32	7.05	6.16	3.83	3.75	0.55	0.61	0.62	5.54	4.23	4.00	1.43	2.01	2.15
	1	0.60	0.50	0.53	0.79	0.89	0.99	0.71	3.00	5.62	0.76	0.87	0.81	0.69	1.58	1.47	3.69	1.95	1.14
	2	0.00	0.48	0.59	0.00	2.07	3.39	0.79	3.41	6.12	0.00	0.72	0.71	0.00	2.78	2.64	0.00	2.12	2.00
SH1	4	0.61	0.52	0.44	1.25	1.12	1.04	0.62	3.17	6.21	1.09	0.94	0.81	1.09	1.32	1.40	4.17	1.74	1.64
	5	0.53	0.48	0.45	3.34	2.77	2.32	0.79	3.41	6.21	0.69	0.73	0.64	2.77	2.81	3.16	2.83	1.70	1.52
	6	0.00	0.43	0.41	0.00	5.55	3.99	0.87	3.69	6.46	0.00	0.68	0.54	0.00	3.73	5.04	0.00	2.14	1.79
	1	0.48	0.49	0.47	1.02	1.01	0.98	1.04	2.50	7.04	0.74	0.82	0.72	1.68	1.53	1.96	1.91	1.88	1.66
	2	0.46	0.50	0.00	1.38	2.76	0.00	1.37	3.08	7.79	0.71	0.74	0.00	3.45	2.56	0.00	1.64	1.01	0.00
SH1	4	0.51	0.52	0.47	1.42	1.15	0.98	1.12	2.67	7.21	0.95	0.95	0.75	1.36	1.30	1.56	2.15	1.59	2.24
G	5	0.47	0.48	0.00	3.43	2.79	0.00	1.29	2.92	7.54	0.91	0.74	0.00	2.14	2.71	0.00	1.34	1.87	0.00
	6	0.43	0.45	0.00	5.60	5.64	0.00	1.37	3.17	7.87	0.68	0.70	0.00	2.53	3.63	0.00	1.57	1.91	0.00
	1	0.45	0.51	0.64	0.77	0.90	1.92	3.73	2.72	1.91	0.73	1.01	1.27	1.66	1.38	0.64	1.74	1.74	1.73
	2	0.50	0.55	0.56	2.61	3.40	2.96	3.39	3.27	2.14	0.69	0.91	1.11	2.79	1.85	1.30	1.78	1.66	1.60
Wa2	4	0.44	0.56	0.58	1.22	1.18	1.09	4.04	3.20	2.03	0.64	1.05	1.44	1.57	1.26	0.74	2.13	1.60	2.38
	5	0.46	0.52	0.57	2.91	2.91	3.18	4.06	2.63	2.21	0.68	0.92	1.14	3.09	2.36	1.77	1.92	2.06	2.45
	6	0.43	0.49	0.00	5.11	6.64	0.00	3.52	4.59	0.00	0.64	0.81	0.96	4.23	2.52	0.00	1.98	2.80	0.00
	1	0.55	0.47	0.45	1.53	0.83	0.65	2.83	3.63	3.19	1.00	0.80	0.79	0.75	1.57	2.35	1.60	1.92	1.95
	2	0.52	0.53	0.44	3.30	3.21	1.61	2.65	3.57	3.31	0.98	0.71	0.63	1.05	2.49	3.95	2.11	1.37	2.63
HS2	4	0.51	0.51	0.50	0.62	1.23	1.50	3.34	3.47	3.96	1.15	0.91	0.72	0.35	1.28	2.15	3.55	1.62	1.38
	5	0.53	0.50	0.46	3.13	2.52	2.55	2.19	3.86	4.25	0.94	0.76	0.67	1.35	2.61	3.75	2.58	1.67	1.80
	6	0.46	0.40	0.38	6.34	5.52	2.58	3.09	3.23	5.50	0.78	0.59	0.61	2.35	4.02	5.55	3.62	2.27	0.94
	1	0.00	0.49	0.53	0.00	0.89	1.11	0.00	3.21	3.17	0.00	0.84	0.83	0.00	1.45	1.36	0.37	1.47	2.71
	2	0.60	0.49	0.48	2.84	2.99	2.21	1.35	3.64	2.51	0.76	0.81	0.72	2.23	2.17	2.79	0.29	1.45	3.04
SH2	4	0.56	0.51	0.49	1.18	1.11	1.25	2.97	3.62	3.19	1.17	0.89	0.88	1.11	1.31	1.33	0.21	1.21	3.04
	5	0.52	0.47	0.46	2.95	2.56	2.99	3.60	4.03	3.32	0.75	0.73	0.77	2.66	2.72	2.61	0.29	1.48	3.12
	6	0.00	0.42	0.45	0.00	5.09	6.47	0.00	3.92	2.17	0.00	0.63	0.77	0.00	3.75	2.40	0.29	1.64	3.46
	1	0.00	0.48	0.51	0.00	0.81	1.66	0.00	2.95	2.31	0.00	0.85	0.76	0.00	1.61	1.77	0.37	1.17	4.96
	2	0.55	0.51	0.55	2.54	3.05	2.51	3.03	3.55	1.96	0.59	0.77	0.70	2.76	2.15	3.36	0.37	1.08	4.87
SH2	4	0.51	0.49	0.52	1.17	1.29	1.01	3.99	3.57	2.91	1.13	0.91	0.86	1.18	1.47	0.87	0.29	0.83	4.46
G	5	0.46	0.47	0.48	2.15	2.66	3.27	3.88	3.99	2.97	0.57	0.71	0.77	3.43	2.83	2.24	0.37	1.08	4.79
	6	0.00	0.41	0.00	0.00	6.22	0.00	0.00	1.91	0.00	0.00	0.60	0.00	0.00	3.00	0.00	0.37	1.25	5.04

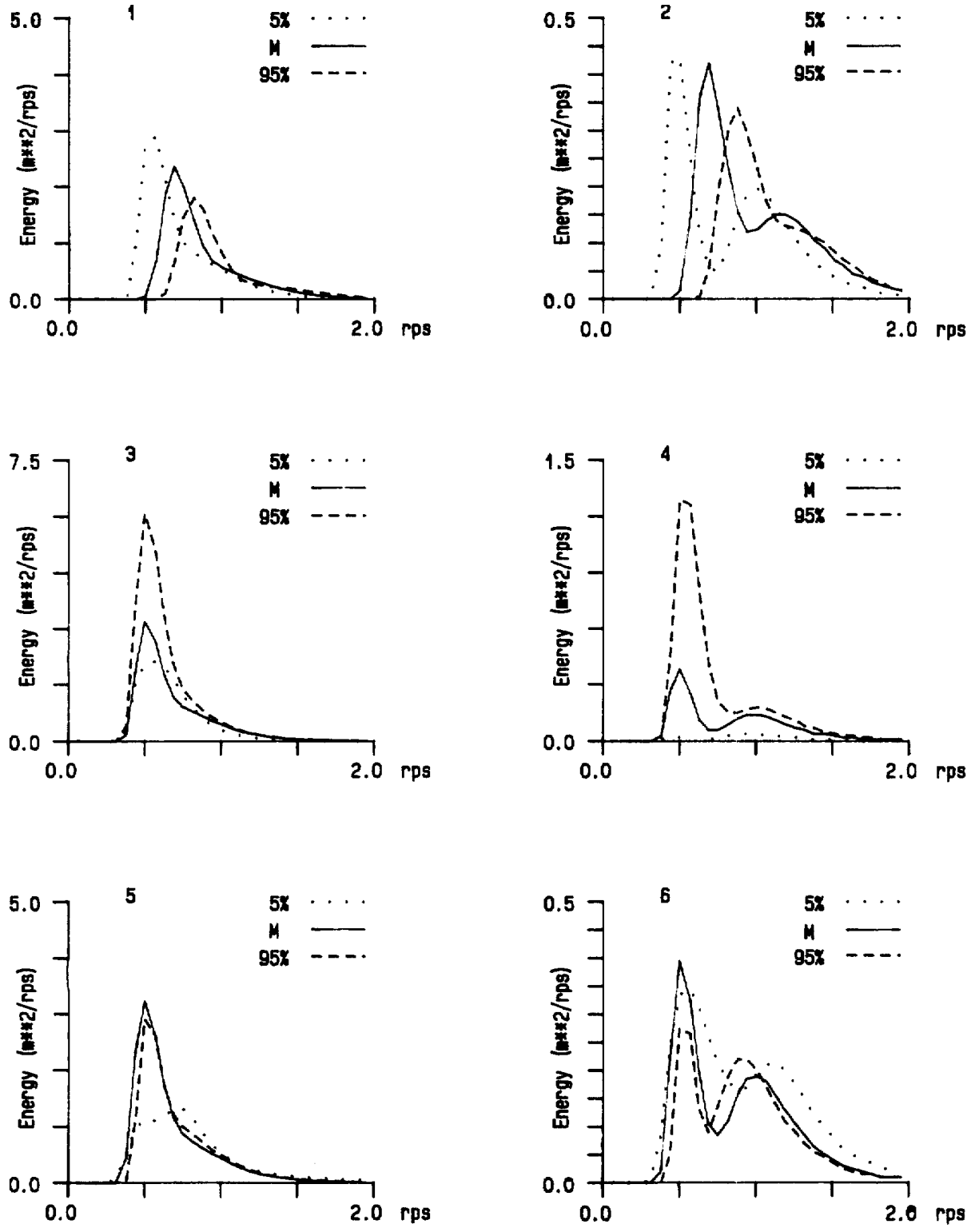

Fig. 23 Examples of the 5% (dotted), modal (solid) and 95% (dashed) probability spectra for Group 2 and 4 spectra and target parameters ωm1 (plot 1,2), HS1 (3,4), SH1 (5,6), ωm2 (7,8), HS2 (9,10) and SH2 (11,12).

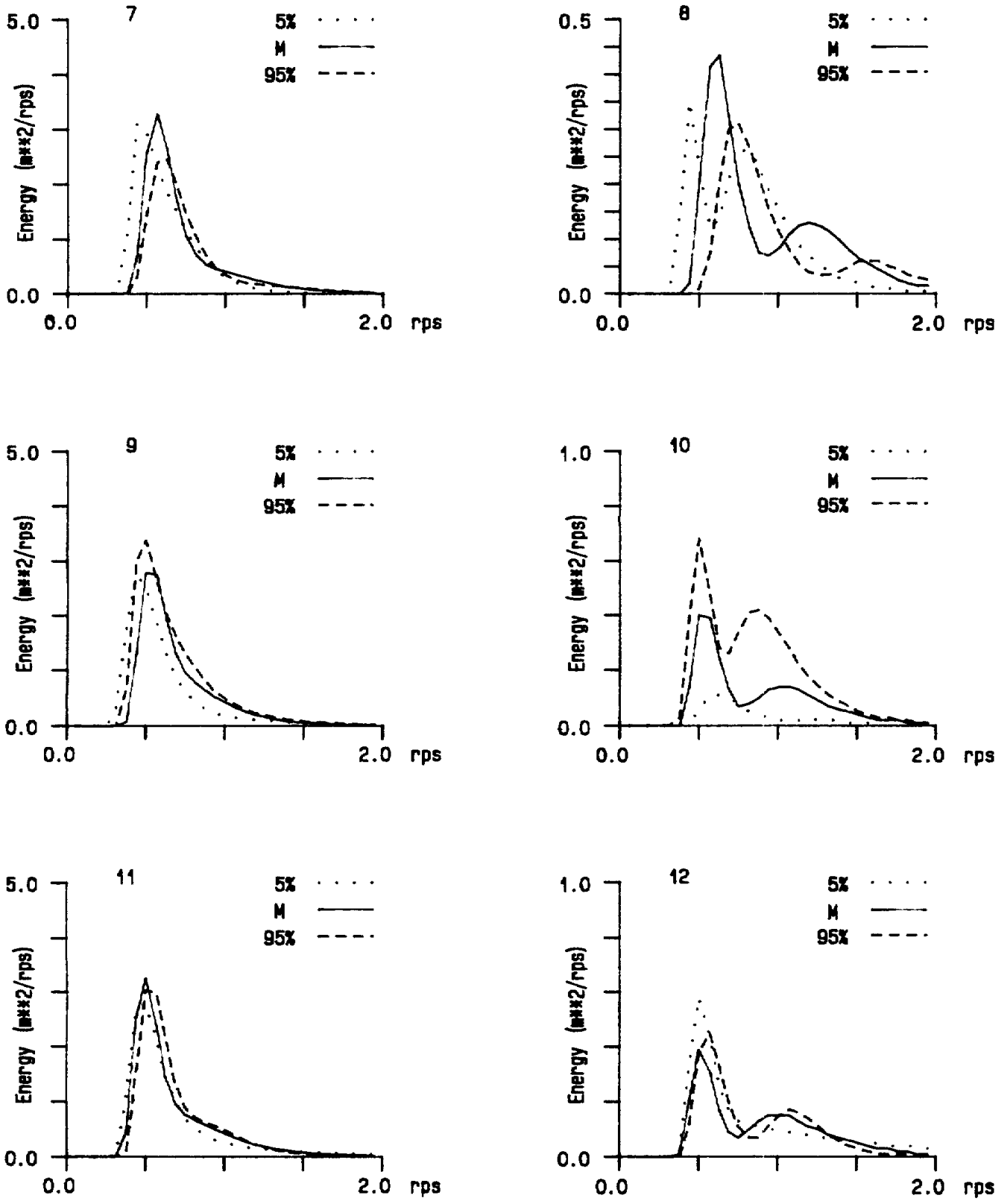

Fig. 23 (continued)

where ωm, HS and λ are the modal frequency, significant wave height and shape parameter, and two other parametric formulations will be examined. These two models are Wallops spectrum (Huang et al. 1981) which contains a variable power law relationship, and the model proposed by Donelan et al.(1985) which represents a class of models enhancement parameter first proposed by Hasselmann et al. (1973) during JONSWAP.

The Wallops spectrum is given as:

$$E_W(\omega) = \frac{\beta g^2}{\omega m^5} \left(\frac{\omega m}{\omega}\right)^M e^{-\left(\frac{M}{4}\right)\left(\frac{\omega m}{\omega}\right)^4}$$

$$\beta = \frac{(2\Pi\Phi)^2 M^{(M-1)/4}}{4^{(M-5)/4}\,\Gamma((M-1)/4)} \qquad \Phi = \frac{(\overline{\delta^2})^{1/2}}{\lambda_o}$$

where Φ is the significant slope defined as the RMS surface elevation (δ) divided by the wavelength (λo) associated with the spectral peak frequency (ωg) and g is the gravitational acceleration. The spectrum consists of two-independent parameters, δ and ωm, as the power law variable, M, was shown by Huang et al, (1981) to be related to the significant slope, through statistical arguments, by:

$$M = \left| \frac{\text{Log}\,(2^{1/2}\Pi\Phi)^2}{\text{Log}\,2} \right|$$

One can readily show that given deep water, sinusoidal wave assumptions, i.e.:

$$\lambda_o = \frac{g(2\Pi)}{\omega m^2} \qquad (\overline{\delta^2})^{1/2} = \frac{Hs}{4} \Rightarrow \Phi = \frac{Hs\ \omega m^2}{4g2\Pi}$$

that the Wallops and OH (3-parameter) spectra are identical expressions when M= 4λ + 1. The Wallops spectrum has been extended to account for finite depth effects, solitary and cnoidal wave theory which affect the M and β calculations and which would be included implicitly in the OH model fit. The relationship between M and significant slope suggests that the λ shape parameter should also be related to significant slope, ie:

$$\lambda = \frac{M-1}{4} = \frac{1}{4}\left(\left|\frac{\mathrm{Log}(\,2^{1/2}\,\Pi\Phi\,)^2}{\mathrm{Log}\ 2}\right| - 1\right)$$

which would improve the ability to predict the shape parameter; however, attempts to reconcile the observed fit parameters with the above expression have not been successful.

The Donelan spectra is given as:

$$E_D(\omega) = \frac{\alpha\, g^2}{\omega m\, \omega^4}\, e^{-\left(\frac{\omega m}{\omega}\right)^4}\, \gamma^{[A]}$$

$$[A] = \mathrm{EXP}\ [\ -(\ 1\ -\ \omega/\omega m)^2\ /\ 2\,\sigma^2\ ]$$

where ωm is the peak frequency, α is a variance constant, γ a peak enhancement parameter and σ a peak width parameter. The peak enhancement parameter, γ, was defined by Hasselmann et al.(1973) to be equal to the ratio of the observed peak energy to that of a Pierson-Moskowitz spectrum of the same peak frequency. It was originally used to reconcile the JONSWAP results as opposed to representing any theoretical relationship. The peak width parameter is sometimes assigned two values in order to represent the differing half-widths of the forward and back faces of the peak.

Donelan's spectrum is a modification of the JONSWAP formulation with the ω**5 relationship of the latter replaced by [ωm* ω**4]. It is equivalent to Toba's spectrum (Phillips, 1985) with

$$\alpha = \left(\frac{\omega m U_*}{g}\right)\beta$$

with β assumed to be a universal constant and U_* the friction wind velocity.

A relationship between the peak enhancement parameter, γ, and the OH shape parameter, λ, can be established. If one normalizes both spectra by the total variance, given as

$$M_0 = \int_{\omega_1}^{\omega_2} E(\omega)\,d\omega = \frac{\alpha g^2}{\omega m^4} \quad \text{or} \quad \frac{Hs^2}{4^2}$$

then the model reduces to:

$$E_D'(\omega) = \frac{\omega m^3}{\omega^4} e^{-\left(\frac{\omega m}{\omega}\right)^4} \gamma^{[A]} \qquad E_{OH}'(\omega) = 4 \frac{\left(\frac{4\lambda+1}{4}\right)^{\lambda} \omega m^{4\lambda} e^{-\frac{(4\lambda+1)}{4}\left(\frac{\omega m}{\omega}\right)^4}}{\Gamma(\lambda)\, \omega^{4\lambda+1}}$$

$$[A] = \mathrm{EXP}\left[-(1 - \omega/\omega m)^2 / 2\sigma^2 \right]$$

If one assumes that both models represent the data spectrum equally well, then for the spectral shapes to be similar:

$$\gamma^{[A]} = 4 \frac{\left(\frac{4\lambda+1}{4}\right)^{\lambda} \left(\frac{\omega m}{\omega}\right)^{4\lambda-3} e^{-\frac{(4\lambda-3)}{4}\left(\frac{\omega m}{\omega}\right)^4}}{\Gamma(\lambda)}$$

At the spectral peak, $\omega = \omega m$, so that

$$\gamma = 4 \frac{\left(\frac{4\lambda+1}{4}\right)^{\lambda} e^{-\frac{(4\lambda-3)}{4}}}{\Gamma(\lambda)}$$

Assuming an ω**-4 relationship, then $\lambda = 3/4$ and $\gamma = 3.26$, while for a -5 high-frequency tail, $\lambda = 1$ and $\gamma = 3.89$. The experimental mean JONSWAP γ value was 3.3, and 3.6 when the data were re-analyzed by Battjes et al.(1987) which could support either a -4 or -5 relationship. A linear regression analysis was performed between the fitted peak enhancement parameter, from Donelan's formulation, and the predicted peak enhancement parameter calculated using λ from the fitted normalized 3 parameter OH spectra for single peak spectra (having assigned Type 2 classes 1, 5, and 9) for Stn. 46005 data. A predicted peak enhancement parameter using $\lambda 1$ from the corresponding six-parameter model fits was also examined. The regression results are given in Table 13 . It can be seen that when the residual fit error (RESH) is low, the predicted γ from λ of the 3-parameter normalized OH expression agrees well with a directly fitted γ, with only slight offset from a zero intercept (A=0) and slope (B) of 1. When predicted from $\lambda 1$ (SH1) of the complete six-parameter expression, the correlation is reduced, particularly for the inshore stations, though still significant.

At first examination, it appears that an estimate of σ could be produced by using the constraint that

$$\int E_D'(\omega)d\omega = \int E_{OH}'(\omega)d\omega = 1$$

and replacing the predicted peak enhancement parameter into Ed'(ω). However, the integral turns out to be insensitive to the value of λ.

Table 13. Regression results for the peak enhancement and shape parameters.

Station	Npts.	Corr. Coeff.	A	SIGA	B	SIGB
46005						
3-par	1018	.87	-.24	.099	1.17	.021
RESH<2%	578	.94	-.11	.08	1.096	.017
SH1	1073	.81	1.98	.074	0.69	.015
RESH<2%	900	.88	1.53	.066	0.76	.014
46004						
	915	.81	2.04	.08	0.68	.017
RESH<2%	772	.87	1.64	.07	0.75	.015
103						
	839	.56	0.36	.31	1.25	.061
RESH<2%	630	.67	-.66	.32	1.42	.062
211	700	.67	0.61	.23	1.23	.052
RESH<2%	632	.68	0.44	.24	1.26	.055
503W	63	.70	2.93	.52	0.68	.017

7SUMMARY

An examination of the West Coast wave climate was conducted based on spectral records for a five year period extending from 1984 to 1989 collected at two offshore and three inshore locations. In Chapter two , the treatment of the data was described. The spectra were truncated between constant frequency limits, their quality assessed and they were examined to ascertain the amount of noise present, it was found that smoothing of the spectra was required only for the three inshore station records in order to remove this variability and increase confidence in the spectral density estimates. Further smoothing would have been desired for the Station 503W WRIPS buoy records, however this was not possible due to the few number of frequencies available to describe the spectra.

In Chapter 3 , summary spectral statistics and spectral Type 1 classification were used to describe the general features of the wave climate. There was an expected seasonal and geographic variation in the wave properties with winter months and offshore locations

experiencing the most severe conditions. The single maximum observed significant wave height was 14.1m at Stn. 46004. of the three inshore stations, Stn. 503W in Queen Charlotte Sound experienced average sea states almost as severe as offshore and, during a later storm analysis, was observed under certain conditions to have a larger storm signal than Stn. 46004 located in the open ocean. The percentage of records having a significant wave height greater than 5m and peak period greater than 14s, for winter months, were 10.2, 9.9, 8.2, 3.3 and 1.1% for Stns, 46005, 46004, 503W, 211 and 103 respectively, which reflect the relative severity of the wave climate at the different sites. All stations showed at least one occurrence of HSIG>8m and TP>17s with the most extreme joint occurrence of HSIG and TP observed at Stn. 46005 (HSIG of 13.6m, TP of 20s). In comparisons with other geographic areas, the West Coast appears to experience more severe long period wave conditions than Hibernia, Sable Island, or the North Sea. Examination of the occurrence of different spectral types indicated a large percentage of swell dominant and multiple peak spectra which has implications towards both parametric and numerical modelling.

In Chapter 4 , the Ochi and Hubble six-parameter model was fit to all the data spectra and its behavior was described. It was shown that this model provided acceptable representation of the spectra, for a wide variety of spectral shapes, over 90% of the time. There was considerable scatter in the fit parameters. However, certain behavioral trends could be observed. The modal frequencies and variance parameters followed the general behavior of decreasing frequency with increasing wave energy. The SH1 parameter tended to decrease with energy, for a given period, and to increase with period for a given energy level. The SH2 parameter generally increased with energy for a given period and with period for a given energy level.

A discussion on observed storms and storm spectra was included in chapter 5 . It was seen that storms were generated by two distinct types of low pressure systems: a slow moving, large scale system and a rapidly moving small scale system, both of which can intensify as they approach the coast. Rapid growth of the seas was observed, with maximum rates on the order of 1m/hr and 1s/hr for HSIG and TP, respectively. With the exception of Queen charlotte Sound, there was a mean decrease in energy between offshore and inshore stations of approximately 30%. In Queen Charlotte Sound, intensification of sea conditions was observed on occasion, generally associated with a small scale disturbance, resulting in a maximum energy intensification of 60% compared to Stn. 46004. The time of sea response to storm winds at the different measurement sites was determined by their relative position to the storm track which would influence characteristics of

local winds as well as travel times for generated swell. Long period swell was observed at all stations.

The ability to predict the Ochi and Hubble model parameters from significant wave height and peak period and from other model parameters was examined in Chapter 6 with varying success. The frequency and variance parameters were better predicted than were the shape parameters, due to the large amount of scatter present in the latter, however no single parameter could be predicted consistently well for all spectral types. More useful information was obtained by examining the probability distribution of the fit parameters. A bounded normal and gamma probability function was fit to the probability density histogram for each fit parameter and then used to produce a "family" of wave model spectra based on the modal and 95% confidence limit values for each parameter. An analytical analysis on the relationships between the Ochi and Hubble spectrum and the Wallops and JONSWAP type spectra showed that the Wallops and Ochi and Hubble spectra are equivalent under certain conditions and that the Ochi and Hubble shape parameter can be used to predict the peak enhancement parameter of a JONSWAP type spectra.

Certain features of the wave climate should be addressed by any hindcast or forecast model of the region. Swell of periods greater than 20 seconds (as long as 25 seconds), were observed at all stations and their modelling could influence the position of the offshore model boundary. The presence of two types of storm generating low pressure systems will dictate the spatial and temporal scales of the model. Specifically, the steep curvature of isobars, rapid movement, and strong interaction between winds and wave field of small-scale pressure systems would have to be properly modelled to provide an accurate prediction of the wave climate in Queen Charlotte Sound and Hecate Strait. These regions are of particular interest as they contain active fishing areas, known gas reserves with potential for offshore drilling, and the major shipping routes to Alaska. The inshore wave climate would further be affected by land sheltering, wave refraction due to changes in bathymetry and current/wave interactions.

8REFERENCES

Baird, W.F, 1984. Comparison of wave data representative of the Hibernia and Venture areas with data representative of the North Sea Wave Climate. Contractor report to the Marine Environmental Data Services Branch, Dept. of Fisheries and Oceans. Unpub. Man.

Battjes J.A, T.J. Zitman and C.H. Holthuijsen, 1987. A reanalysis of the spectra observed in JONSWAP. J. Phys. Ocean. 17: 1288-1295.

Bretschneider, C.L. 1959. Wave variability and wave spectra for wind-generated gravity waves. U.S. Army Corps of Engineers, Beach Erosion Board, Tech. Memo no. 118.

Donelan M.A., J. Hamilton and W.H. Hui, 1985. Directional spectra of wind-generated waves. Phil. Trans. R. Soc. Lond. A315: 509-562.

Ewing, J.A., 1980. Observations of wind-waves and swell at an exposed coastal location. Estuarine and Coastal Mar. Sci., 10, 543-554.

Hasselmann K., T.P. Barnett, E. Bouws. H. Carlson, D.E. Cartwright, K. Enke, J.A. Ewing. H. Gienapp, D.E. Hasselmann, P. Kruseman. A. Meerburg, P. Muller, D.J. Olbers, K. Richter, W. Sell and H. Walden, 1973. Measurements of wind-wave growth and swell decay during the Joint North Sea Wave Project (JONSWAP). Dtsch. Hydrogr. Z. A8(12):1-95.

Hodgins D.O, P.H. LeBlond, D.S. Dunbar and C.T. Niwinski, 1985. A wave climate study of the Northern British Columbia coast. Vol. 2, Wave Properties and Wave Prediction. Contractor report R-48-1 prepared for the Marine Environmental Data Services Branch, Dept. of Fisheries and Oceans. 236pp.

Huang N.E., S.R. Long, C.C. Tung, Y. Yuen and C.F. Bliven, 1981. A unified two-parameter wave spectral model for a general sea state. J. Fluid Mech. 112:203-224.

Huang N.E., P. Hwang, H. Wong, S.R. Long and L.F. Bliven, 1983. A study on the spectral models for waves in finite water depth. J. Geophys. Res. 88:9579-9587.

James, R.W., 1969. Abnormal changes in wave heights. Mar. Weather Log 13: 252-255.

Juszko B,-A, 1989. Parameterization of directional spectra -Part 1. DREA CR/89/414, March 1989. 141pp.

Juszko B,-A., 1989. Parameterization of Directional spectra -Part 2. DREA CR/89/445 Vol.I. December 1989. 115pp.

Juszko B.-A., R. Brown, B. de Lange Boom and D. Green, 1985. A wave climate study of the Northern British Columbia coast. Vol. 1, Wave Observations. Contractor report R-48-1 prepared for the Marine Environmental Data Services Branch, Dept. of Fisheries and Oceans. 164pp.

Kitaigorodskii, S.A., 1983. On the theory of the equilibrium range in the spectrum of wind-generated gravity waves. J. Phys. Ocean. 13:816-827.

Neu, H., 1982. 11-year deep water wave climate of Canadian Atlantic waters. Can. Tech. Rep. Hydrogr. Ocean Sci. 13:7.41pp.

Ochi M.K. and E.N. Hubble, 1976. Six-parameter wave spectra. Proceedings of the 15th Coastal Engineering Conference,Honolulu, 1976. P301-328.

Phillips, O.M., 1958. The equilibrium range in the spectrum of wind generated waves. J. Fluid Mech. 4:426-434.

Phillips, O.M. 1985, Spectral and statistical properties of the equilibrium range in wind-generated gravity waves. J. Fluid Mech. 156:505-531.

Pierson, W.J. and L. Moskowitz, 1964. A proposed spectral form for fully-developed wind seas based on the similarity theory of S.A. Kitaigorodskii, J. Geophys. Res. 69., 5181-5190.

Quayle, R.G. and D.C. Fulbright, 1975. Extreme wind and wave periods for the U.S. coast. Mar. Weather Log 19:67-70.

Toba. Y. 1972. Local balance in the air-sea boundary processes. I: On the growth of wind waves. J. Ocean. Soc. Japan. 28:109-121.

Toba, Y., 1973. Local balance in the air-sea boundary processes. III: On the spectrum of wind waves. J. ocean. Soc. Japan. 29:209-220.

9ACKNOWLEDGEMENTS

This work was supported by a Department of Supply and Services Contract No. W7707-9-0286/01-OSC. We would like to give special thanks to the Scientific Authority, Dr. Ross Graham of the Defence Research Establishment Atlantic, Dept. of National Defence, for his support and helpful comments. We would also like to thank Dr. R. Wilson, J. Gagnon, C. Glennie and D. Spear of the Marine Environmental Data Service, Dept. of Fisheries and Oceans, and R, Beale and E. Coatta of the Atmospheric Environment Service, Environment Canada, for providing the background information, wave data and surface air pressure maps used in the study.

UNCLASSIFIED
SECURITY CLASSIFICATION OF FORM
(highest classification of Title, Abstract, Keywords)

DOCUMENT CONTROL DATA

(Security classification of title, body of abstract and indexing annotation must be entered when the overall document is classified)

1. ORIGINATOR (the name and address of the organization preparing the document Organizations for whom the document was prepared, e.g. Establishment sponsoring a contractor's report, or tasking agency, are entered in section 8.)

Juszko Scientific Services

2. SECURITY CLASSIFICATION (overall security classification of the document including special warning terms if applicable).

Unclassified

3. TITLE (the complete document title as indicated on the title page. Its classification should be indicated by the appropriate abbreviation (S,C,R or U) in parentheses after the title).

Analysis of the West Coast Wave Climate

4. AUTHORS (Last name, first name, middle initial. If military, show rank, e.g. Doe, Maj. John E.)

Juszko, Barbara-Ann

5. DATE OF PUBLICATION (month and year of publication of document)

March 1990

6a. NO OF PAGES (total containing information Include Annexes, Appendices, etc).

105

6b. NO. OF REFS (total cited in document)

22

6. DESCRIPTIVE NOTES (the category of the document, e.g. technical report, technical note or memorandum. If appropriate, enter the type of report, e.g. interim, progress, summary, annual or final. Give the inclusive dates when a specific reporting period is covered).

Contractor Report

8. SPONSORING ACTIVITY (the name of the department project office or laboratory sponsoring the research and development. Include the address).

Defence Research Establishment Atlantic, PO Box 1012, Dartmouth, N.S.
B2Y 3Z7

9a. PROJECT OR GRANT NO. (If appropriate, the applicable research and development project or grant number under which the document was written. Please specify whether project or grant).

1AG

9b. CONTRACT NO. (If appropriate, the applicable number under which the document was written).

W7707-9-0286/01-OSC

10a. ORIGINATOR'S DOCUMENT NUMBER (the official document number by which the document is identified by the originating activity. This number must be unique to this document).

DREA/CR/90/424

10b. OTHER DOCUMENT NOS. (Any other numbers which may be assigned this document either by the originator or by the sponsor).

11. DOCUMENT AVAILABILITY (any limitations on further dissemination of the document, other than those imposed by security classification)

(X) Unlimited distribution
( ) Distribution limited to defence departments and defence contractors; further distribution only as approved
( ) Distribution limited to defence departments and Canadian defence contractors; further distribution only as approved
( ) Distribution limited to government departments and agencies; further distribution only as approved
( ) Distribution limited to defence departments; further distribution only as approved
( ) Other (please specify):

12. DOCUMENT ANNOUNCEMENT (any limitation to the bibliographic announcement of this document. This will normally correspond to the Document Availability (11). However, where further distribution (beyond the audience specified in 11) is possible, a wider announcement audience may be selected).

UNCLASSIFIED
SECURITY CLASSIFICATION OF FORM

DCD03 2/06/87-M

UNCLASSIFIED
SECURITY CLASSIFICATION OF FORM

13. ABSTRACT (a brief and factual summary of the document. It may also appear elsewhere in the body of the document itself. It is highly desirable that the abstract of classified documents be unclassified. Each paragraph of the abstract shall begin with an indication of the security classification of the information in the paragraph (unless the document itself is unclassified) represented as (S), (C), (R), or (U). It is not necessary to include here abstracts in both official languages unless the text is bilingual).

Surface displacement spectra, collected at five locations off Canada's West Coast over a period extending from 1984 to 1989, were used to describe the overall wave climate, spectral types and storm characteristics of this region. Offshore waters experienced the most severe wave climate, as indicated by the joint occurrence of significant wave height (HSIG) and peak period (TP). Conditions of HSIG>8m and TP>17s were observed at all locations while the most severe record was represented by an HSIG>13m and TP of 20s. Examination of the spectral types indicated a large percentage of swell dominant and multiple peak spectra which has implications towards both their numerical and parametric modelling. Fifteen storms, driven by both small and large scale pressure systems, were examined in detail and showed the presence of rapid sea growth (maximum rates on the order of 1 m/hr and 1s/hr for HSIG and TP) and, with the exception of Queen Charlotte Sound, an average 30% decrease in energy between offshore and inshore stations. Intensification of sea conditions in Queen Charlotte Sound was observed on occasion (maximum intensification of 60%). The Ochi and Hubble six-parameter model was fit to all spectra. The statistical distribution of the fit parameters was calculated and an attempt was made to predict these parameters with varying success. The probability distribution of the fit parameters was also examined to define design spectra with known confidence limits.

14. KEYWORDS, DESCRIPTORS or IDENTIFIERS (technically meaningful terms or short phrases that characterize a document and could be helpful in cataloguing the document. They should be selected so that no security classification is required. Identifiers, such as equipment model designation, trade name, military project code name, geographic location may also be included. If possible keywords should be selected from a published thesaurus. e.g. Thesaurus of Engineering and Scientific Terms (TEST) and that thesaurus-identified. If it not possible to select indexing terms which are Unclassified, the classification of each should be indicated as with the title).

Waves
Ocean Waves
Wave Spectra
Wave Climate
Pacific Ocean

UNCLASSIFIED
SECURITY CLASSIFICATION OF FORM